REDUCTION AND UTILIZATION OF EMITTING CO_2 BY USING MOLTEN CARBONATE FUEL CELL (MCFC) STACK FOR SUSTAINABLE DEVELOPMENT IN BANGLADESH

by

MD. MATIUR RAHMAN

MINHAZ UR RASHID

BACHELOR OF SCIENCE IN ELECTRICAL AND ELECTRONIC ENGINEERING

Department of Electrical and Electronic Engineering
INTERNATIONAL ISLAMIC UNIVERSITY CHITTAGONG

December 2017

REDUCTION AND UTILIZATION OF EMITTING CO_2 BY USING MOLTEN CARBONATE FUEL CELL (MCFC) STACK FOR SUSTAINABLE DEVELOPMENT IN BANGLADESH

by

MD. MATIUR RAHMAN

MINHAZ UR RASHID

A thesis
Submitted as partial fulfilment of the requirement for the degree of

BACHELOR OF SCIENCE IN ELECTRICAL AND ELECTRONIC ENGINEERING

Department of Electrical and Electronic Engineering
INTERNATIONAL ISLAMIC UNIVERSITY CHITTAGONG

December 2017

CERTIFICATE OF APPROVAL

The thesis entitled as "**Reduction and utilization of emitting CO_2 for sustainable development in Bangladesh**" submitted by **Md. Matiur Rahman**, bearing Matric ID. **ET-133020** and **Minhaz ur Rashid**, bearing Matric ID. **ET-131072** of session **Autumn 2017**, to the Department of Electrical and Electronic Engineering, International Islamic University Chittagong, has been accepted as satisfactory in partial fulfilment of the requirements for the degree of Bachelor of Science in Engineering and approved for the examination held on **14 December, 2017**.

_____

Supervisor
Engr. Md. Shahid Ullah
Assistant Professor,
Department of Electrical and Electronic Engineering
International Islamic University Chittagong.

DECLARATION

It is hereby declared that this work has been done by us and no portion of the work contained in this thesis/project has been submitted elsewhere for the award of any degree or diploma.

_____

Md. Matiur Rahman

_____

Minhaz ur Rashid

ACKNOWLEDGMENT

All praises and thanks to Allah, the Lord of the world, the most Beneficent, the most Merciful for helping us to accomplish this work. For this Prototype development and report preparation we would like to thank our thesis supervisor Engr. Md. Shahid Ullah, Asst. Professor, EEE or his massive support and watchful guidance. Without his guidance, it was almost impossible to continue with the thesis work. He was very helpful and ever affectionate to endure the mistakes we had committed in the thesis work and always encouraged us by correcting our wrong proceedings. It was only the endless support offered by him that enabled us to complete this devoted task. We would also like to thank our parents who gave inspirations all the time for completing the thesis.

Authors

ABSTRACT

Reduction of the CO_2 emission from the existing natural gas and coal based power plant is a great challenge. Existing power plants of Bangladesh emit CO_2 at a concerning rate. Meanwhile, that causes serious greenhouse effect. But Bangladesh government cannot afford to simply stop producing power from the existing power plants just because they are harmful to the environment. In this research work molten carbonate fuel cell implementation with the existing power plant has been proposed. This proposed hybrid power supply system not only reduces CO_2 emission but also produces power by utilizing that CO_2. Meanwhile, it makes the existing power plant environment friendly as well. After observation from MATLAB Simulink and COMSOL results it can be concluded that this proposed hybrid power plant is able to reduce CO_2 emission by 70% from existing power plant and at the same time by using the reduced CO_2, MCFC stack can produce power with an efficiency of 41.19% for a cell number of 1000. In the inverter section for discrete time operation, the maximum efficiency was found to be 59.81%. Again, from the mathematical analysis it was seen that Ghorashal and Ashuganj have the capability of producing 53.46 MW and 16.16 MW respectively. Meanwhile, considering 1 KW to be the maximum demand of each house it is possible to supply 53000 and 16000 houses respectively by using CO_2 from both Ghorashal and Ashuganj power plant. Finally, this proposed hybrid power supply system would be a solution to ensure CO_2 reduction, utilization and sustainable development in Bangladesh.

TABLE OF CONTENTS

LIST OF FIGURES

LIST OF TABLES

LIST OF ABBREVIATIONS

IPCC	Intergovernmental Panel on Climate Change
GDP	Gross Domestic Product
MCFC	Molten Carbonate Fuel Cells
PEMFC	Polymer Electrolyte Membrane Fuel Cells
DMFC	Direct Methanol Fuel Cells
AFC	Alkaline Fuel Cells
PAFC	Phosphoric Acid Fuel Cells
SOFC	Solid Oxide Fuel Cells
DIF	Direct Internal Reformer
PDE	Partial Differential Equations
ODE	Ordinary Differential Equations
KEPCO	Korea Electric Power Corporation
CC	Carbon Capture
ORC	Organic Ranking Cycle
ITM	Ion Transfer Membrane
COE	Cost Of Electricity
RMS	Root Mean Square
DC	Direct Current
AC	Alternating Current
IGBT	Insulated-Gate Bipolar Transistor
BDT	Bangladesh Taka

CHAPTER 1

INTRODUCTION

1.1 Introduction:

Global warming, greenhouse effect and natural disaster these are now very common scenario in all over the world. In one sense people are responsible for that because people are not careful about the environment. Honestly speaking still people always try cope up with the modern world for that they can sacrifice the environment issue as well. One of the major causes of greenhouse effect is the carbon dioxide emission from the power plant, industry etc. As days goes energy demand increases day by day due to globalization. Electricity is the major source of power for most of the country's economic activities. Bangladesh's total installed electricity generation capacity (including captive power) was 15,351 MW as of January 2017 [1]. As of 2015, 92% urban population and 67% rural population have access to electricity. Average of 77.9% population have access to electricity in Bangladesh.

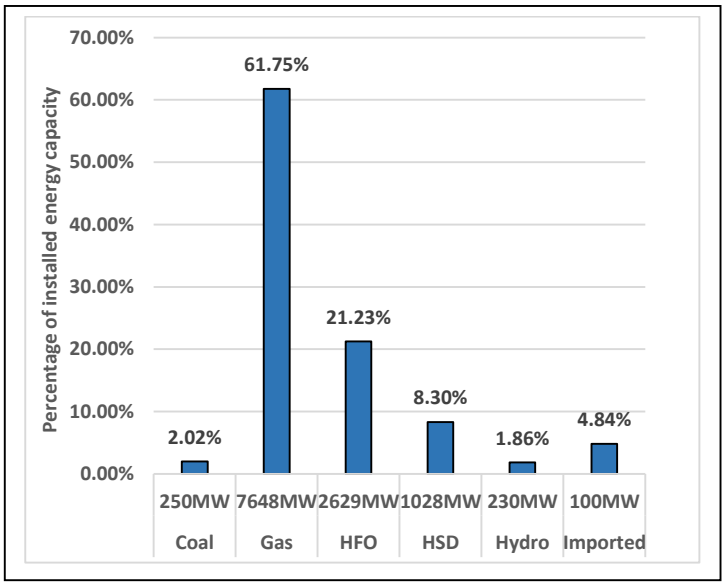

Fig. 1.1 Total installed energy capacity of Bangladesh.[2]

From Fig. 1.1, we can easily say that, maximum amount of power we consume comes from the natural gas based power plant. That means we are very much dependent on the conventional energy sources rather than renewable energy. Again, coal and gas based power plant emit carbon di-oxide at a concerning rate which is really harmful for our environment.

If we look at Table 1.1 below we can easily come to the conclusion that, in Bangladesh maximum amount of CO_2 is emitted by power sector as well.

Table 1.1: Top ten CO_2 emitting power plant list. [3]

Name of sector	**Installation name**	**Estimated annual CO_2 emissions(kilotons)**
Power	Ghorashal	4,731
Power	Barapukuria	2,075
Power	Ashuganj	1,502
Refinery	Eastern Refinery Ltd	983
Power	Haripur Barge	980
Power	Khulna	938
Power	Chittagong	914
Power	Haripur AES	653
Power	Shajibazar	631
Power	Shiddhirganj	631

Some graphical representation of the severity of the rise of CO_2 has been shown here. Fig. 1.2 and 1.3 represents the emission of CO_2 from Fossil and Natural gas fired power plants in Bangladesh. From the figures, it is clear to see that carbon emission is increasing at a concerning rate which could destroy the environment and unfortunately it is still on rise. Another graphical representation has also been shown in Fig. 1.4 to highlight how much CO_2 emission has been increasing over the year of 2010-2012 in different sectors of power sources and industries of Bangladesh.

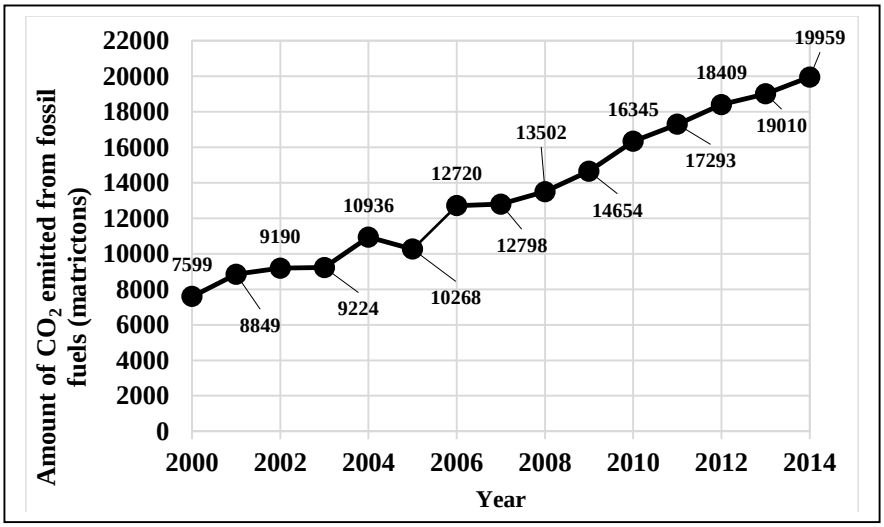

Fig. 1.2 Annual CO_2 emitted by fossil fuel based power plant in Bangladesh [4][5].

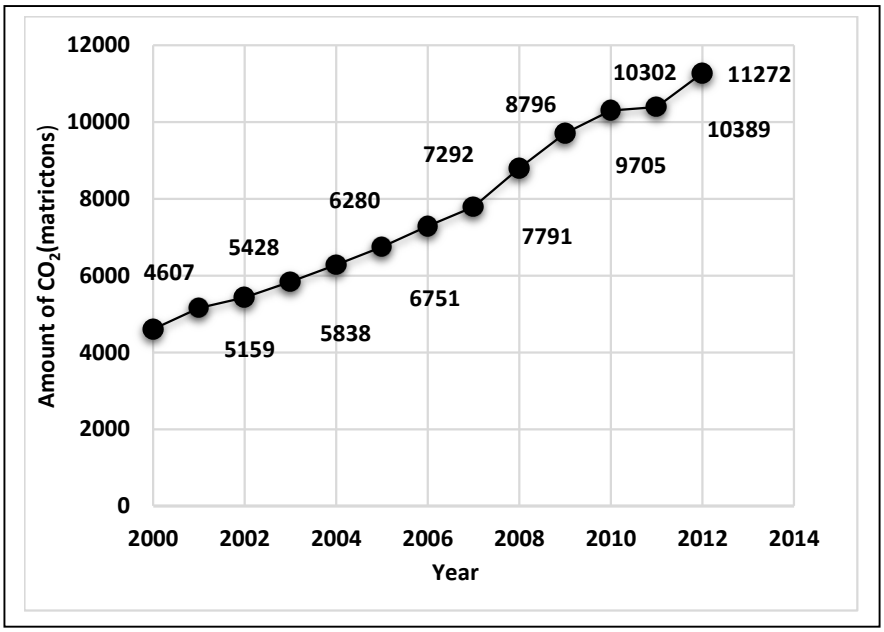

Fig. 1.3 Annual CO_2 emitted by Natural gas fired power plant in Bangladesh [5].

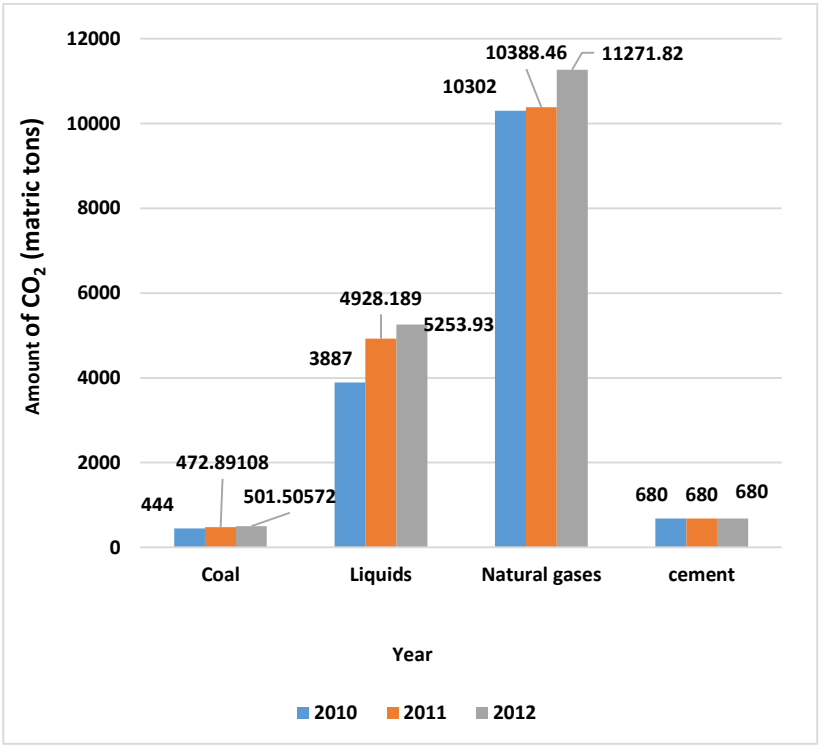

Fig. 1.4 CO_2 emission from different types of power sources and industries from 2010-2012.[5]

Looking at the above Fig 1.4, we can see that the emission of CO_2 is on the rise every year. That is not all in the upcoming years with the inclusion of two 1320MW coal fired power plant one in Rampal [6] and another in Banshkhali [7] the percentage of emission is only going rise even further. Experts have predicted that almost 15 percent of

Bangladesh will go underwater within the next 50 years. According to the Intergovernmental Panel on Climate Change (IPCC) Fifth Assessment Report published recently, the sea-level of the Bay of Bengal is rising at a rate of 1.5 mm per year. If the sea-level rises by 45 cm, a permanent loss of up to 15600 square kilometers of land is expected. The increase of CO_2 emission is also causing a rise in temperature every year. Researchers at BUET predicted that this temperature could rise to 3-5% by 2100 [8].If temperature increases by 3°C than 250-550 million people will be in the risk of hunger. Also, the rising CO_2 concentrations are likely to have huge effects on the growth, physiology, and chemistry of the plant life. It is estimated that if temperature increases by 2°C-3°C within 2100 than the GDP could be reduced by more than 3% and if that temperature increases by 5°-6° than we could be looking at a GPD reduction of 5-6%. Even the fishery sector will suffer consequences which contributes 3-5% of the total gross domestic product (GDP). As the oxygen level deceases with the increasing temperature. Not only that the recent addition of the unpredictable weather pattern is also the result of this increase of global emission of CO_2.

From Fig. 1.2,1.3 and 1.4, it is also easily perceivable that carbon dioxide emission rate in Bangladesh is a great waring for us. It is high time to think about that, otherwise we have to pay for that in future. We have to find out a way of CO_2 reduction and use that carbon dioxide to produce power. For that we considered a hybrid power supply system which includes a carbon capture unit and after that process that carbon and produce power from that carbon. For our base study in carbon capture unit we use Molten Carbonate Fuel Cell (MCFC).

1.2 Background:

MCFC is one of the many branches of the fuel cell technology which captures carbon dioxide and produces power from the captured power. Normally fuel cell is an electrochemical device which converts the chemical energy of a fuel into an electrical energy. MCFC consists of anode, cathode and an electrolyte. Where both anode and cathode are separated by the electrolyte. MCFC operates when CO_2 and oxygen reactant pass through the cathode. The operating temperature of MCFC is 650^0C.The high temperature increases the conductivity of carbonate electrolyte. The half-cell reaction is given below:

$$H_2 + CO_3^- \rightarrow H_2O + CO_2 + 2e(at\ anode) \quad (1)$$

$$½\ O_2 + CO_2 + 2e^- \rightarrow CO_3(at\ cathode) \quad (2)$$

The total cell reaction:

$$H_2 + \frac{1}{2} O_2 + CO_2\,(cathode) \rightarrow H_2O + CO_2\,(anode) \quad (3)$$

The total cell reaction is shown in Fig. 1.5:

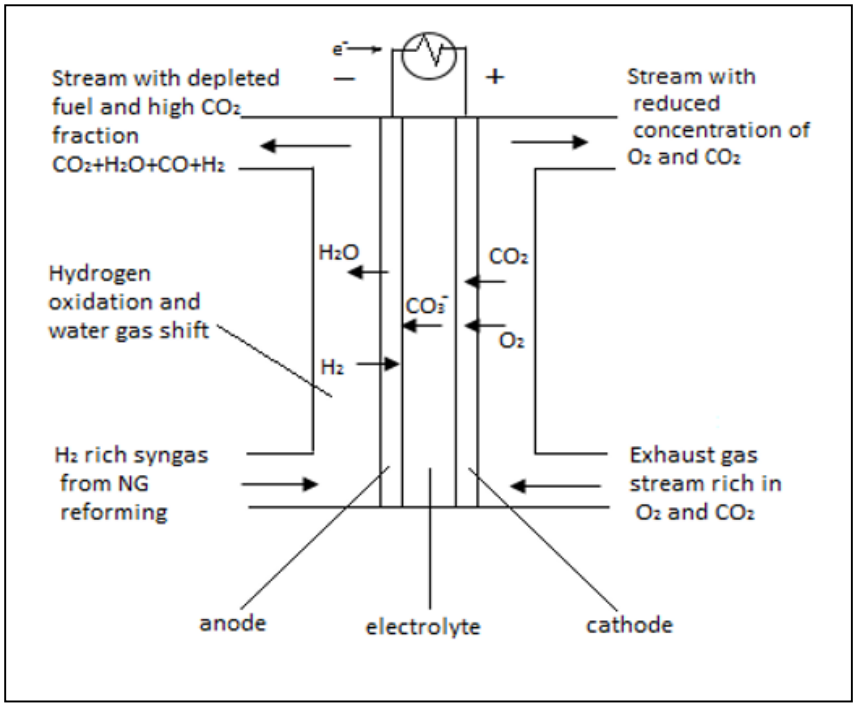

Fig. 1.5 Total cell reaction of MCFC. [9]

1.3 Problem Statement:

To meet the increasing demand government, need to increase the generation but most of the power plant available in Bangladesh are mostly conventional power plant. As the generation increases CO_2 emission increases also. Since we are developing country we cannot afford to stop power generation from the existing conventional power plant. If we don't think about the environment now, we will have to face serious natural disaster in future and for that we will be responsible. Again, if developing country like Bangladesh can ensure carbon free power generation then our government can force other developed countries to do so as well.

1.4 Objective:

- Make the existing power plant environmental friendly
- Reduce CO_2 emission in Bangladesh
- Produce energy from the captured CO_2 and supply that energy to the addition household and reduces the energy crisis as well.

1.5 Thesis Outline

In this thesis, we described and discussed about our project in 5 chapters. The outlines of our thesis are as follows:

Chapter 1 contains the introduction. In this chapter, introduction of the thesis topic has been discussed.

Chapter 2 contains literature review. All the previous works related to this thesis has been discussed in this chapter.

Chapter 3 contains methodology where the method of developing the Simulink model and Comsol model has been discussed.

Chapter 4 contains result and discussion where the result of our thesis has been discussed.

Chapter 5 contains conclusion where conclusion and future work has been discussed.

1.6 Summary:

As we all know Bangladesh is a developing country and for a country such as Bangladesh power crisis is a major issue. So, in order to deliver as much power as possible to the population they tent to opt for coal and natural gas fired power plants due to their cheaper nature. Which also leads to environment pollution. But in order to keep supplying our population with we cannot just stop producing power from these existing sources just because of environmental issue. This is where MCFC systems comes in handy as they have the ability to run these existing plants while reducing CO_2 emission and from that reduced CO_2 they can also produce power which could contribute to the energy crisis situation.

CHAPTER 2

LITERATURE REVIEW

2.1 Introduction to fuel cell and its origin:

Fuel cells are electro chemical devices which has the ability to convert the chemical reaction between molecules into electrical energy. Generally, fuel cells rely on the principle reaction between H_2 and O_2 over a catalyst which produces water, heat and electricity. The first concept of fuel cell was laid out in the early nineteenth century by Humphry Davy. This was later picked up by a scientist named Christian Friedrich Schönbein in 1838.Moving on to the 1939 William Grove [10], a chemist, physicist and lawyer had started performing numerous experiments on what he named as gas voltaic battery. It was him who first discovered that the reaction between H_2 and O_2 within a catalyst made of platinum could produce electricity. For this reason, he is also renowned as the inventor of fuel cell.

2.2 Branches of fuel cell modules:

Ever since the first discovery of fuel cell it has taken many routes in the field of research and spread into many branches. Some of the main branches of fuel cells have been given below:

1. Polymer electrolyte membrane fuel cells (PEMFC)
2. Direct methanol fuel cells (DMFC)
3. Alkaline fuel cells (AFC)
4. Phosphoric acid fuel cells (PAFC)
5. Molten carbonate fuel cells (MCFC)
6. Solid oxide fuel cells (SOFC).

2.3 History of molten carbonate fuel cell:

MCFC is one of the many branches of the fuel cell technology. As a technology MCFC's are still relatively new in the commercial world. Even so research work around MCFC's are being done since the 19^{th} century. In 1950 G.H.J. Broers and J. A. A. Ketelaar began evaluating the work of the Russian scientist Davtyan who in 1930's had made significant advancement to this field [11][12][13]. Then in the 1960's it was their work that had established the fact that molten carbonates are the best choices for electrolytes for handling fuels that contained carbon [11]. In the late 1990's the work on demonstration

and commercialization of MCFC's had started and ever since 2003, commercial power plants based on MFCF's have been available [12]. Currently researchers of many countries such as North America, Japan, Europe and Korea are trying to improve the materials used in MCFC to increase its cell performance, lifetime and at the same time trying reduce its costs [11]. As of 2014 there are about 50 sites worldwide being powered by MCFC power plants having around 300 MW installed capacity and 18 of them are installed in Korea where a total of 144.6 MW power is produced by the MCFC power plants [14].Currently the most popularly used products of fuel cell for stationary application of MCFC are the DFC 300,DFC 1500 and the DFC 3000. Their pictorial view has been represented down below with Fig. 2.1, 2.2 and 2.3:

Fig. 2.1 DFC 300.[14]

Fig. 2.2 DFC 1500 [14]

Fig. 2.3 DFC 3000 [14]

2.4 Previous works:

2.4.1 MCFC modelling and designing [H. Kim et al. (2011)]:

In 2011, Kim et al.[15] proposed a model where they designed a model of MCFC and a control scheme to go along with it. In their proposed model they used a single direct internal reformer(DIF) with the help of numerical process by reducing the partial

differential equations(PDE) for a number of ordinary differential equations(ODE). In order to accomplish their mathematical derivation of the proposed model they used the cubic spline collocation method and the finite difference method. In their research they used the change in power demand to measure the performance of their control scheme and they were really satisfied with their outcome. The concept of their proposed work has been given below in Fig 2.4:

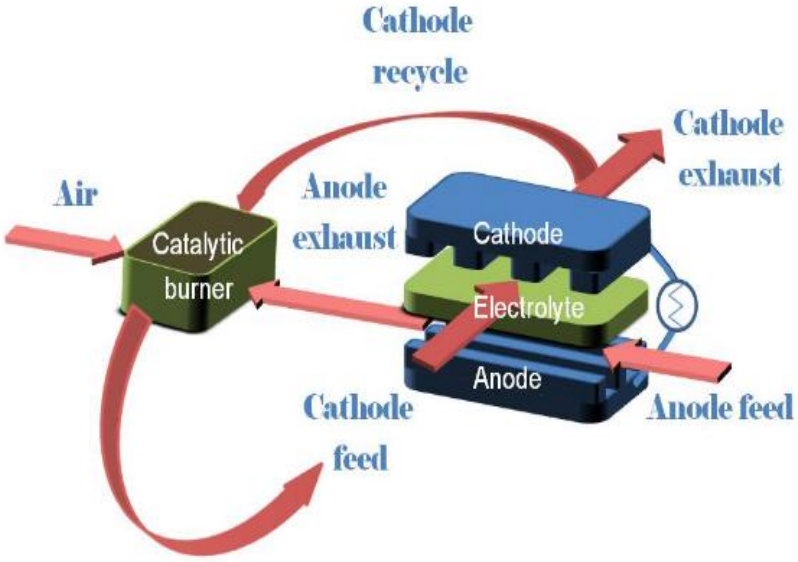

Fig. 2.4 The concept of direct fuel molten carbonate fuel cell [15]

2.4.2 MCFC combined cycle with integrated cryogenic CO_2 Separation unit [P. Chiesa et al. (2011)]:

In 2011, Chiesa et al.[16] conducted an investigative analysis on a natural gas combined MCFC power plant where the amount of CO_2 emitted is lower than other fossil sources. In their analysis they developed a model with cryogenic CO_2 removal chamber. This chamber was positioned in such a way that the captured flue gases are used for cathode feeding where CO_2 shifts from the cathode side to the anode side while increasing the amount of CO_2 concentration in the anode exhaust. From there exhausted CO_2 are taken to the heat recovery steam generator where they are cooled off and finally sends them to the cryogenic chamber. Fig. 2.5 shows the layout of the combined cycle with cryogenic chamber. From their analysis it has been seen that the proposed model has the potential to capture 80% of the exhausted CO_2 from the plant while decreasing 72% of the captured CO_2. At the same time, it was also able to add 22% more electrical output along with the original cycle's 58% efficiency.

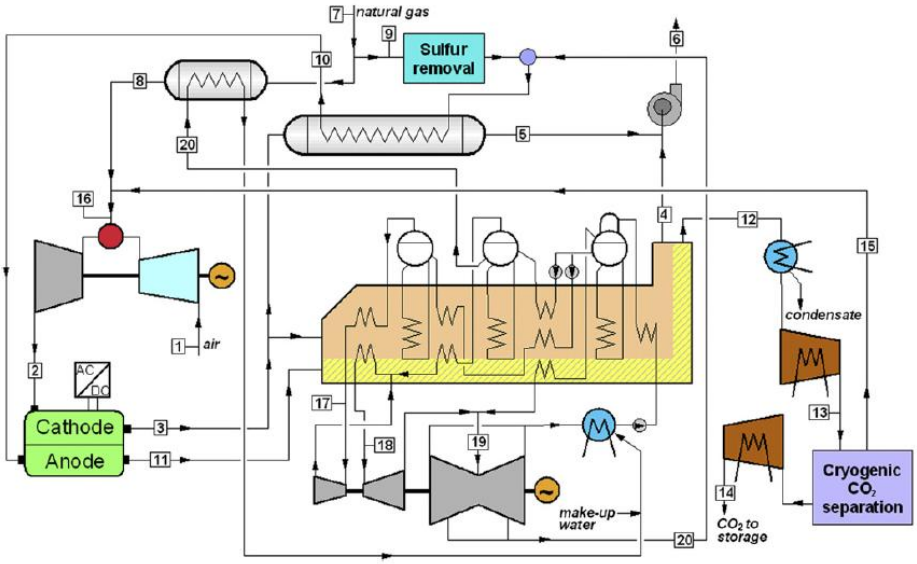

Fig. 2.5 Plant layout of MCFC combined gas cycle with cryogenic chamber.[16]

2.4.3 125 kW MCFC's operation results [B. Kim et al. (2012)]:

In 2012, Kim et al. [17] conducted a series of test experiments on 125 kW unit MCFC module at Boryeong thermal power plant in Korea. The models name was KPCFC125 manufactured by KEPCO (Korea Electric Power Corporation). This MCFC unit consisted of 200-unit cells and covered an area of 10000 cm^2.This unit was operational for a testing period of December 2009 to March 2010.From their tests it was confirmed that the stack showed an open circuit voltage of 214 volts while producing a maximum of 120 kW DC output power. Fig. 2.6 shows the schematic layout of the 125-kW unit MCFC model while Fig. 2.7 shows the exterior of the KPFCFC125 module and Fig. 2.8 shows the MCFC stack of KPFCF125.

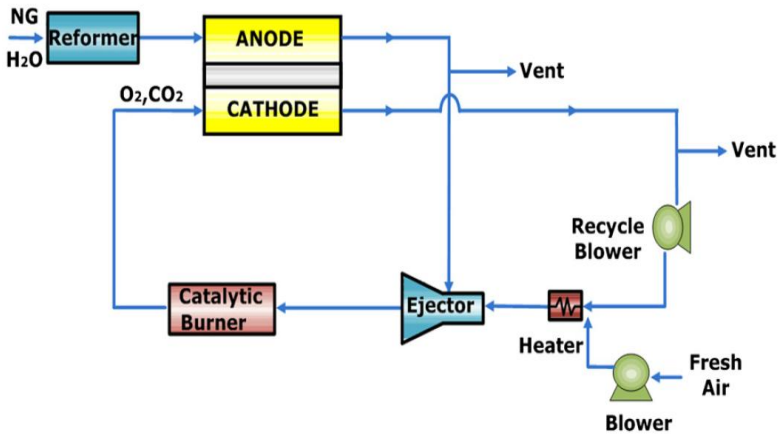

Fig. 2.6 Schematic layout of 125 kW KPFCF125 module.[17]

Fig. 2.7 Exterior outlook of KPFCF125.[17] **Fig. 2.8** MCFC stack of KPFCF125.[17]

2.4.4 Integration of MCFC as a CO_2 separation unit from flue gases [J. Milewski and J. Lewandowski (2012)]:

In 2012, Milewski and Lewandowski [18] made some analysis on the perspective of combining MCFC with Coal fired power plant in order to reduce CO_2 being emitted from the said power plant. In their analysis they placed the MCFC in between the gas streamer of the coal fired boiler where flue gases pass through. With this arrangement they tried to gain better system efficiency to gain more electrical power and reduce CO_2 at the same time. From their analysis it has been observed that 56% of the CO_2 can be reduced from the total emitted CO_2 from the coal fired plant with the use of MCFC. In their work they had also collected data for three different scenarios which were the maximum number of efficiency, maximum number of CO_2 being reduced and lastly the optimal variant. From their analysis they were able to conclude that up to a maximum of 70 percent of CO_2 can be reduced while maintaining an electrical efficiency of about 40% at max.

2.4.5 Potential of MCFC in reducing carbon emission [D. Sánchez et al. (2014)]:

In 2014, Sánchez et al. [19] published his research work on the potential of MCFC. In his research he compared MCFC in different scenarios which were the performance of conventional source without carbon capture(CC), conventional source with chemical absorption and conventional source with MCFC. For each instance he has shown that MCFC yields better result when combined with a conventional source based power plant. From his study it is also apparent that even when the capture efficiency is lower than that of the conventional source MCFC still holds many advantages over the power management. In his paper he has also shown a figure representing how the carbon capture in MCFC works which has been shown below in Fig. 2.9:

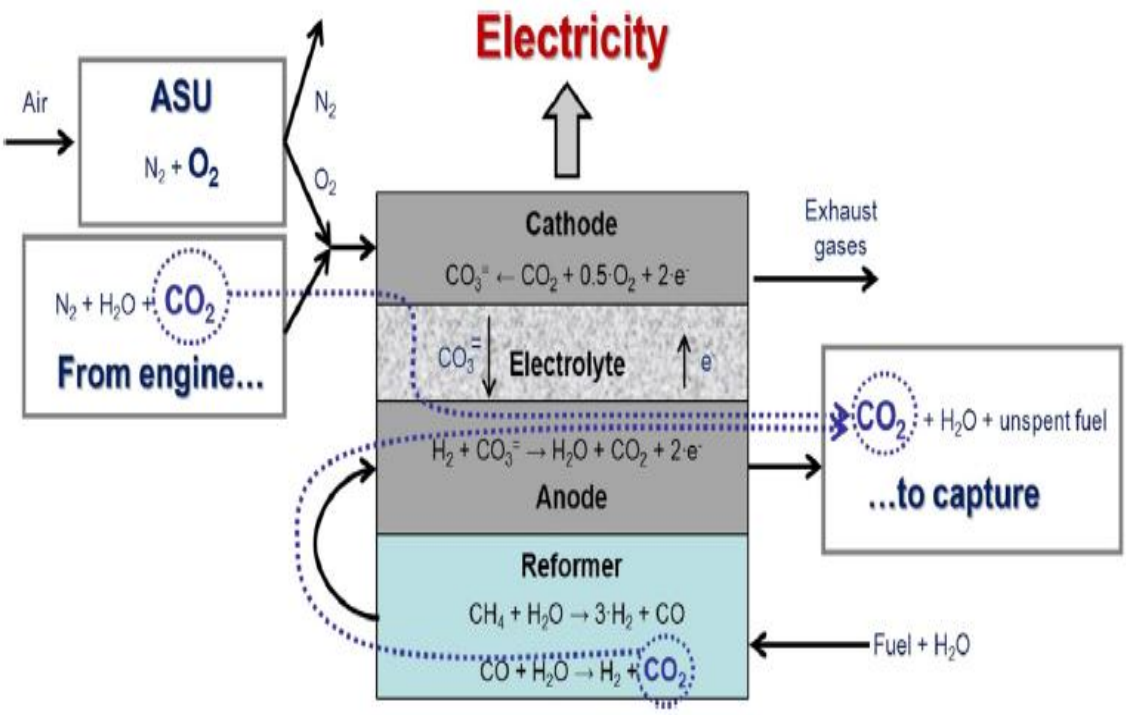

Fig. 2.9 Flow diagram of MCFC for CC.[19]

2.4.6 4E analysis and multi-objective optimization of MCFC [A. H. Mamaghani et al. (2015)]:

In 2015, Mamaghani et al. [20][21] developed mathematical models in order to analyze four different scenarios of MCFC combined with gas cycle which they dubbed 4E analysis. The 4E analysis included comprehensive energetic, exergetic, economic and the environmental evaluations. In their study they included an organic ranking cycle(ORC) which from their study shows that it grants a Significant 5% efficiency boost to the exergetic efficiency. Furthermore, they had also developed a multi objective optimization method which was simultaneously calculated considering economic and exergetic relations in order to provide an optimal solution. From their analysis it has been seen that the optimal solution brought the overall efficiency of the fuel cell to about 35.6%,44.3% and 54.9%. A sensitivity analysis was also conducted to investigate the effect of variation in economic parameters, the fuel unit cost and interest rate, on the Pareto optimal solutions. The algorithm used in order to develop this multi objective optimum solution has been given in Fig. 2.10:

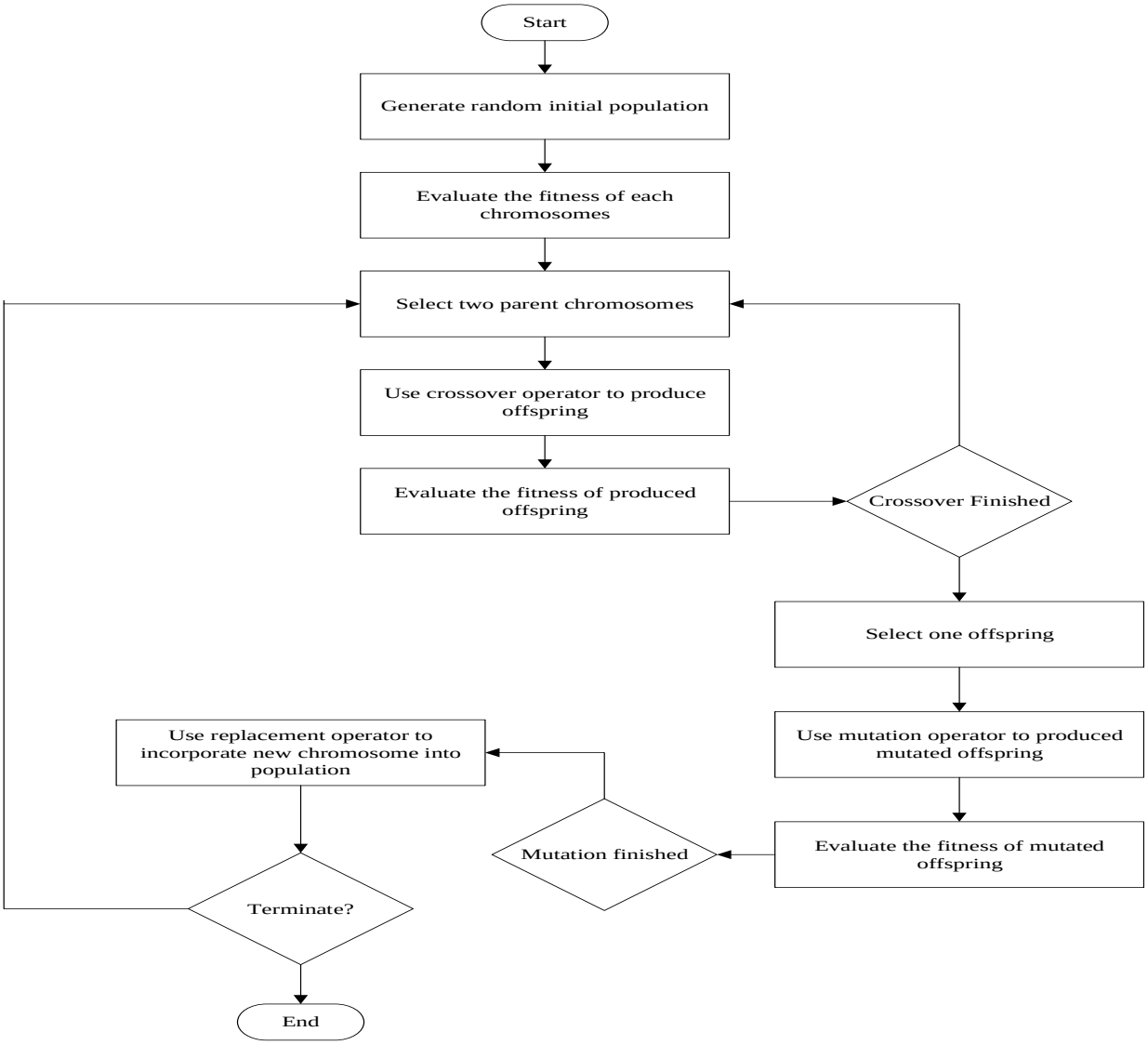

Fig. 2.10 Flow chart of multi objective optimization algorithm.[20]

2.4.7 Study of MCFC integrated with coal fired power plant [L. Duan et al. (2015)]:

In 2015, Duan et al.[22] made some benchmark on a MCFC hybrid system that did not have any CO_2 capture unit and proposed a model for that power plant with the integration of oxygen ion transfer membrane (ITM) along with a CO_2 capture unit. In order to do so they made use of the software named aspen plus [23] in which they made their model and performed a series of benchmarking for different cases such as the MCFC in its hybrid form without CO_2 capture unit, MCFC integrated with air separation unit with CO_2 capture unit and MCFC integrated with ITM with CO_2 capture unit. In Fig. 2.11 the model used for benchmarking the MCFC combined with ITM unit has been shown. From his benchmarking results it has been observed that the efficiency of the hybrid MCFC without CO_2 capture is 63.36% while the inclusion of ITM lowers the system efficiency

by 0.68% making it 62.68%. They have also concluded that increasing the ITM temperature within the permitted ranges will increase the system net efficiency.

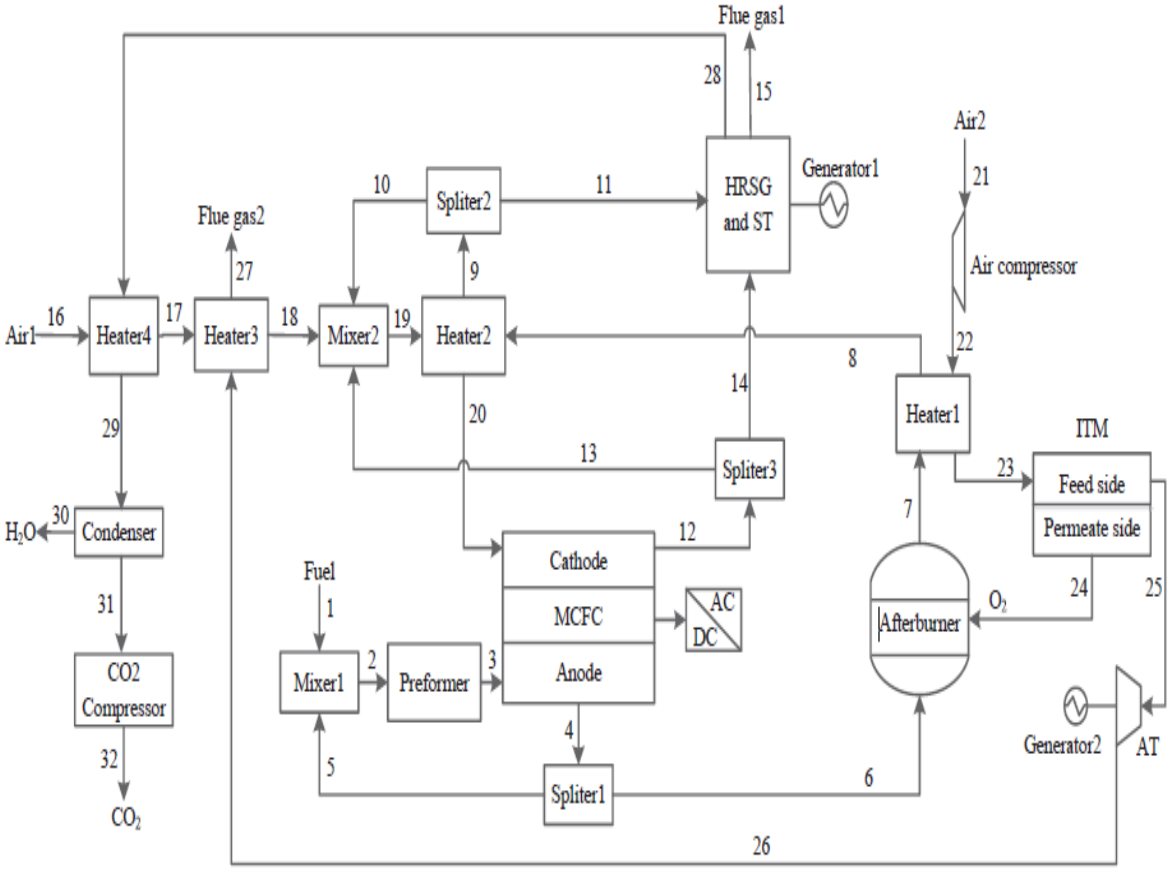

Fig. 2.11 Aspen model used for benchmarking MCFC with ITM unit.[22]

2.4.8 Analysis of MCFC integrated with an existing 250 MW coal fired power plant [S. Samanta and S. Ghosh (2016)]:

In 2016, Samanta and Ghosh[24] analysed the integration of MCFC with 250 MW already existing old coal fired power plant from the perspective of thermo-economic stance. Their proposed schematic for the repowering of an existing plant with MCFC has been shown in Fig. 2.12 from which they have observed that this configuration gives a total of 27% boost to the plant capacity while 67% of CO_2 is captured. From their analysis it also become clear that the inclusion of MCFC didn't hamper the efficiency of the plant but rather increased it by 1.1%. However, they have also entailed that the inclusion of MCFC with CO_2 capture unit does increase the cost per kW production. They have summed up that the value of cost of electricity(COE) is increased by 46% in comparison to the COE of the conventional power plant. The tool they used for the production of this model was cycle tempo software.

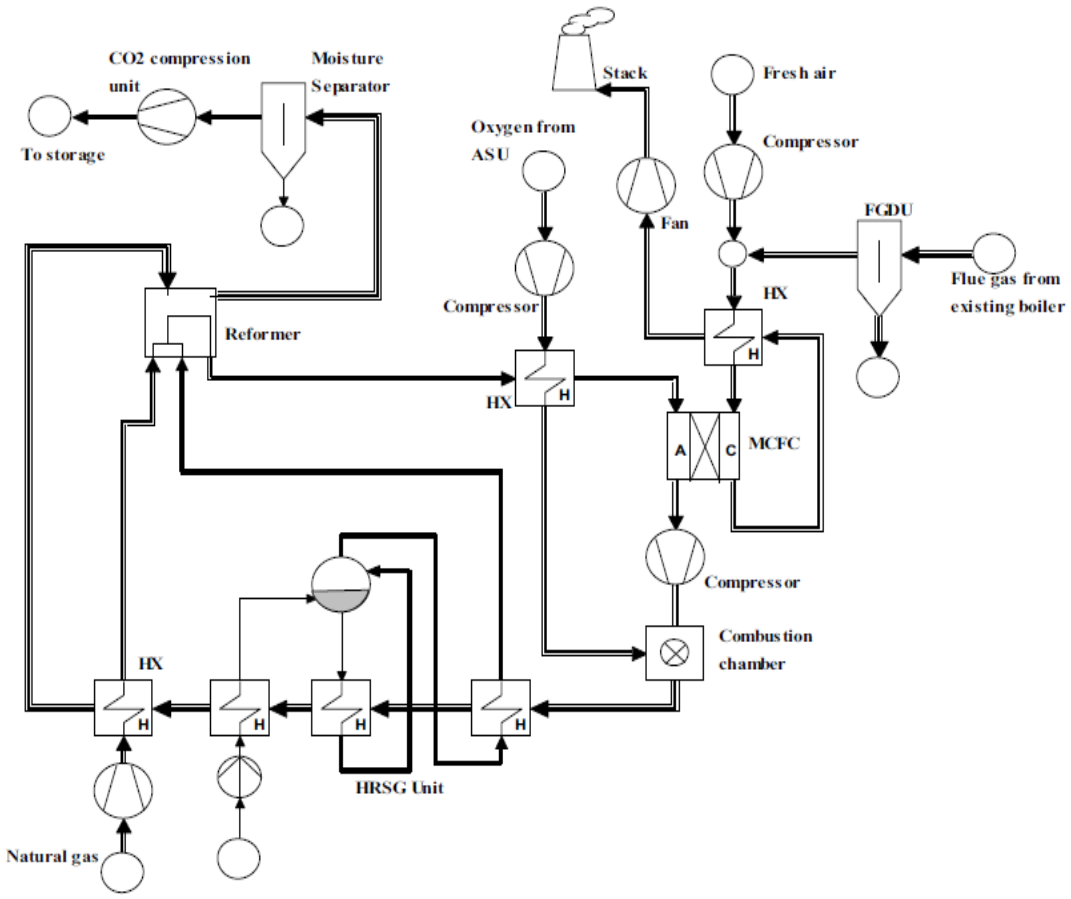

Fig. 2.12 Schematic of MCFC with existing plant used for thermos-economic analysis.

2.5 Summary:

From previous study it can be concluded that MCFC holds a huge potential in both reduction of CO_2 as well as producing power from it. As seen from above research works it is also safe to assume that the electrical efficiency of this system is around 40-50% while its CO_2 reduction capability is around 70%. But due to the involvement of carbon capture mechanism involved in MCFC, the overall price of these systems are quite a lot. But this is a small price to pay in order to save the environment. As one of its most beneficial aspect is that it can make existing power plants to run in an environment friendly nature.

CHAPTER 3

METHODOLOGY

3.1 Introduction

In this section we have used MATLAB Simulink and Comsol as helping tool for our analysis. The process involved in developing these models in their respective software has been shown with proper explanation and figures. Here we have built a model in Simulink which can give output regarding voltage, current, power by varying the cell number. While in the Comsol section we have analysis the gas diffusion layer of the gases.

3.2 Build of MCFC stack:

MCFC block in Fig. 3.1 is generated in Simulink by using the following equation [24]. Here, resistance loss of MCFC is neglected.

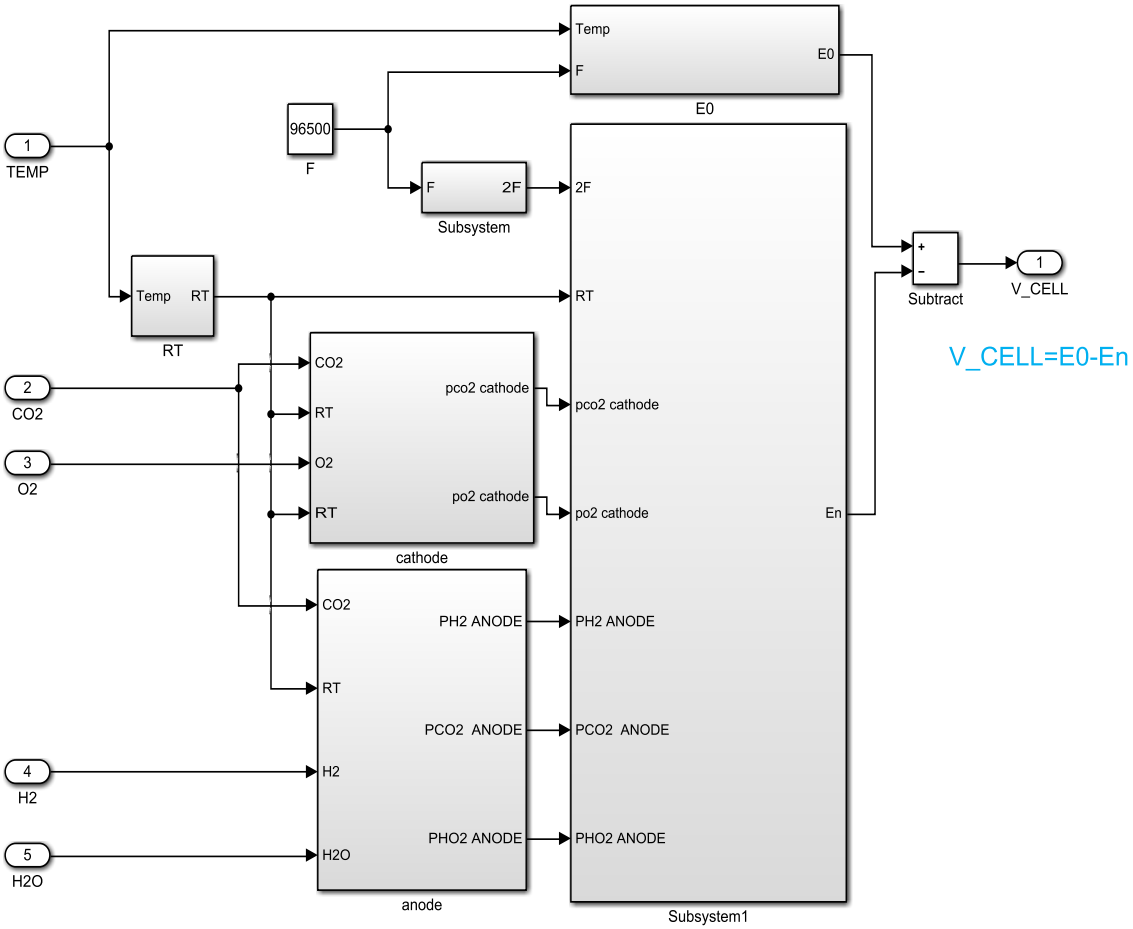

Fig. 3.1 Internal view of the MCFC stack

Where,

$P_{H_{2,an}}$ = Partial pressure of H_2 in anode side

$P_{H_{2,ca}}$ = Partial pressure of H_2 in cathode side

$P_{CO_{2,Ca}}$ = Partial pressure of CO_2 in cathode side

$P_{CO_{2,an}}$ = Partial pressure of CO_2 in anode side

$P_{O_{2,an}}$ = Partial pressure of O_2 in anode side

$P_{O_{2,Ca}}$ = Partial pressure of O_2 in cathode side

$P_{H_{2,Oan}}$ = Partial pressure of H_2Oin anode side

$P_{H_{2O,Ca}}$ = Partial pressure of H_2O in cathode side

T_{cell}= Cell temperature

F= Faraday constant

ΔG= Gibbs energy

V=Output voltage of MCFC

$$V = E^0 - E_n$$

$$E^0 = -\frac{\Delta G}{2F}$$

$$\Delta G = -242000 + 45.8 \times T_{cell}$$

$$E_n = \frac{RT_{cell}}{2F} \ln\{\frac{P_{O_{2,Ca}}^{0.5} P_{H_{2,an}} P_{CO_{2,Ca}}}{P_{H_2O,an} P_{CO_{2,an}}}\}$$

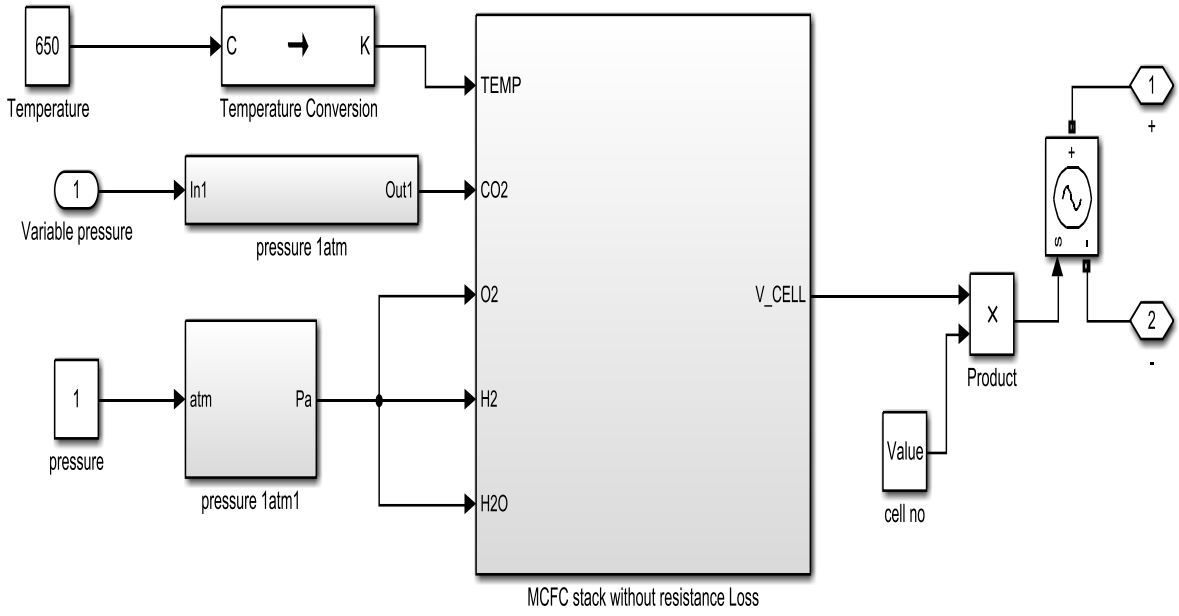

Fig. 3.2 Simulink Model of MCFC by using partial pressure equation

Here we designed the MCFC stack shown in Fig. 3.2 which has been done in MATLAB Simulink without the resistance loss. Where we supplied the temperature, pressure of the CO_2. Again, we keep the pressure of O_2, H_2, and H_2O fixed at 1 atm.

The internal view of the MCFC stack as like as above Fig. 3.2. Where we have the following section-

- Anode side
- Cathode side
- Subsystem 1
- E°

The output of the cathode and anode sides enters into the subsystem 1. Then with the addition of the out of the E° and subsystem 1, we have the output of the MCFC stack.

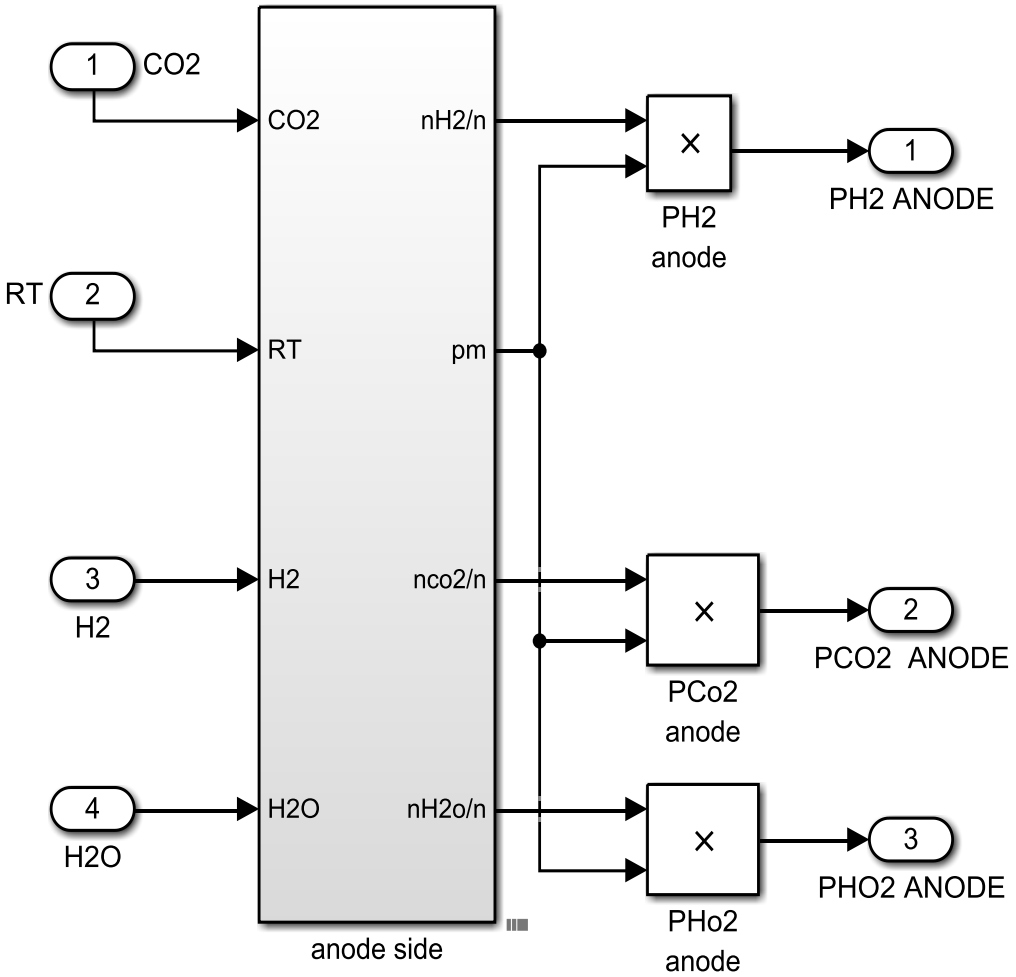

Fig. 3.3 Internal view of the anode side of the MCFC stack

Above Fig. 3.3 shows the internal view of the anode side of the MCFC stack. In the anode side we supply the pressure of CO_2, H_2 and H_20 and product of R and T as an input and after that we have output as

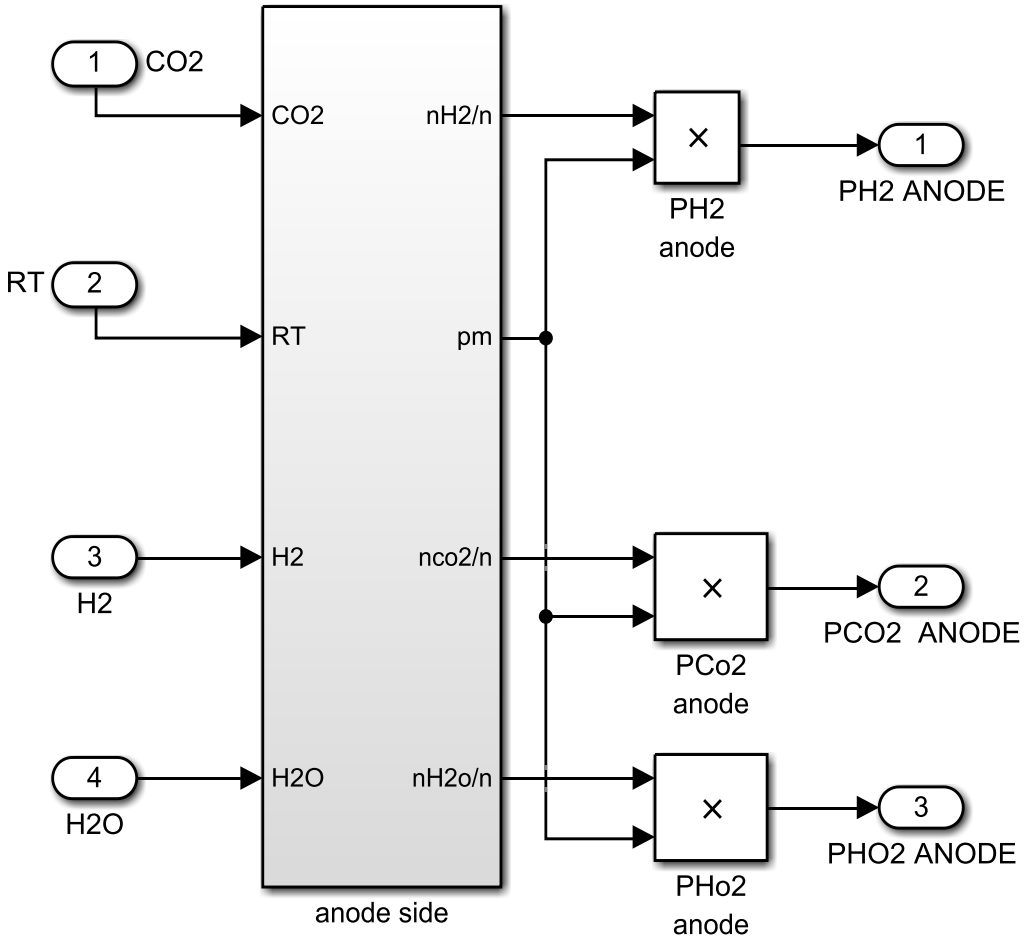

Fig. 3.4 Internal view of the cathode side of the MCFC stack

Above Fig. 3.4 shows the internal view of the cathode side of the MCFC stack.

Where input RT, O_2, CO_2

Output P_{CO2}, cathode, P_{O2} anode.

3.3 Carbon Capture Unit:

Amount of CO_2 supply = $0.0085 \times P^2 + 6.5 \times p + 15$ Kg/hr

Using the above equation Carbon supply block in Fig. 3.5 is generated. That supply the carbon from the power plant.

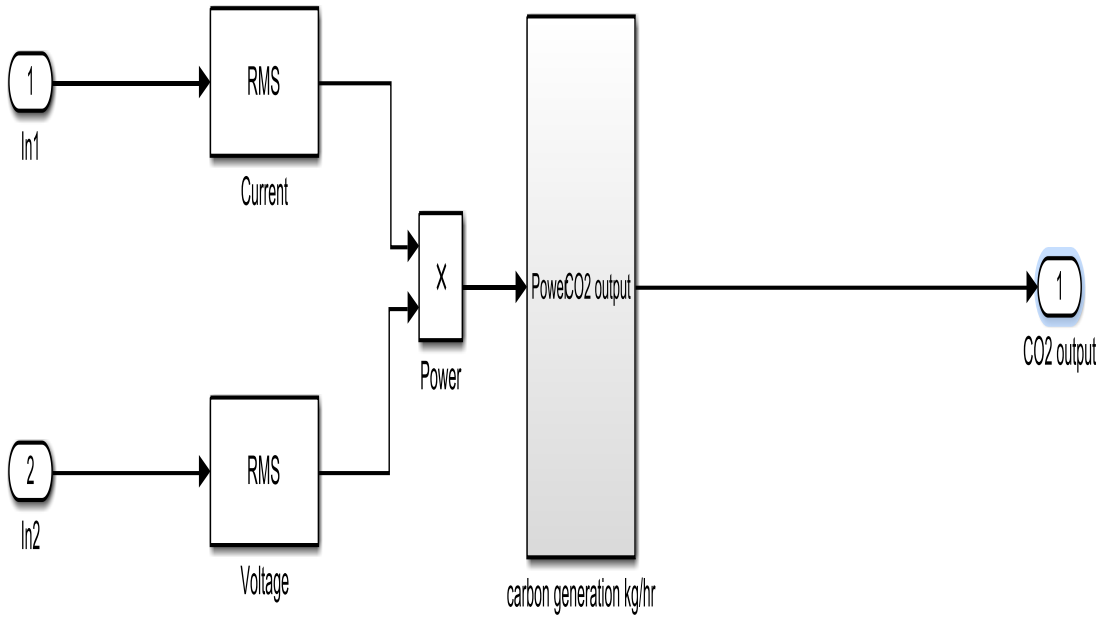

Fig. 3.5 Internal view of the carbon supply unit

This unit generate the CO_2 which a power plant generates in one hour. Where inputs are rms value of the current and voltage which gives the power. That power supplies to the carbon generation block that gives the output Kg/hr has been shown in Fig. 3.6

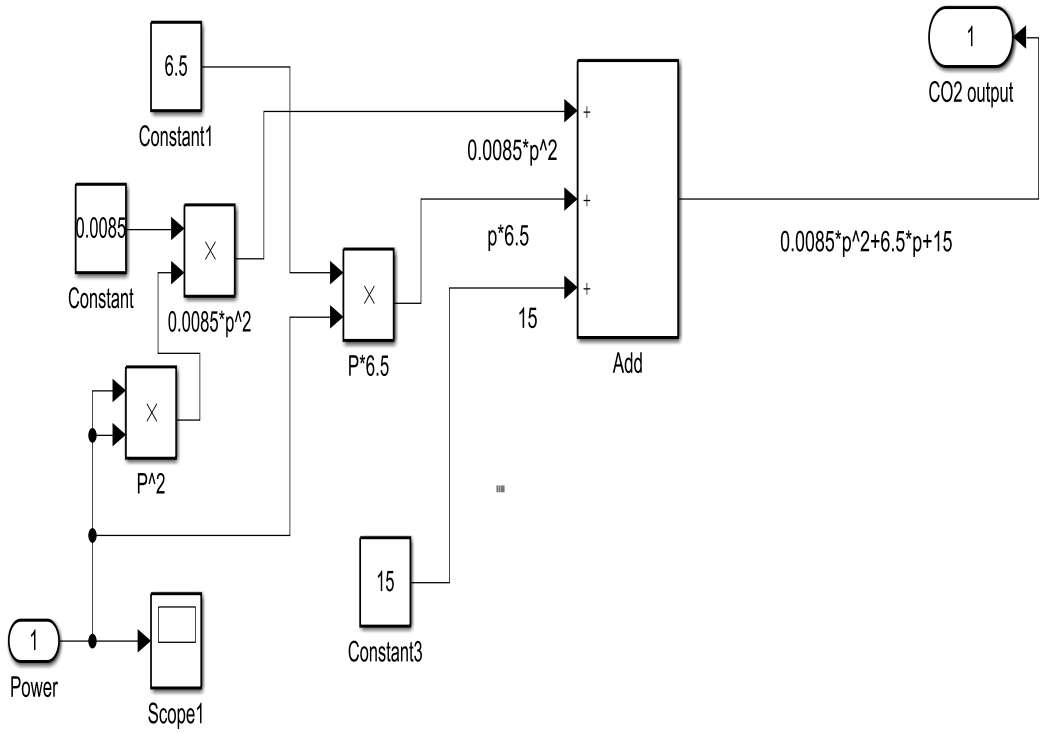

Fig. 3.6 Internal view of the Carbon generator unit

3.4 Connection for DC to AC conversion:

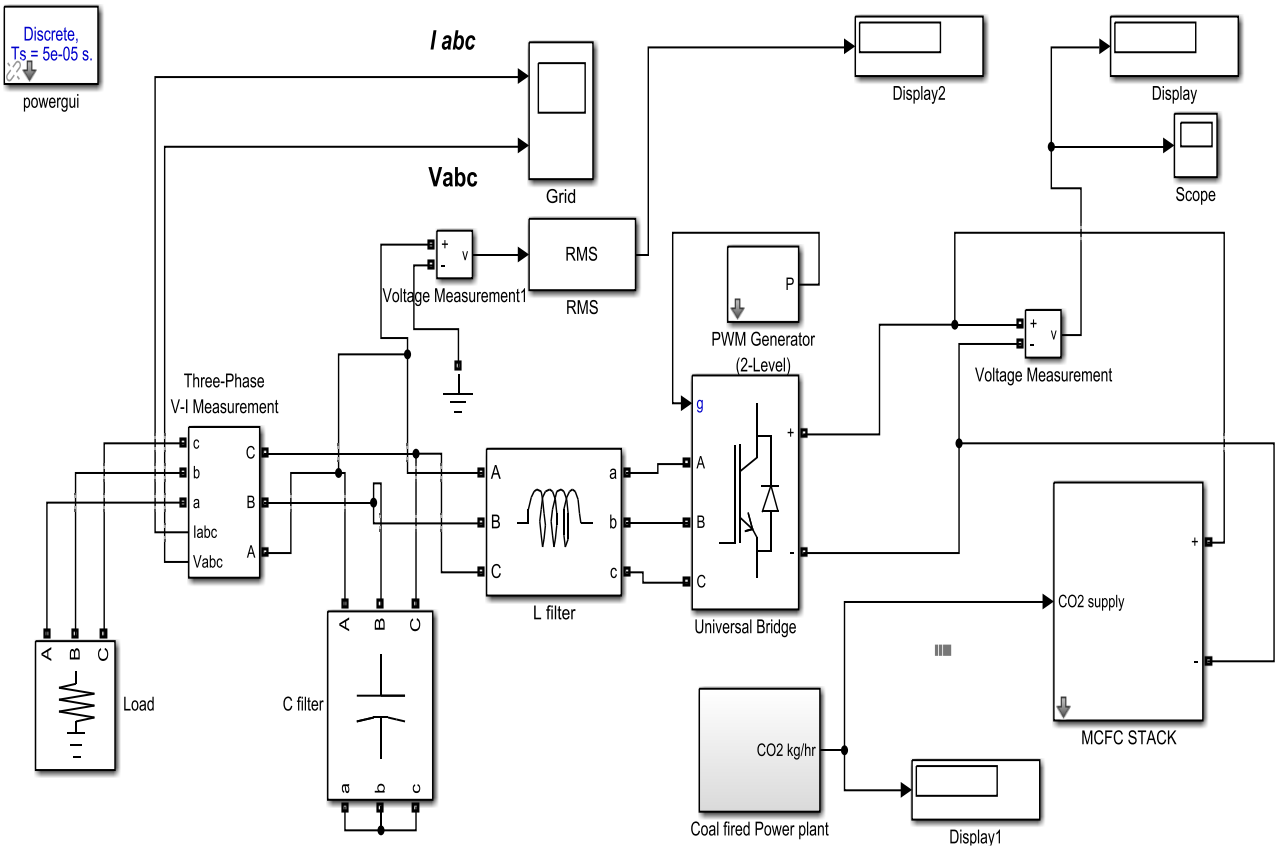

Fig. 3.7 Simulink model to observe the ac and dc output voltage with the variation of cell number

The output terminal of MCFC block is connected with the universal bridge that actually IGBT. Then the output of the IGBT (Insulated-gate bipolar transistor) is connected with the L filter block where the value of the inductance 2.97 micro henry. Three phase capacitance branches (capacitance is 5.33e-5 Faraday), R load (Nominal phase to phase voltage 220V and nominal frequency 50 Hz) and three phases VI measurement block are connected in parallel. Here the PMW generator 2 level pulse is the basically three phase bridge (6 pulse) type generator which operates in unsynchronized mode and its frequency 50 Hz. The three-phase output taken from the scope as shown in the above Fig. 3.7.

3.5 Gas diffusion layer of MCFC using Comsol:

Here a model has been built using Comsol software in order to observe the species transport in gas diffusion layer of a MCFC. Here the geometry for the model was built with two adjacent flow channels consisting of different pressure. In Fig. 3.8 the model used has been represented. For this model the following equations were used in order to determine the MCFC's internal behaviour:

- the current balance,
- Maxwell Stefan diffusion equation [25] and
- Darcy's law for the gas flow [25]

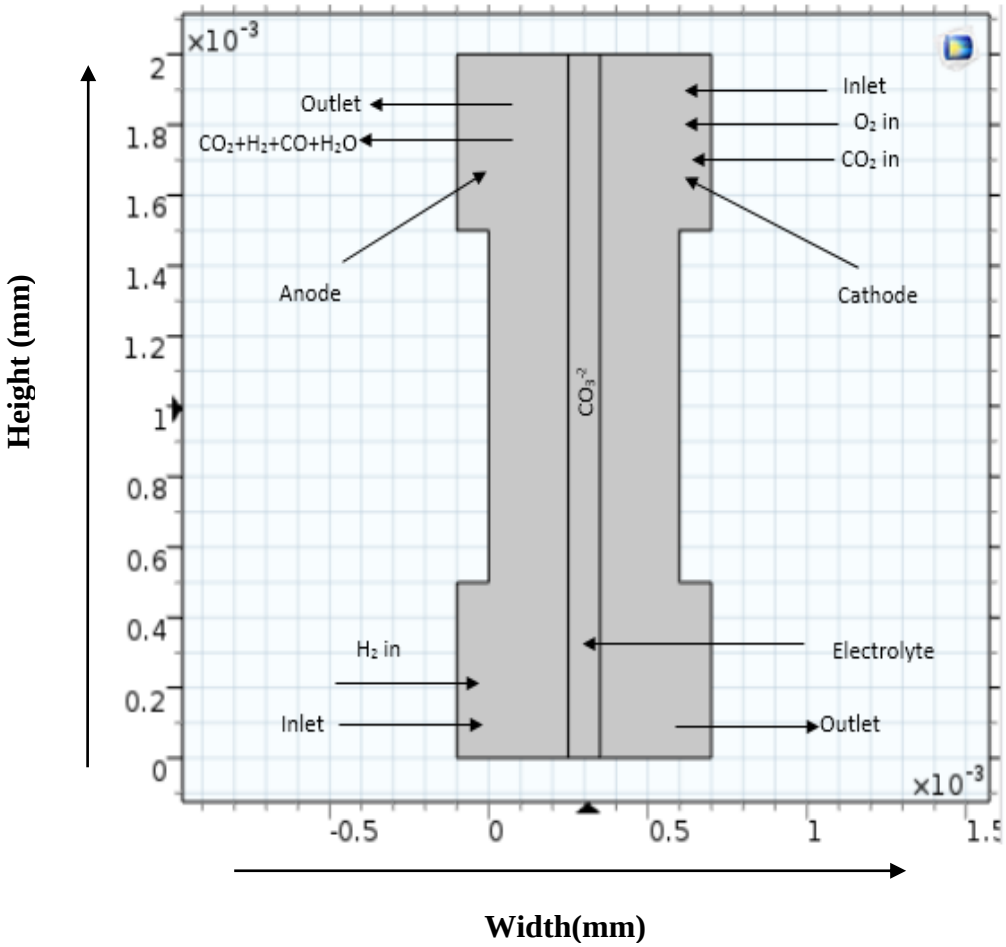

Fig. 3.8 Analysis of Gas diffusion layer in MCFC using Comsol.

3.5.1 Parameters used in model:

kappa_s = Conductivity, solid phase

kappa_m = Conductivity, membrane

V_cell = Cell voltage

T = Temperature

kappa_p = GDL permeability

eta = Fluid viscosity

p_ref = Reference pressure

p_a_in = Anode inlet pressure

p_c_in = Cathode inlet pressure

drag = Proton-Water drag coefficient through membrane

E_eq_a = Equilibrium potential, anode

E_eq_c = Equilibrium potential, cathode

i0_a = Exchange current density, anode

i0_c = Exchange current density, cathode

S = Specific surface area

R_agg = Aggregate radius

eps_mic = Microscopic porosity inside agglomerates

eps_mac = Macroscopic porosity between agglomerates

D_agg = Effective diffusion coefficient inside agglomerates

$D_{eff}H_2\_H_2O$ = Effective binary diffusivity, $H_2\_H_20$

$D_{eff}O_2\_CO_2$ = Effective binary diffusivity, $O_2\_CO_2$

$D_{eff}H_2O\_CO_2$ = Effective binary diffusivity, $H_2O\_CO_2$

$D_{eff}O_2\_H_2O$ = Effective binary diffusivity, $O_2\_H_2O$

wH_2_in = Inlet weight fraction H_2

wO_2_in = Inlet weight fraction O_2

wH_2Oc_in = Cathode inlet weight fraction, H_2O

MH_2 = Molar mass, H_2

MO_2 = Molar mass, O_2

MH_2O = Molar mass, H_2O

MCO_2 = Molar mass, CO_2

xH_2_in = Inlet molar fraction, H_2

KH_2 = Henry's law constant, H_2 in agglomerate

KO_2 = Henry's law constant, O_2 in agglomerate

cH_2_ref = Reference concentration, H_2

cO_2_ref = Reference concentration, O_2

l_act = Active layer thickness

xO_2_in = Inlet molar fraction, O_2

K = Agglomerate current density subexpression

3.5.2 Model design:

In order to make this model three domains were created in Comsol which are:

- An anode (Ω_a)
- A cathode (Ω_c) and
- A proton exchange membrane (Ω_m)

For this model the height and width for the electrode were considered as 2mm and .25mm respectively. Also, the collector height was considered as 1mm.

Here, there are many contact points in the electrode and each of contacts are interconnected with a gas distributor. This gas distributor has an inlet ($\partial\Omega_{a,inlet}$),outlet ($\partial\Omega_{a,outlet}$) and a current collector ($\partial\Omega_{a,cc}$) channel. This configuration is same for both cathode and anode. In the cathode side flow of CO_2 and O_2 are inserted while in the anode side flow of H_2 is inserted.

3.6 Summary:

The main target of this thesis was to make the existing power plants environment friendly. In order to do so a hybrid power plant has been considered for this aim. A complete Simulink model of hybrid power plant has been represented here. For the purpose of building this hybrid power plant a MCFC has been used here which has been built in both Matlab Simulink and Comsol. So, in this section both the Simulink and Comsol models has been explained in details with their respective figures.

CHAPTER 4

RESULT AND DISCUSSION

4.1 Introduction

In this section we have shown all the results of our research. Here both economical and analytical portions regarding MCFC has been shown. Including the cost needed to build the system, space required and how many houses can be supplied with electricity using this system. In the analytical portion results regarding MATLAB Simulink and Comsol has been shown.

4.2 Results of Comsol analysis:

4.2.1 Current density in electrode of MCFC:

Using comsol the current distribution in a cell of MCFC has been represnted in Fig. 4.1 where the left side is anode and the right side is cathode.It can be observed from the plot that there are significant concentration of spikes at the corners of the current collectors.This cell is operating at 0.7 V.

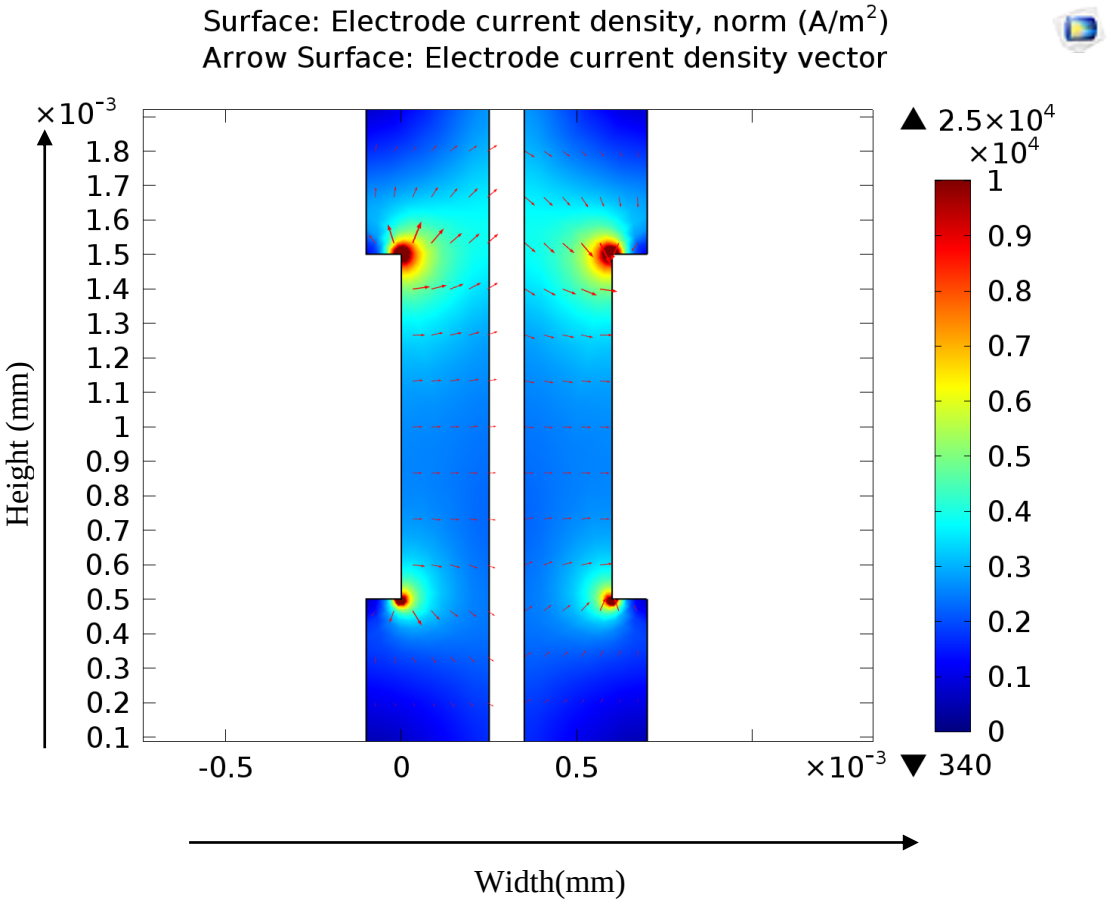

Fig. 4.1 Current density analysis of MCFC.

In order to better understand the cell's behaviour further analysis has been made by plotting the current density distribution at the active layer of the anode side. The results of which has been shown in Fig. 4.2.

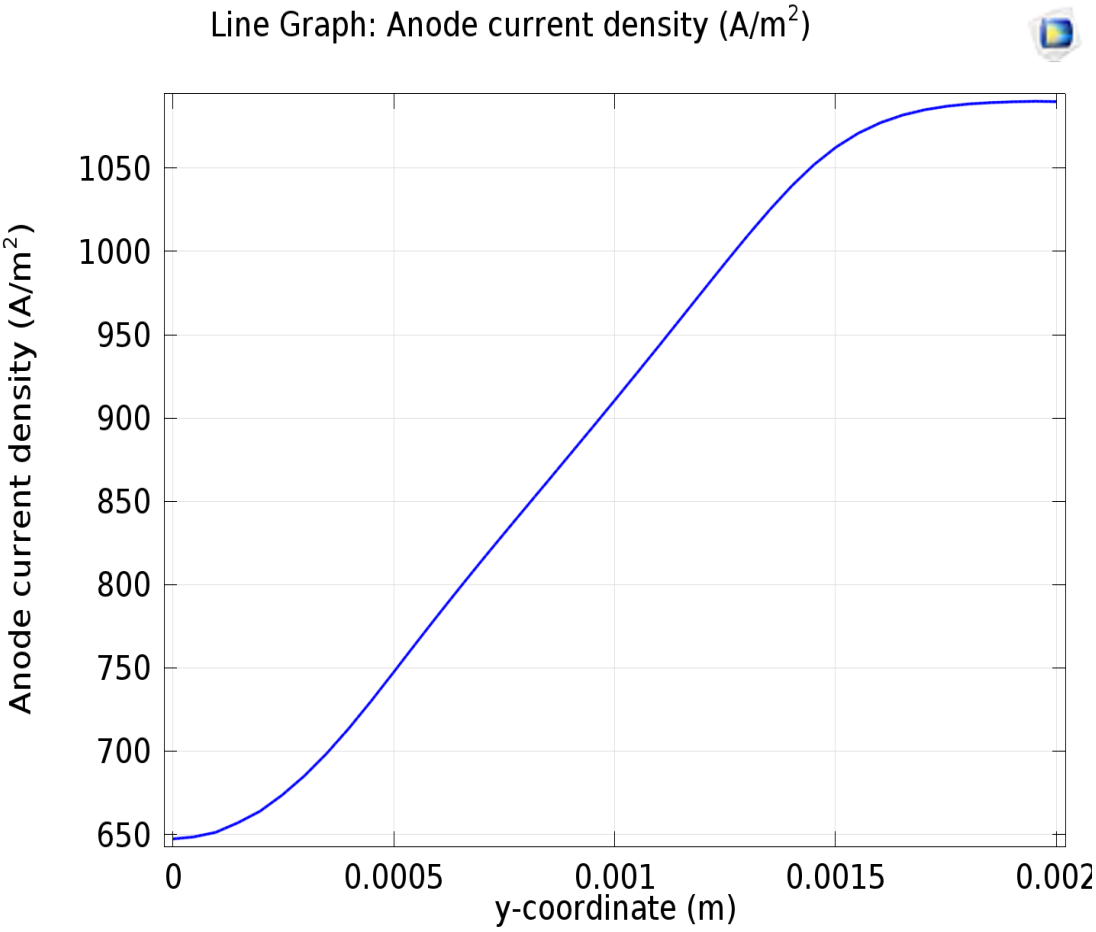

Fig. 4.2 Anode current density distribution

It can be seen in Fig. 4.2 that the current density is not even with the highest density in the cell's upper region which means that the reaction rate of the oxygen reduction in the cathode side determines the distribution of current density. From this we can also conclude that at the air inlet the maximum current density arises. Here value of current density found at anode ranges from 650 to 1050 A/m^2 which can be verified from the works of Brenna et al. [26] where they have also found quite similar results.

4.2.2 Analysis of gas flow behaviour using Darcy's law:

Generally, convective fluxes denominate mass transport in the cell. A plot has been shown in Fig. 4.3 of gas velocity field in both the anode and cathode side. This has been plotted in order to understand the convective effects in the cell. From the plot it can be

seen that at current collector corners the highest values of flow velocity magnitude is attained.

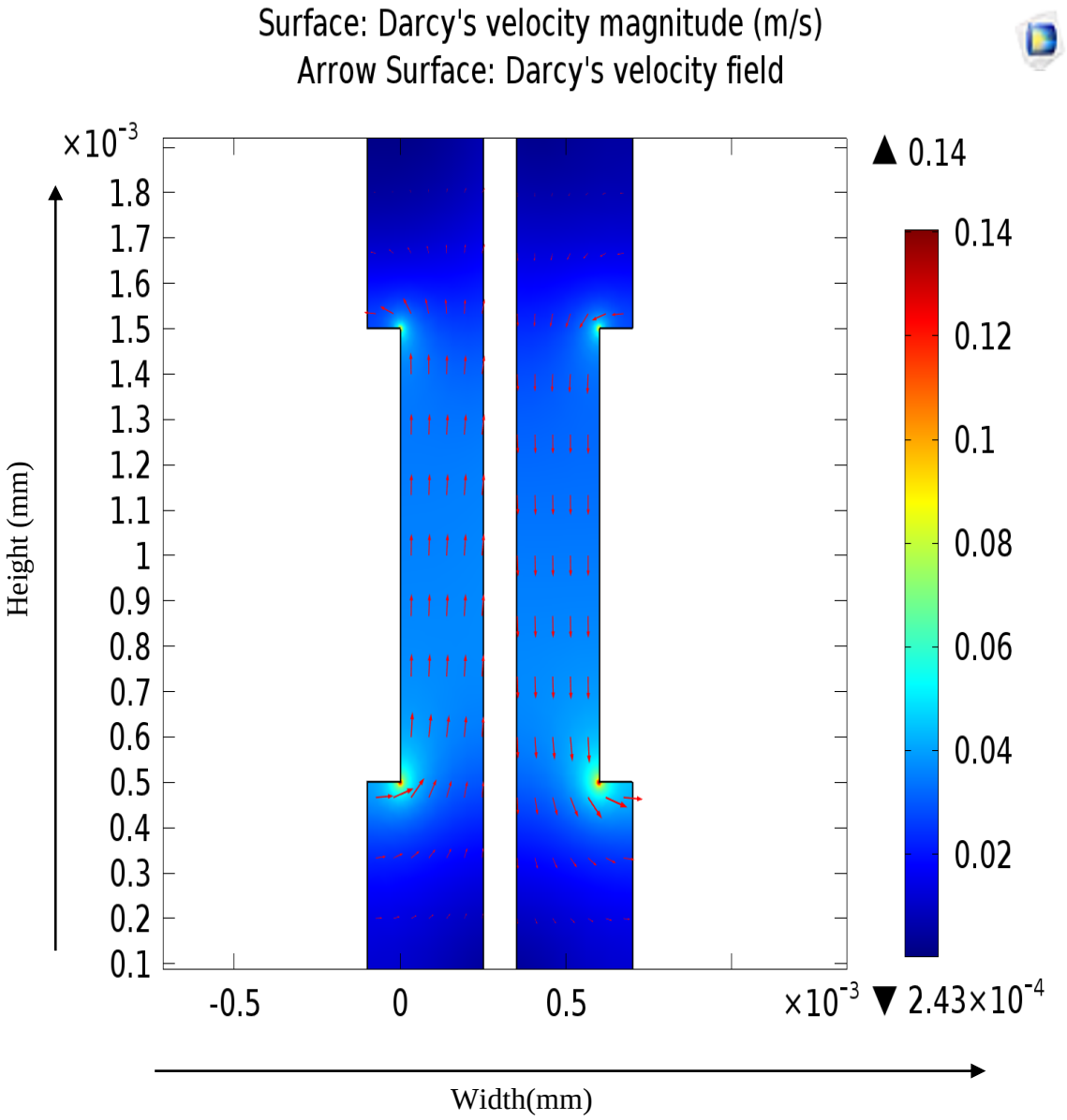

Fig. 4.3 Field velocity of gas in the cathode and anode.

Another analysis has been shown in Fig 4.4which represents the reactants H_2 and O_2's weight fraction for both cathode and anode side gases. In Fig. 4.4 the reactant in the anode side is H_2 while on the cathode side the reactant is O_2. From the plot on the anode side it can be observed that hydrogen fraction increases from the inlet at the bottom to the outlet of the upper side This happens due to osmotic drag of water the electrode which means a higher number flux is produced than the consumption of hydrogen. While on the cathode side there is a decrease in O_2 content in the direction of flow.

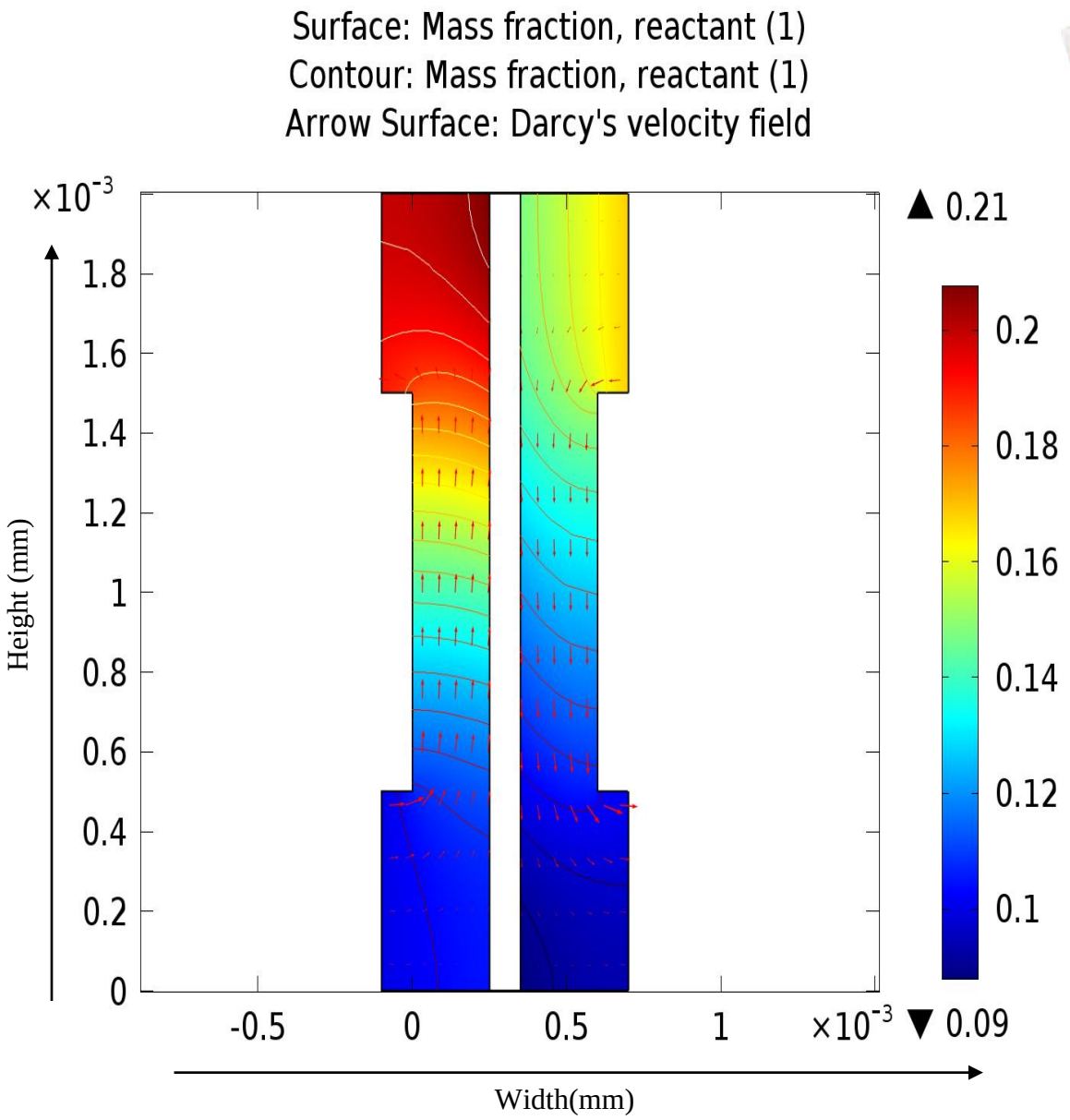

Fig. 4.4 Mass fraction of reactants using Darcy's law.

Although oxygen consumption is small, the concentration over-voltage in the agglomerates gives a substantial contribution to the concentration over-voltage. A small change in the oxygen flow gives a substantial change in cell polarization. Fig. 4.4 depicts the water mass fraction in the anode and cathode gases as well as the diffusive flux of water in the anode. It is apparent that water is transported through both diffusion and convection to the membrane on the anode side. The results show a minimum occurring in the upper corner of the membrane on the anode side. This is known to limit fuel cell performance. If the anode gas becomes too dry, the membrane dries out, resulting in decreasing ionic conductivity and the cell subsequently fails. On the other hand, on the

cathode side water levels increase with the direction of flow, and a local maximum in water current occurs in the lower corner to the membrane. This might also be critical because water droplets can clog the pores and effectively hinder gas transport to the active layer.

4.3 Output characteristics of MCFC stack:

The output of the MCFC stack with the variation of cell number is shown in the following Table 4.1-

Table 4.1: Output results of MCFC in relation to cell number

Sl	Number of cell	voltage output V_{DC}(V)	Current output I_{DC}(A)	Power output P_{DC}(kW)	Efficiency %
01	65	49.47	265.82	13.15KW	0.174
02	75	57.09	306.71	17.51KW	0.23
03	85	64.7	347.60	22.49KW	0.298
04	100	76.11	408.88	31.12KW	0.412
05	150	114.2	613.13	70.02KW	0.927
06	200	152.2	817.94	124.49KW	1.64
07	250	190.3	1022.12	194.51KW	2.58
08	300	228.3	1225.89	280.1KW	3.71
09	500	380.6	2044.14	0.778MW	10.30
10	1000	761.1	4086.20	3.11MW	41.19

From the above table 4.1 it is clear that as the cell number increases the output DC voltage V_{dc}, DC current I_{dc} and DC power P_{dc} also increases. Here we have the maximum V_{dc}, I_{dc}, P_{dc} at cell number 65 and maximum V_{dc}, I_{dc} and P_{dc} at the 1000 cell number. Also by increasing cell number, it can be seen that the efficiency is also increasing. Also the maximum number of power was attained here at 1000 number of cell. So having higher number of cell also increases the MCFC performance. The increasing characteristics easily perceivable from the output curve which shown in the following subsection

4.3.1 Variation of V_{dc} with varying cell number of MCFC stack:

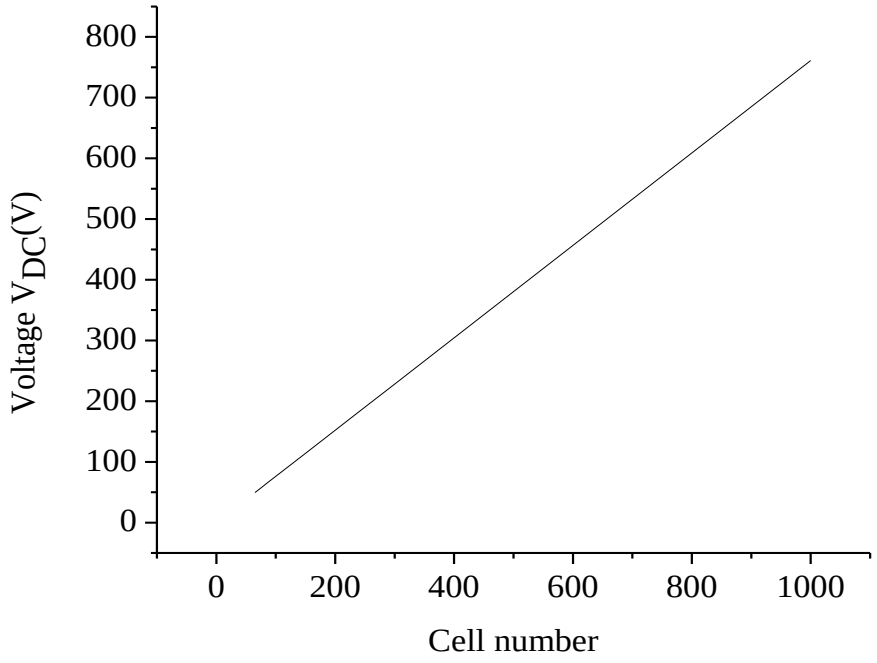

Fig. 4.5 Cell number Vs MCFC stack DC voltage

From the above Fig 4.5 it clear that, V_{dc} shows a liner relationship with the varying cell number. Whereas the cell number increases I_{dc} also increases. We have the minimum I_{dc} =265.82 A at cell number 65 and maximum I_{dc} =4086.20 A value at cell number 1000.

4.3.2 Variation of I_{dc} with varying cell number of MCFC stack:

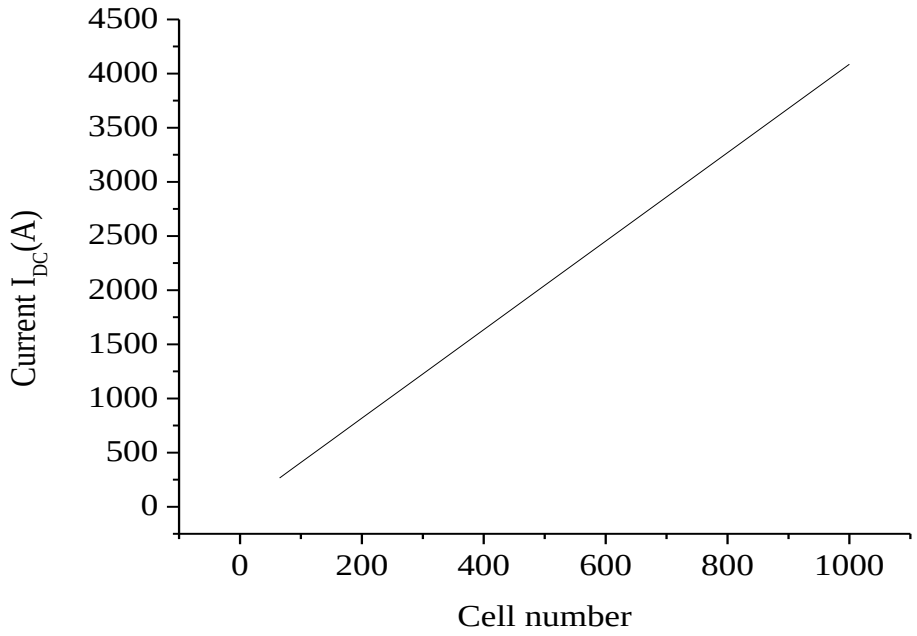

Fig. 4.6 Cell number Vs MCFC stack DC current I_{dc}

From the above Fig. 4.6 it is clear that, V_{dc} shows a liner relationship with the varying cell number. Whereas the cell number increases V_{dc} also increases. We have the minimum V_{dc} =49.47V at cell number 65 and maximum V_{dc} =761.1 V value at cell number 1000.

4.3.3 Variation of P_{dc} with varying cell number of MCFC stack:

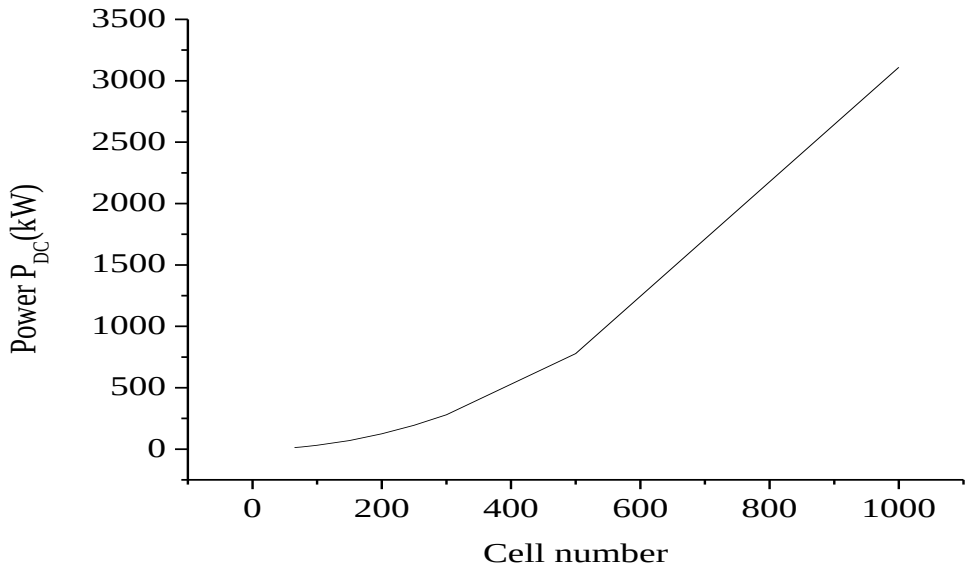

Fig. 4.7 Cell number Vs P_{dc} of MCFC stack

From the above Fig 4.7 it is clear that, P_{dc} shows an exponential relationship with the varying cell number. As the cell number increases P_{dc} also increases. Here, we minimum P_{dc}=13.15 KW at cell number 65. Again, we have maximum P_{dc}=3.11 MW.

4.3.4 Variation of efficiency with varying cell number of MCFC stack:

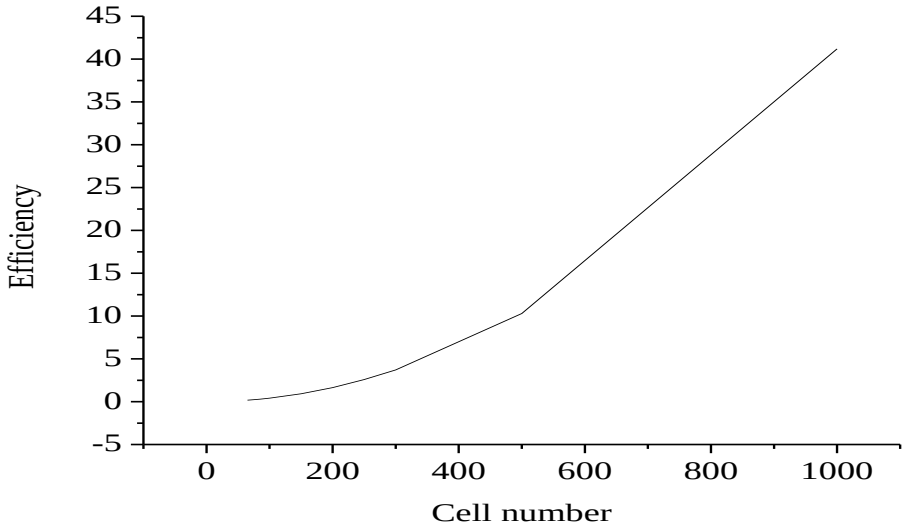

Fig. 4.8 Cell number Vs MCFC stack efficiency

From the above Fig. 4.8 it is quite clear that as the cell number increases efficient of MCFC stack also increases. That means MCFC stack efficiency shows an exponential relationship with the increasing cell number. Here, we have minimum efficiency 0.174% at cell number 65. Again, we have maximum efficiency 41.19% at cell number 1000.

4.3.5 I-V characteristics and I_{dc} Vs P_{dc} characteristics of MCFC stack:

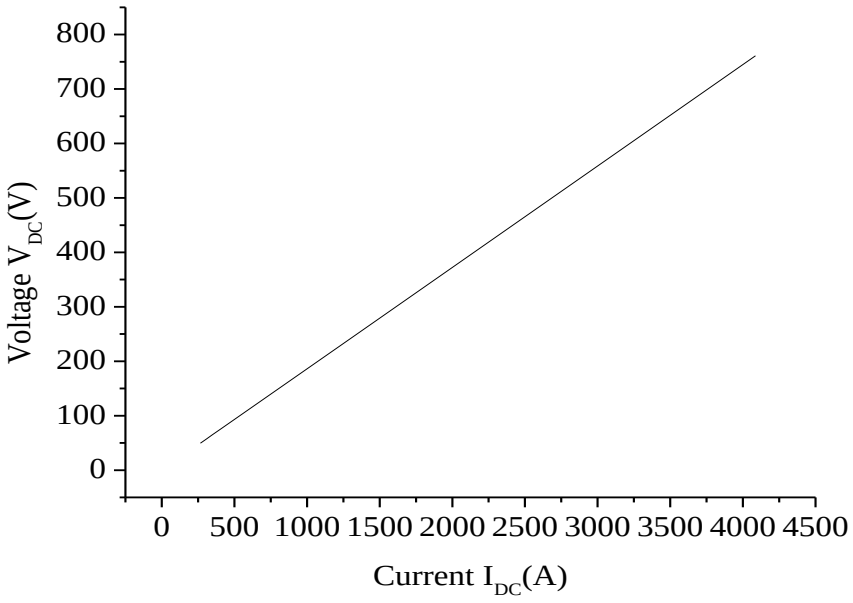

Fig. 4.9 I-V characteristics curve of MCFC stack

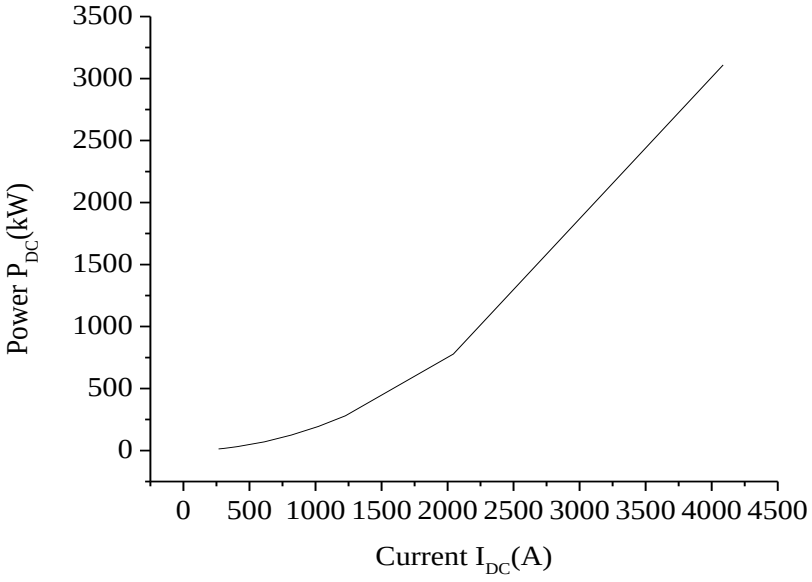

Fig. 4.10 Current vs power characteristics curve of MCFC stack

From the Fig. 4.10 it can be said I_{dc} and Vdc have a liner relationship with each other that means as the current increases voltage increases linearly with the increasing current. And again, I_{dc} and P_{dc} have an exponential relationship with each other. As the I_{dc} increases P_{dc} increases exponentially with the increasing current.

4.4 Output of inverter section for discrete time analysis:

The output results of inverter section for discrete time analysis has shown below in Table 4.2

Table 4.2: Output results of inverter section for discrete time analysis

SL	**Cell number**	**Output power P_{dc}**	**I_{rms} (A)**	**V_{rms} (V)**	**P_{ac}**
01	65	13.15KW	171.19	15.27	7.84 Kw
02	75	17.51KW	198.3	17.62	10.49Kw
03	85	22.49KW	224.8	19.97	13.47 Kw
04	100	31.12KW	264.5	23.5	18.65KW
05	150	70.02KW	396.7	35.25	41.95KW
06	200	124.49KW	528.9	47	74.57KW
07	250	194.51KW	661.1	58.75	116.52KW
08	300	280.1KW	793.4	70.5	167.80KW
09	500	0.778MW	1322	117.5	466.01KW
10	1000	3.11MW	2645	235	1.86MW

From the discrete time inverter analysis table 4.2 it can be seen that by varying the number of cell output result also increases. The current and voltage seems shows a linear characteristic while power shows an exponential characteristic. For a cell number of 1000 it can be seen that DC output power is 3.11 MW while in the inverter section this value is reduced to 1.86 MW due to loss in inversion process. As for voltage and current for a 1000 number cell, they show 235 V and 2645 A respectively. Also it can be understood from table 4.2 that higher output number can be found by having higher number of cells in a stack

4.4.1 Variation of V_{rms} with varying cell number of MCFC stack:

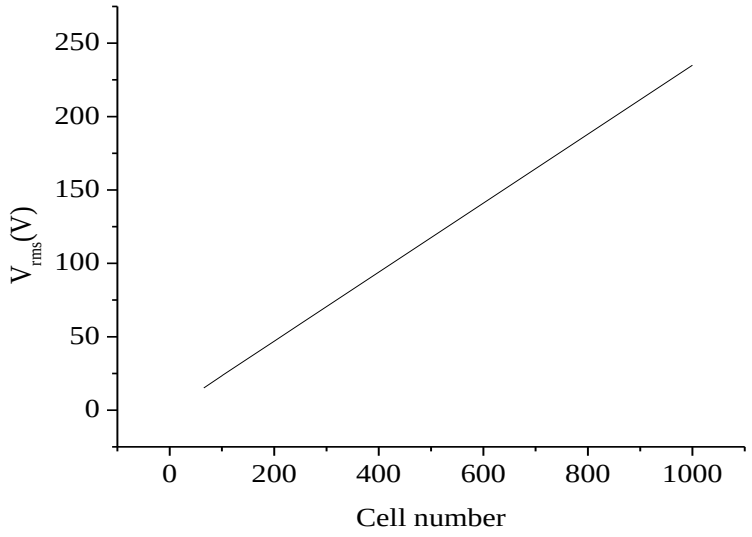

Fig. 4.11 Cell number Vs V_{rms} for discrete time inverter operation

From the above Fig. 4.11 it is clear that, V_{rms} shows a liner relationship with the varying cell number. Whereas the cell number increases V_{rms} also increases. We have the minimum V_{rms} =15.27 V at cell number 65 and maximum V_{rms} =235 V value at cell number 1000.

4.4.2 Variation of I_{rms} with varying cell number of MCFC stack:

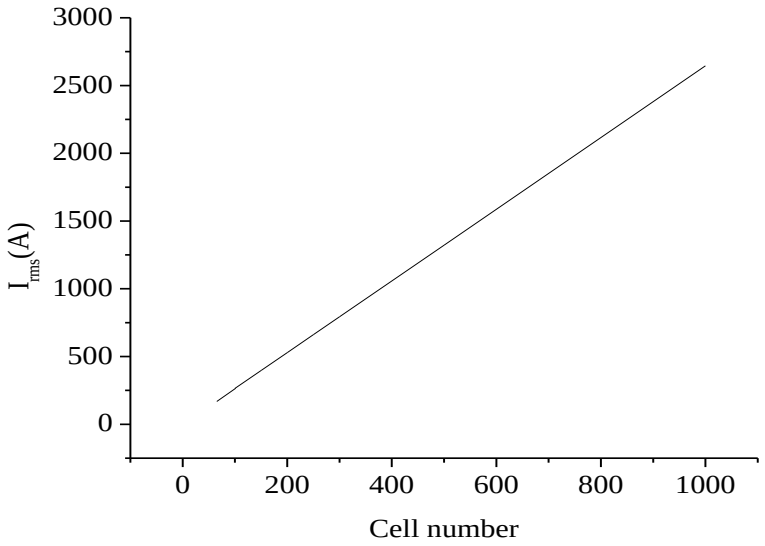

Fig. 4.12 Cell number Vs I_{rms} for discrete time inverter operation

From the above Fig. 4.12 it is clear that, I_{rms} shows a liner relationship with the varying cell number. Whereas the cell number increases I_{rms} also increases. We have the

minimum I_{rms} =171.19 A at cell number 65 and maximum I_{rms} =2645 A value at cell number 1000.

4.4.3 Variation of P_{ac} with varying cell number of MCFC stack:

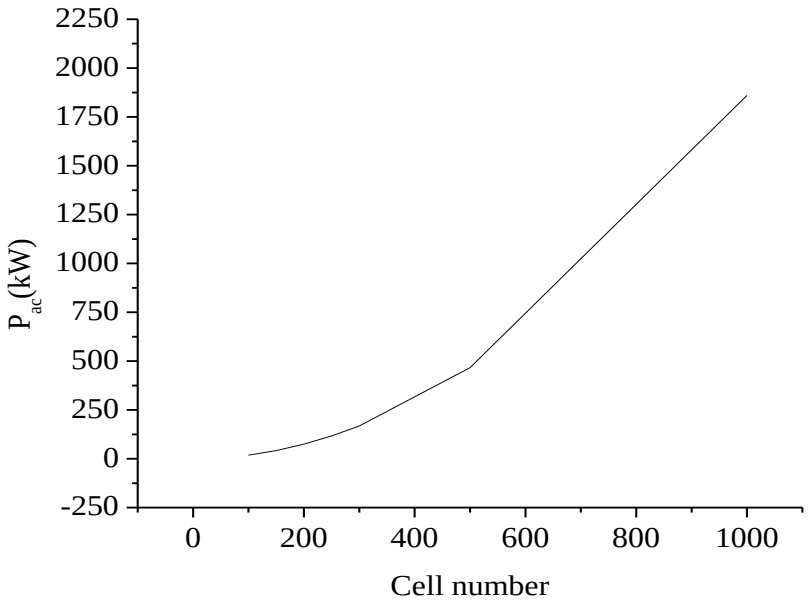

Fig. 4.13 Cell number Vs P_{ac} for discrete time inverter operation

From the above Fig. 4.13 it is clear that, P_{ac} shows an exponential relationship with the varying cell number. As the cell number increases P_{ac} also increases. Here, we minimum P_{ac}=7.84 Kw at cell number 65. Again, we have maximum P_{ac}=1.86MW.

4.4.4 Variation of efficiency of inverter with varying cell number of MCFC stack:

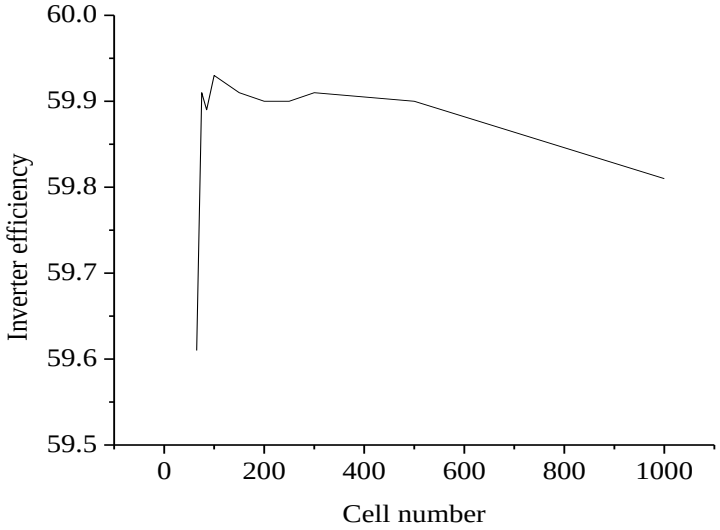

Fig. 4.14 Cell Vs inverter efficiency for continuous time operation

From the above Fig. 4.14 it is clear that, we have maximum efficiency 59.93% at cell number 150. Minimum efficiency 59.61% at the cell number 65. We have 59.81% efficiency at cell number 1000.

4.4.5 Output characteristics curve of single phase current and voltage:

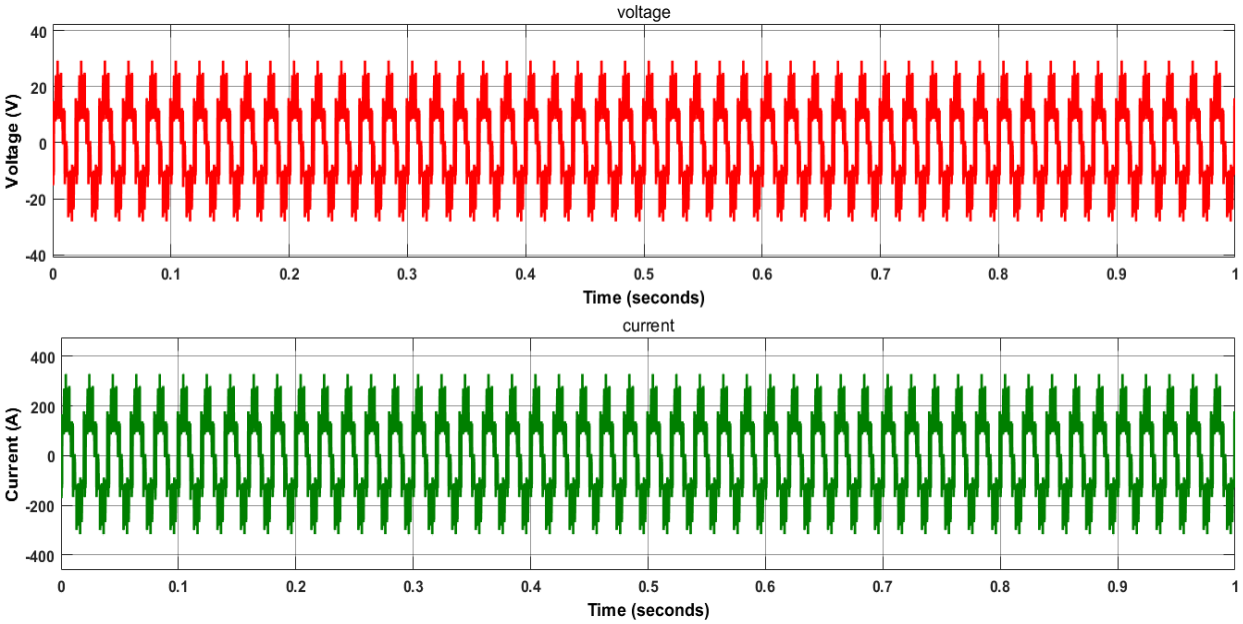

Fig. 4.15 Single phase current and voltage output when cell no 65

The above Fig. 4.15 represents the single-phase voltage and current after DC to AC conversion for 65 cell number. For phase current 1 and phase voltage 1 we have the following Table 4.3-

Table 4.3: Output results of single phase current and voltage output when cell no 65

Contents	**Phase current I_A**	**Phase voltage V_A**
Maximum peak value	329.1 A	29.24 V
Maximum peak value Time	0.825 Sec	0.825 Sec
Minimum phase value	316.3 A	-28.11 V
Minimum phase value Time	0.175 Sec	0.175 Sec
Peak to peak value	645.4A	57.35 V
Rams value	171.19 A	15.2 V
Rise time	122.308 us	122.308us
Fall time	125.49 us	125.49 us
Overshoot	18.559%	18.559%

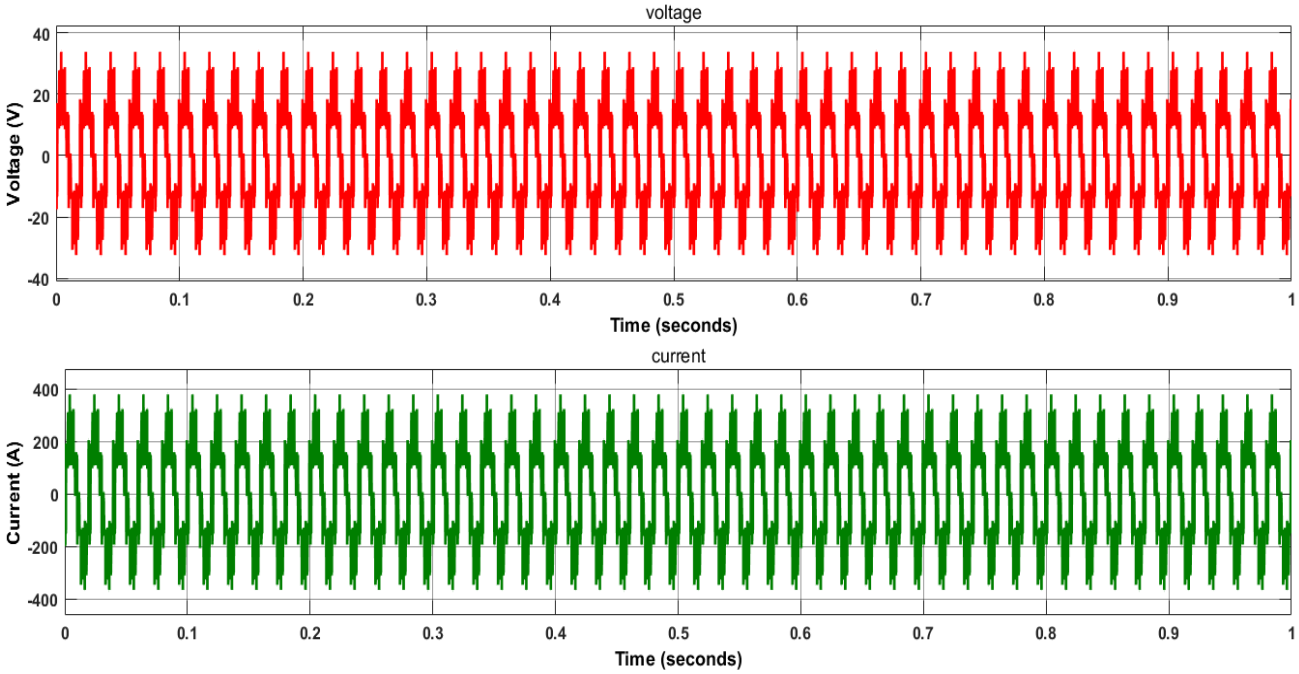

Fig. 4.16 Single phase current and voltage output when cell no 75

The above Fig. 4.16 represents the single-phase voltage and current after DC to AC conversion for 65 cell number. For phase current 1 and phase voltage 1 we have the following Table 4.4-

Table 4.4: Output results of single phase current and voltage output when cell no 75

Contents	Phase current I_A	Phase voltage V_A
Maximum peak value	179.7A	33.74V
Maximum peak value Time	0.684 second.	0.784 second.
Minimum phase value	364.9 A	-32.43 V
Minimum phase value Time	0.996 second	0.996 second
Peak to peak value	744.6A	66.17V
Rams value	198.3 A	15.2 V
Rise time	122.308us	122.308us
Fall time	125.49 us	125.49 us
Overshoot	18.559%	18.559%

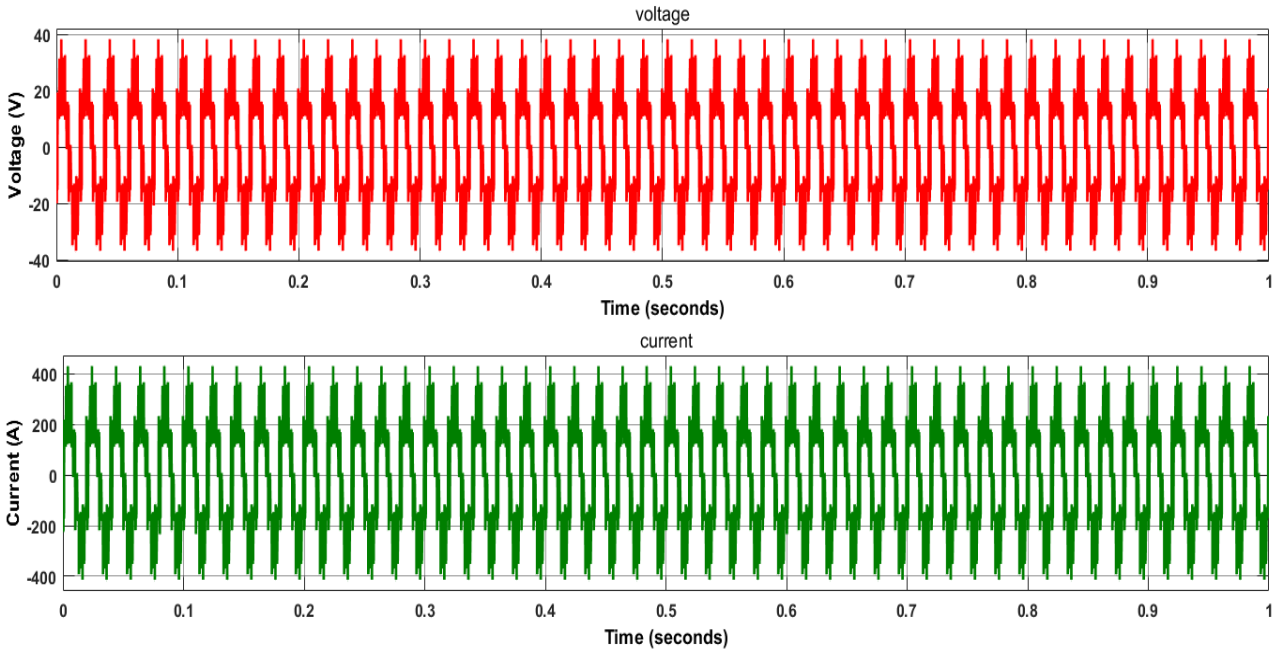

Fig. 4.17 Single phase current and voltage output when cell no 85

The above Fig. 4.17 represents the Single-phase voltage and current after DC to AC conversion for 85 cell number. For phase current 1 and phase voltage 1 we have the following Table 4.5-

Table 4.5: Output results of single phase current and voltage output when cell no 85

Contents	**Phase current I_A**	**Phase voltage V_A**
Maximum peak value	430.3A	38.24V
Maximum peak value Time	0.684 second.	0.784 second.
Minimum phase value	-413.6 A	-36.75 V
Minimum phase value Time	0.996 second	0.996 second
Peak to peak value	843.9A	74.99V
Rams value	224.8A	19.7V
Rise time	122.308us	122.308us
Fall time	125.49 us	125.49 us
Overshoot	18.559%	18.559%

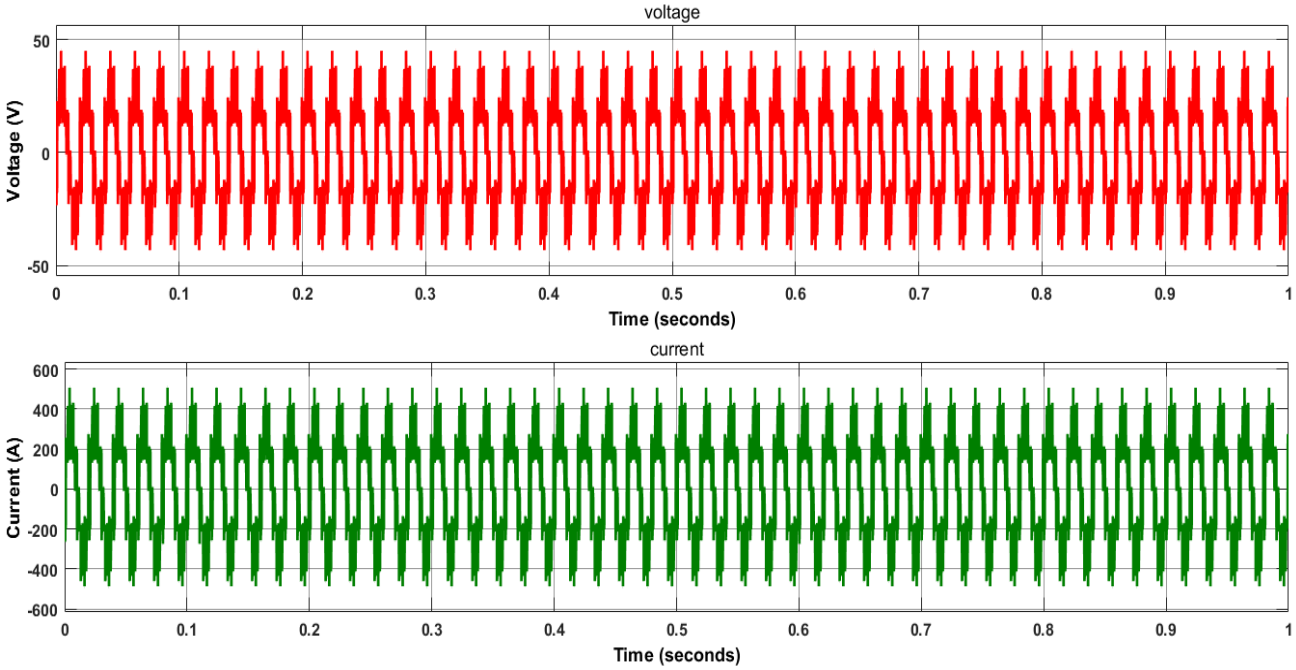

Fig. 4.18 Single phase current and voltage output when cell no 100

The above Fig. 4.18 represents the Single-phase voltage and current after DC to AC conversion for 100 cell number. For phase current 1 and phase voltage 1 we have the following Table 4.6-

Table 4.6: Output results of single phase current and voltage output when cell no 100

Contents	**Phase current I_A**	**Phase voltage V_A**
Maximum peak value	506.3A	44.99V
Maximum peak value Time	0.684 second.	0.784 second.
Minimum phase value	-486.6 A	-43.24 V
Minimum phase value Time	0.996 second	0.996 second
Peak to peak value	992.9A	88.23V
Rams value	264.5A	23.5V
Rise time	122.308us	122.308us
Fall time	125.49 us	125.49 us
Overshoot	18.559%	18.559%

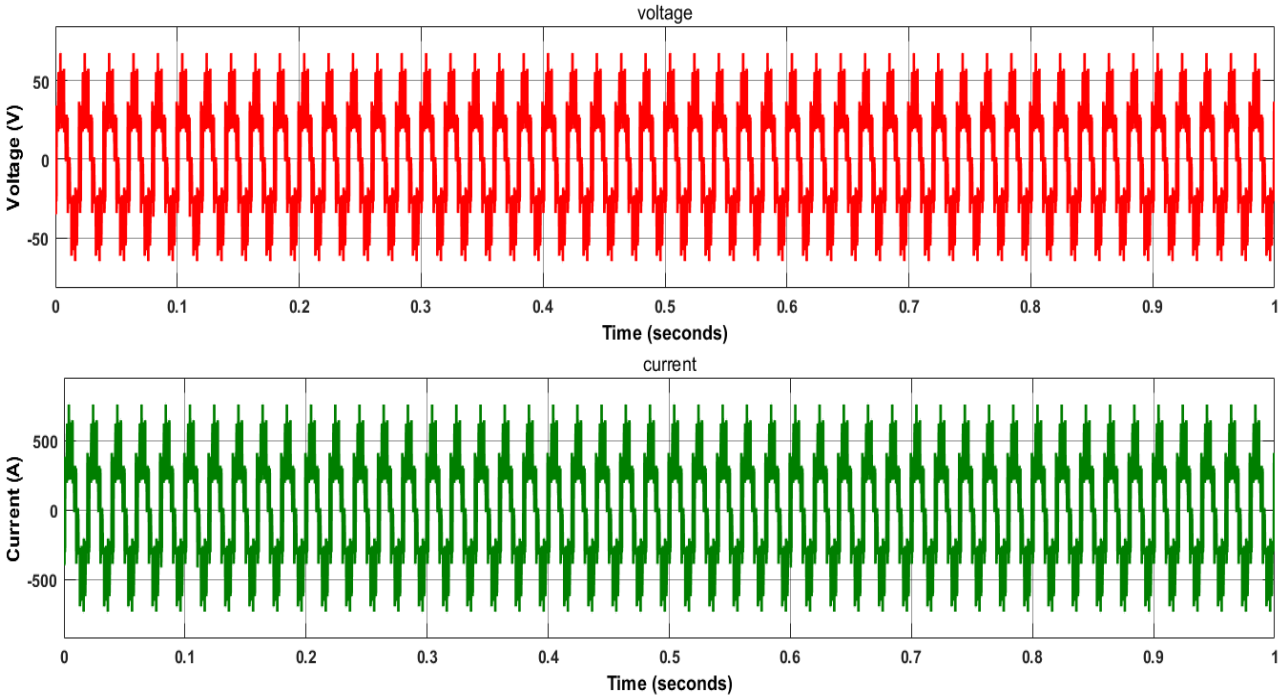

Fig. 4.19 Single phase current and voltage output when cell no 150

The above Fig. 4.19 represents the single-phase voltage and current after DC to AC conversion for 150 cell number. For phase current 1 and phase voltage 1 we have the following Table 4.7-

Table 4.7: Output results of single phase current and voltage output when cell no 150

Contents	**Phase current I_A**	**Phase voltage V_A**
Maximum peak value	759.4A	67.48V
Maximum peak value Time	0.684 second.	0.784 second.
Minimum phase value	-729.9 A	-64.86 V
Minimum phase value Time	0.996 second	0.996 second
Peak to peak value	1489A	132.3V
Rams value	396.7A	19.7V
Rise time	122.308us	122.308us
Fall time	125.49 us	125.49 us
Overshoot	18.559%	18.559%

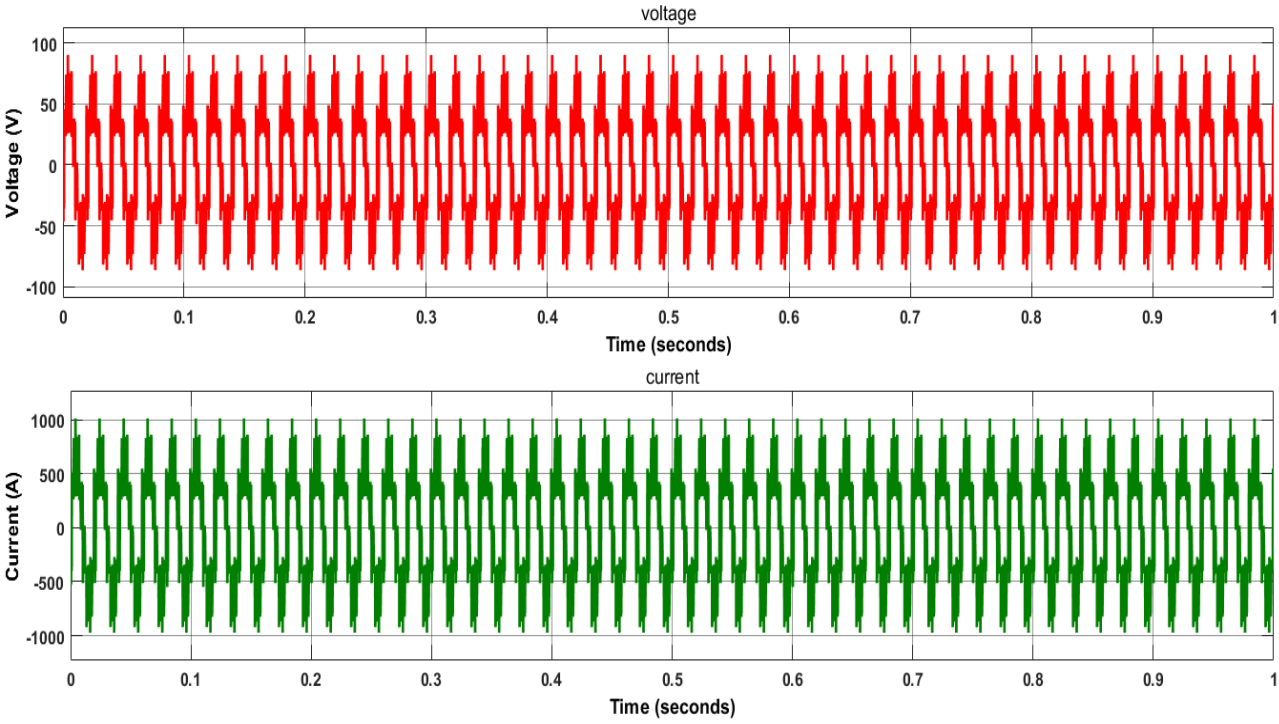

Fig. 4.20 Single phase current and voltage output when cell no 200

The above Fig. 4.20 represents the single-phase voltage and current after DC to AC conversion for 200 cell number. For phase current 1 and phase voltage 1 we have the following Table 4.8-

Table 4.8: Output results of single phase current and voltage output when cell no 200

Contents	**Phase current I_A**	**Phase voltage V_A**
Maximum peak value	1013A	89.98V
Maximum peak value Time	0.684 second.	0.784 second.
Minimum phase value	-973.2 A	-86.48V
Minimum phase value Time	0.996 second	0.996 second
Peak to peak value	1986A	176.5V
Rams value	528.9A	47V
Rise time	122.308us	122.308us
Fall time	125.49 us	125.49 us
Overshoot	18.559%	18.559%

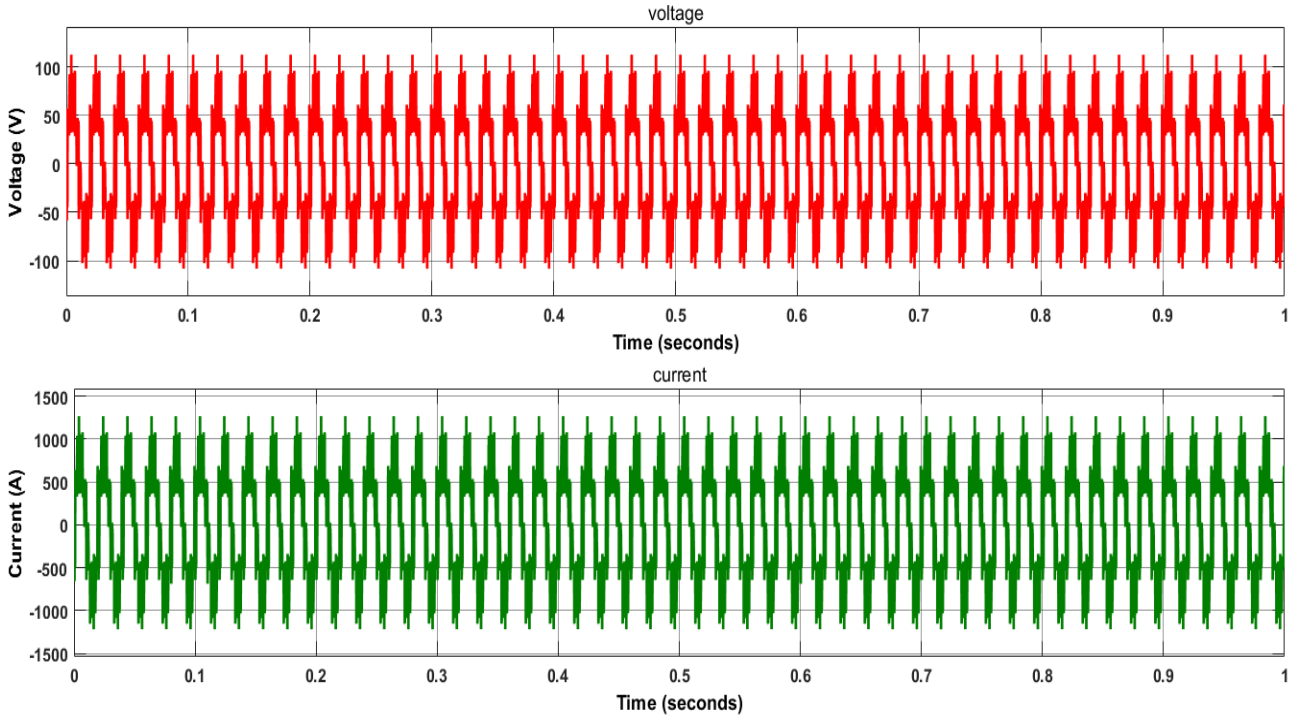

Fig. 4.21 Single phase current and voltage output when cell no 250

The above Fig. 4.21 represents the Single-phase voltage and current after DC to AC conversion for 250 cell number. For phase current 1 and phase voltage 1 we have the following Table 4.9-

Table 4.9: Output results of single phase current and voltage output when cell no 250

Contents	**Phase current I_A**	**Phase voltage V_A**
Maximum peak value	1266A	112.5V
Maximum peak value Time	0.684 second.	0.784 second.
Minimum phase value	-1216 A	-108.1 V
Minimum phase value Time	0.996 second	0.996 second
Peak to peak value	2482A	220.6V
Rams value	661.1A	58.75V
Rise time	122.308us	122.308us
Fall time	125.49 us	125.49 us
Overshoot	18.559%	18.559%

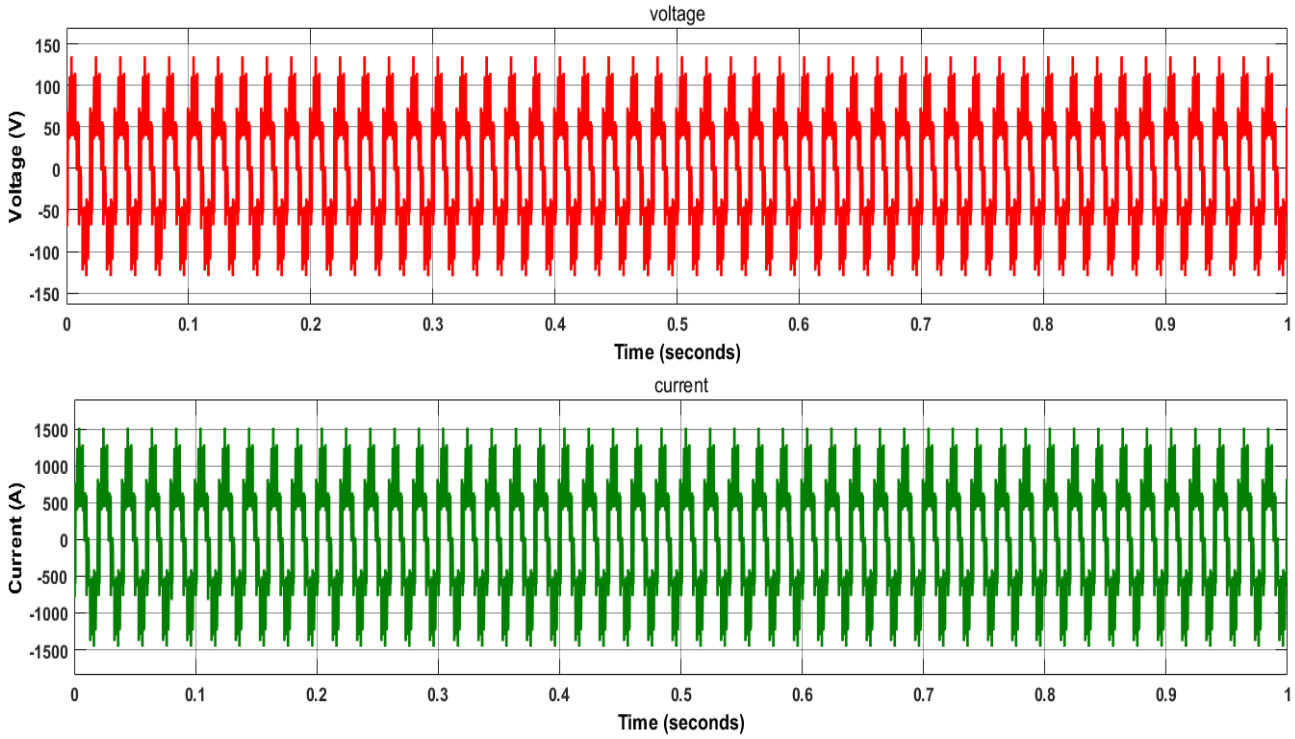

Fig. 4.22 Single phase current and voltage output when cell no 300

The above Fig. 4.22 represents the single-phase voltage and current after DC to AC conversion for 300 cell number. For phase current 1 and phase voltage 1 we have the following- Table 4.10

Table 4.10: Output results of single phase current and voltage output when cell no 300

Contents	**Phase current I_A**	**Phase voltage V_A**
Maximum peak value	1519 A	135V
Maximum peak value Time	0.684 second.	0.784 second.
Minimum phase value	-1460 A	-129.7V
Minimum phase value Time	0.996 second	0.996 second
Peak to peak value	2979A	264.7V
Rams value	793.4A	70.5V
Rise time	122.308us	122.308us
Fall time	125.49 us	125.49 us
Overshoot	18.559%	18.559%

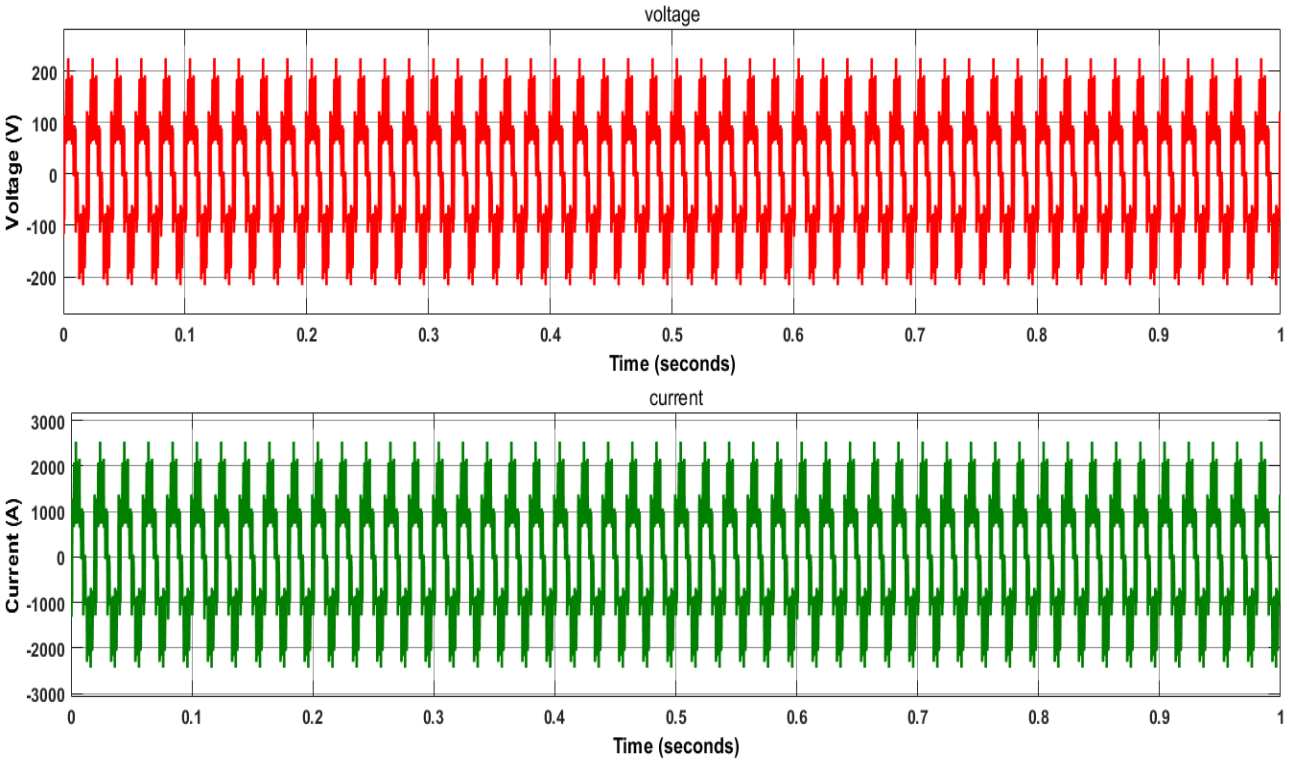

Fig. 4.23 Single phase current and voltage output when cell no 500

The above Fig. 4.23 represents the single-phase voltage and current after DC to AC conversion for 500 cell number. For phase current 1 and phase voltage 1 we have the following Table 4.11-

Table 4.11: Output results of single phase current and voltage output when cell no 500

Contents	**Phase current I_A**	**Phase voltage V_A**
Maximum peak value	2531A	224.9V
Maximum peak value Time	0.684 second.	0.784 second.
Minimum phase value	-2433A	-216.2 V
Minimum phase value Time	0.996 second	0.996 second
Peak to peak value	4964 A	441.1 V
Rams value	1322A	117.5V
Rise time	122.308us	122.308us
Fall time	125.49 us	125.49 us
Overshoot	18.559%	18.559%

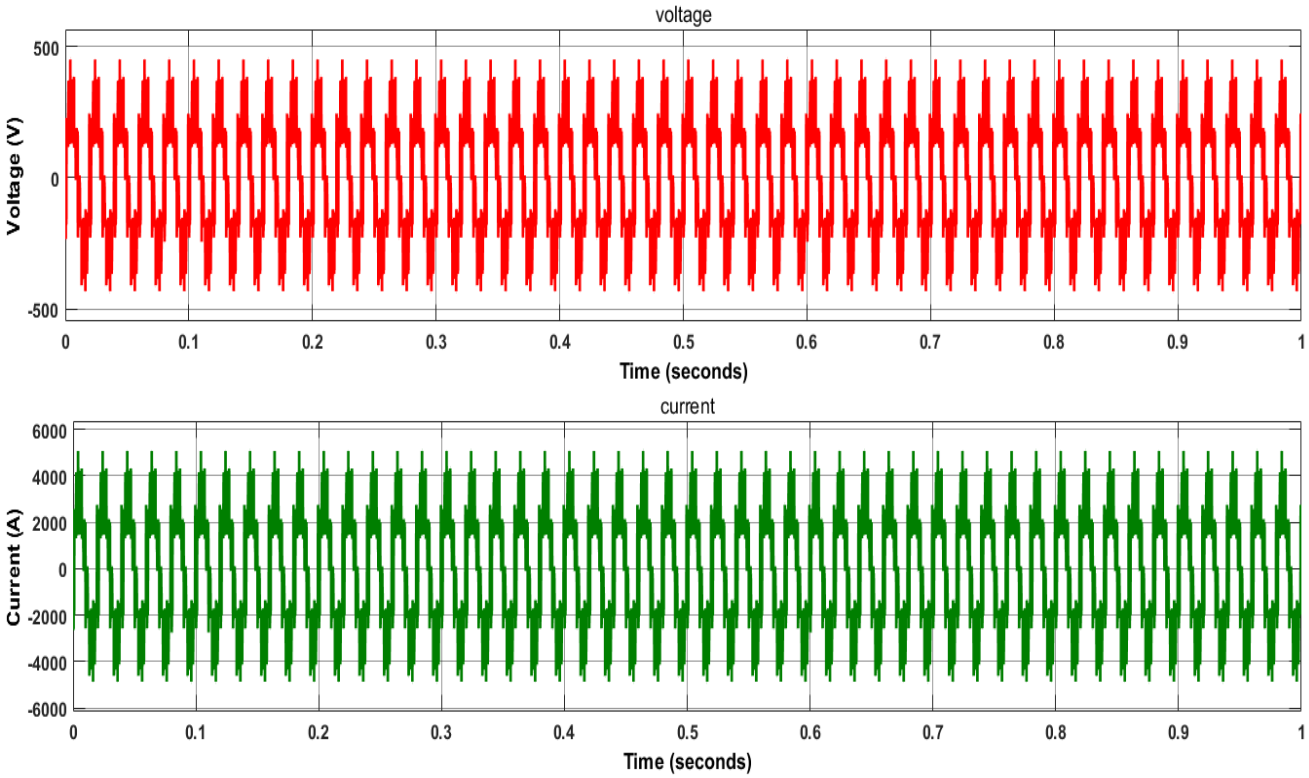

Fig. 4.24 Single phase current and voltage output when cell no 1000

The above Fig. 4.24 represents the single-phase voltage and current after DC to AC conversion for 1000 cell number. For phase current 1 and phase voltage 1 we have the following Table 4.12-

Table 4.12: Output results of single phase current and voltage output when cell no 1000

Contents	**Phase current I_A**	**Phase voltage V_A**
Maximum peak value	5063A	449.9V
Maximum peak value Time	0.684 second.	0.784 second.
Minimum phase value	-4866 A	-432.4V
Minimum phase value Time	0.996 second	0.996 second
Peak to peak value	9929A	882.3V
Rams value	2645A	235V
Rise time	122.308us	122.308us
Fall time	125.49 us	125.49 us
Overshoot	18.559%	18.559%

4.2.6 Output characteristics curve of three phase current and voltage:

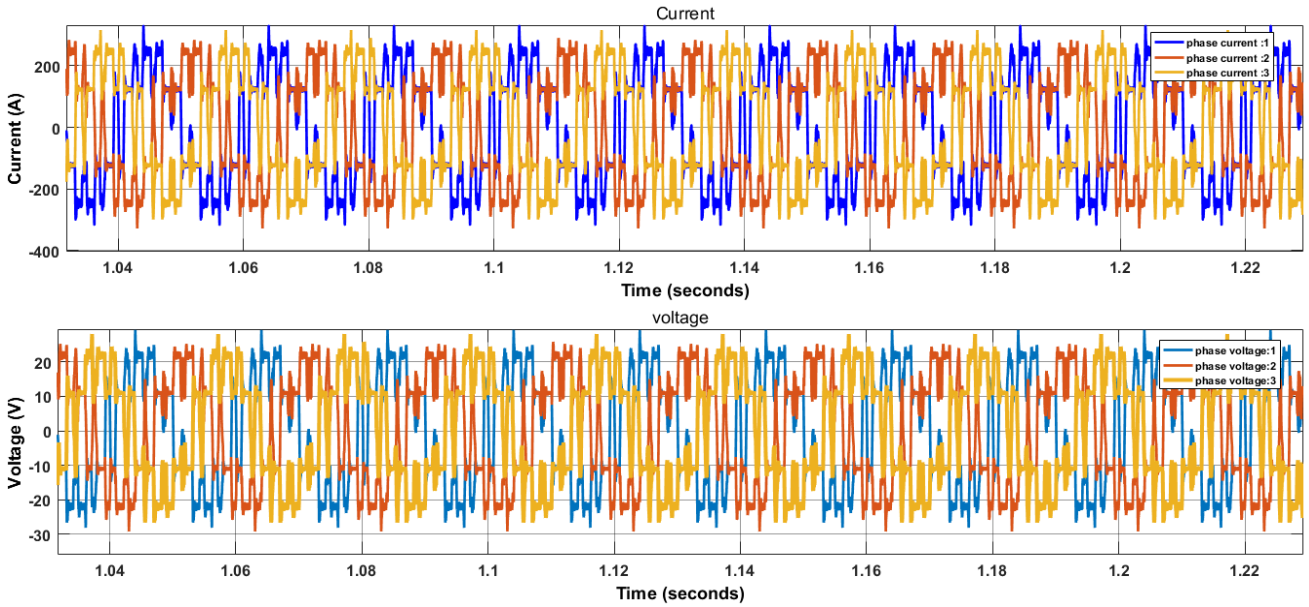

Fig. 4.25 Three phase current and voltage output when cell no 65

The above Fig. 4.25 represents the three-phase voltage and current after DC to AC conversion for 65 cell number. For phase current 1 and phase voltage 1 we have the following Table 4.13-

Table 4.13: Output results of three phase current and voltage output when cell no 65

Contents	**Phase current I_A**	**Phase voltage V_A**
Maximum peak value	329.1 A	29.24 V
Maximum peak value Time	1.684 second.	1.784 second.
Minimum phase value	316.3	-28.11 V
Minimum phase value Time	1.996 second	1.996 second
Peak to peak value	645.4A	645.4A
Rams value	171.19 A	15.2 V
Rise time	122.308us	122.308us
Fall time	125.49 us	125.49 us
Overshoot	18.559%	18.559%

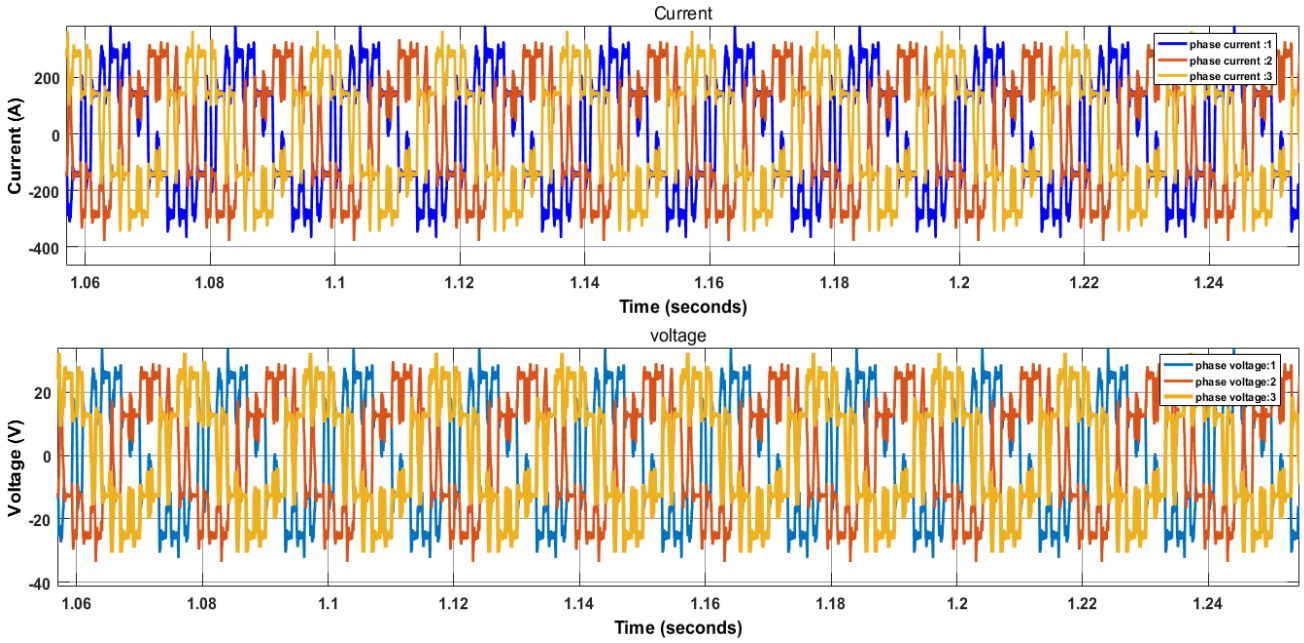

Fig. 4.26 Three phase current and voltage output when cell no 75

The above Fig. 4.26 represents the three-phase voltage and current after DC to AC conversion for 75 cell number. For phase current 1 and phase voltage 1 we have the following Table 4.14-

Table 4.14: Output results of three phase current and voltage output when cell no 75

Contents	**Phase current I_A**	**Phase voltage V_A**
Maximum peak value	179.7A	33.74V
Maximum peak value Time	1.684 second.	1.784 second.
Minimum phase value	-364.9 A	-32.43 V
Minimum phase value Time	1.996 second	1.996 second
Peak to peak value	744.6A	66.17V
Rams value	198.3 A	15.2 V
Rise time	122.308us	122.308us
Fall time	125.49 us	125.49 us
Overshoot	18.559%	18.559%

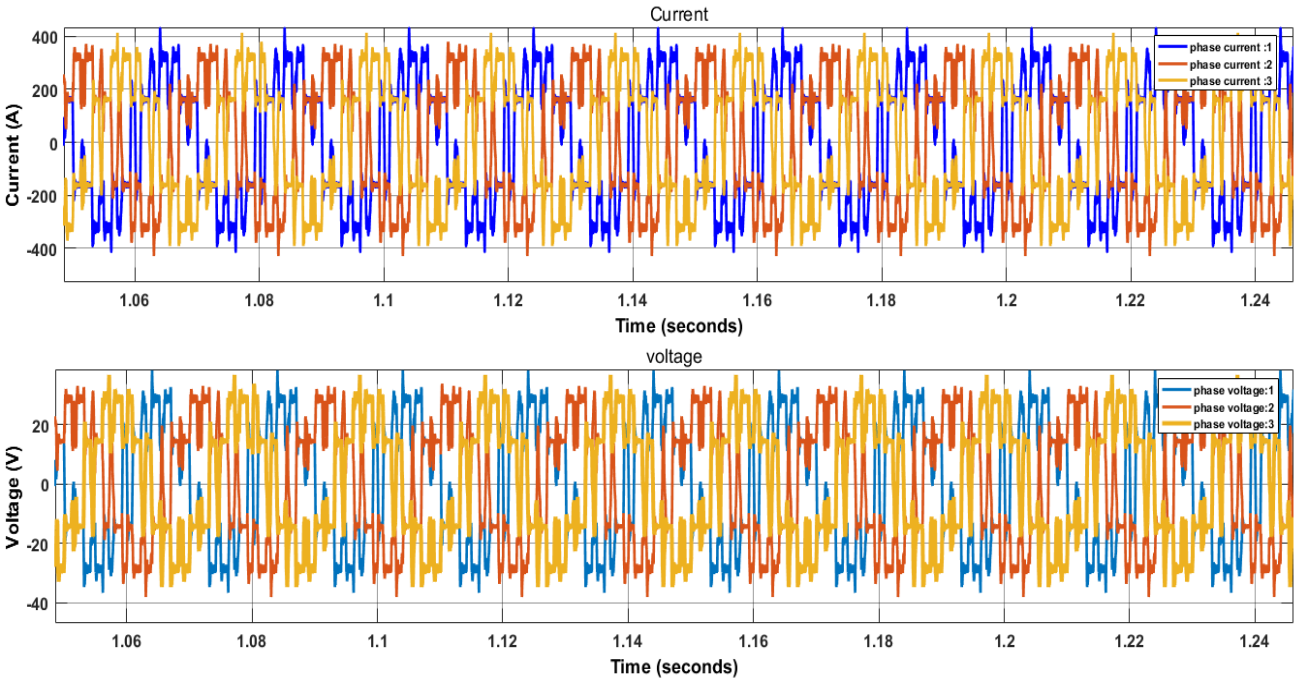

Fig. 4.27 Three phase current and voltage output when cell no 85

The above Fig. 4.27 represents the three-phase voltage and current after DC to AC conversion for 85 cell number. For phase current 1 and phase voltage 1 we have the following Table 4.15-

Table 4.15: Output results of three phase current and voltage output when cell no 85

Contents	**Phase current I_A**	**Phase voltage V_A**
Maximum peak value	430.3A	38.24V
Maximum peak value Time	1.684 second.	1.784 second.
Minimum phase value	-413.6 A	-36.75 V
Minimum phase value Time	1.996 second	1.996 second
Peak to peak value	843.9A	74.99V
Rams value	224.8A	19.7V
Rise time	122.308us	122.308us
Fall time	125.49 us	125.49 us
Overshoot	18.559%	18.559%

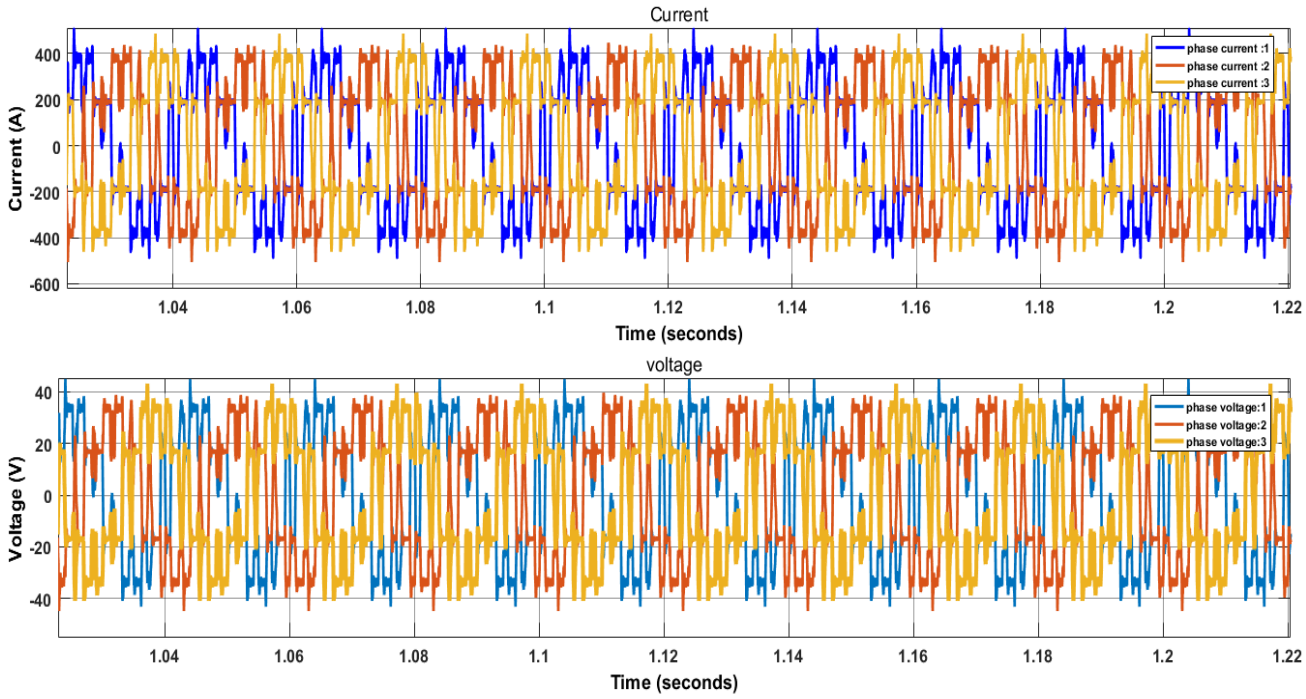

Fig. 4.28 Three phase current and voltage output when cell no 100

The above Fig. 4.28 represents the three-phase voltage and current after DC to AC conversion for 100 cell number. For phase current 1 and phase voltage 1 we have the following Table 4.16-

Table 4.16: Output results of three phase current and voltage output when cell no 100

Contents	**Phase current I_A**	**Phase voltage V_A**
Maximum peak value	506.3A	44.99V
Maximum peak value Time	1.684 second.	1.784 second.
Minimum phase value	-486.6 A	-43.24 V
Minimum phase value Time	1.996 second	1.996 second
Peak to peak value	992.9A	88.23V
Rams value	264.5A	23.5V
Rise time	122.308us	122.308us
Fall time	125.49 us	125.49 us
Overshoot	18.559%	18.559%

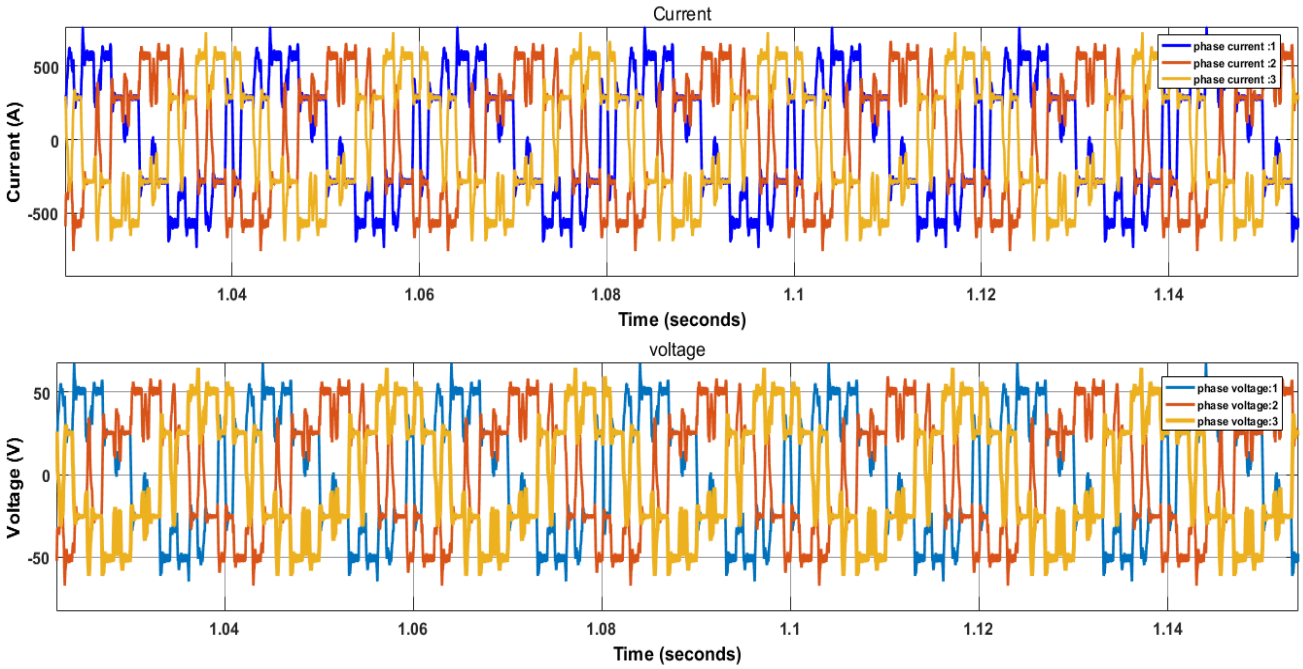

Fig. 4.29 Three phase current and voltage output when cell no 150

The above Fig. 4.29 represents the three-phase voltage and current after DC to AC conversion for 150 cell number. For phase current 1 and phase voltage 1 we have the following Table 4.17-

Table 4.17: Output results of three phase current and voltage output when cell no 150

Contents	**Phase current I_A**	**Phase voltage V_A**
Maximum peak value	759.4A	67.48V
Maximum peak value Time	1.684 second.	1.784 second.
Minimum phase value	-729.9 A	-64.86 V
Minimum phase value Time	1.996 second	1.996 second
Peak to peak value	1489A	132.3V
Rams value	396.7A	19.7V
Rise time	122.308us	122.308us
Fall time	125.49 us	125.49 us
Overshoot	18.559%	18.559%

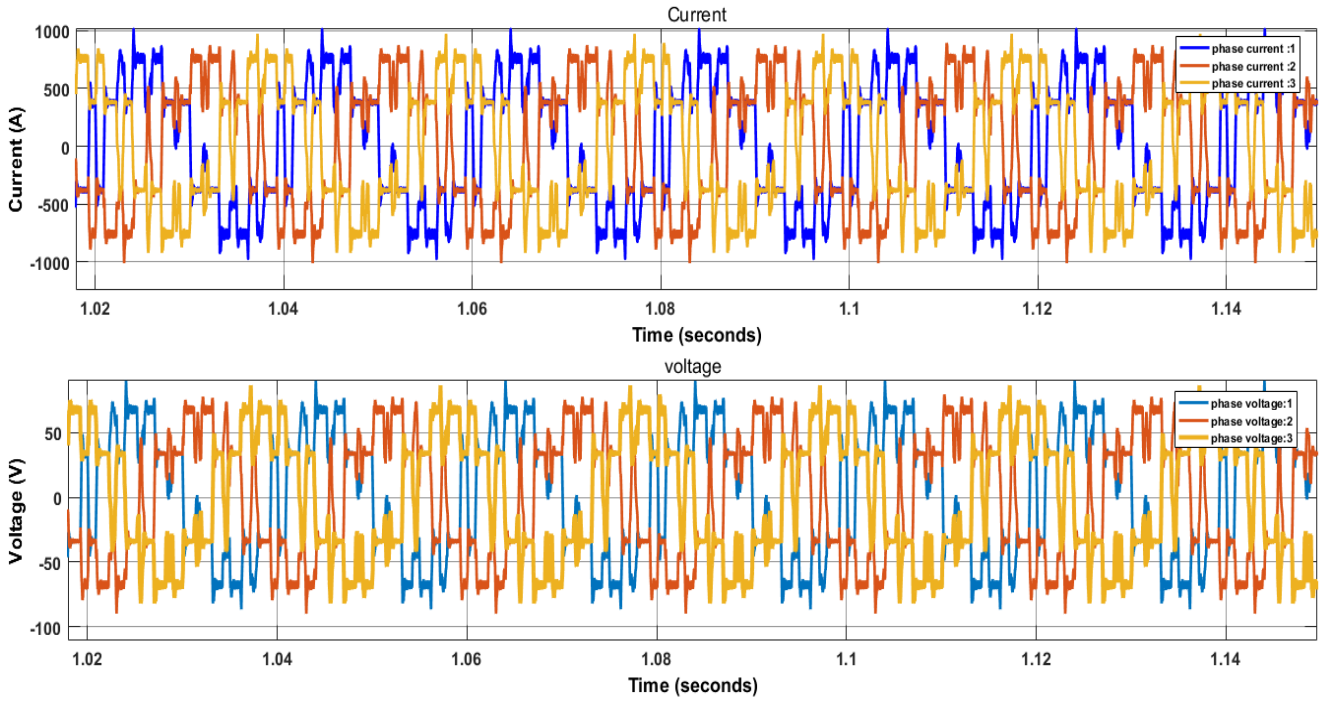

Fig. 4.30 Three phase current and voltage output when cell no 200

The above Fig. 4.30 represents the three-phase voltage and current after DC to AC conversion for 200 cell number. For phase current 1 and phase voltage 1 we have the following Table 4.18-

Table 4.18: Output results of three phase current and voltage output when cell no 200

Contents	**Phase current I_A**	**Phase voltage V_A**
Maximum peak value	1013A	89.98V
Maximum peak value Time	1.684 second.	1.784 second.
Minimum phase value	-973.2 A	-86.48V
Minimum phase value Time	1.996 second	1.996 second
Peak to peak value	1986A	176.5V
Rams value	528.9A	47V
Rise time	122.308us	122.308us
Fall time	125.49 us	125.49 us
Overshoot	18.559%	18.559%

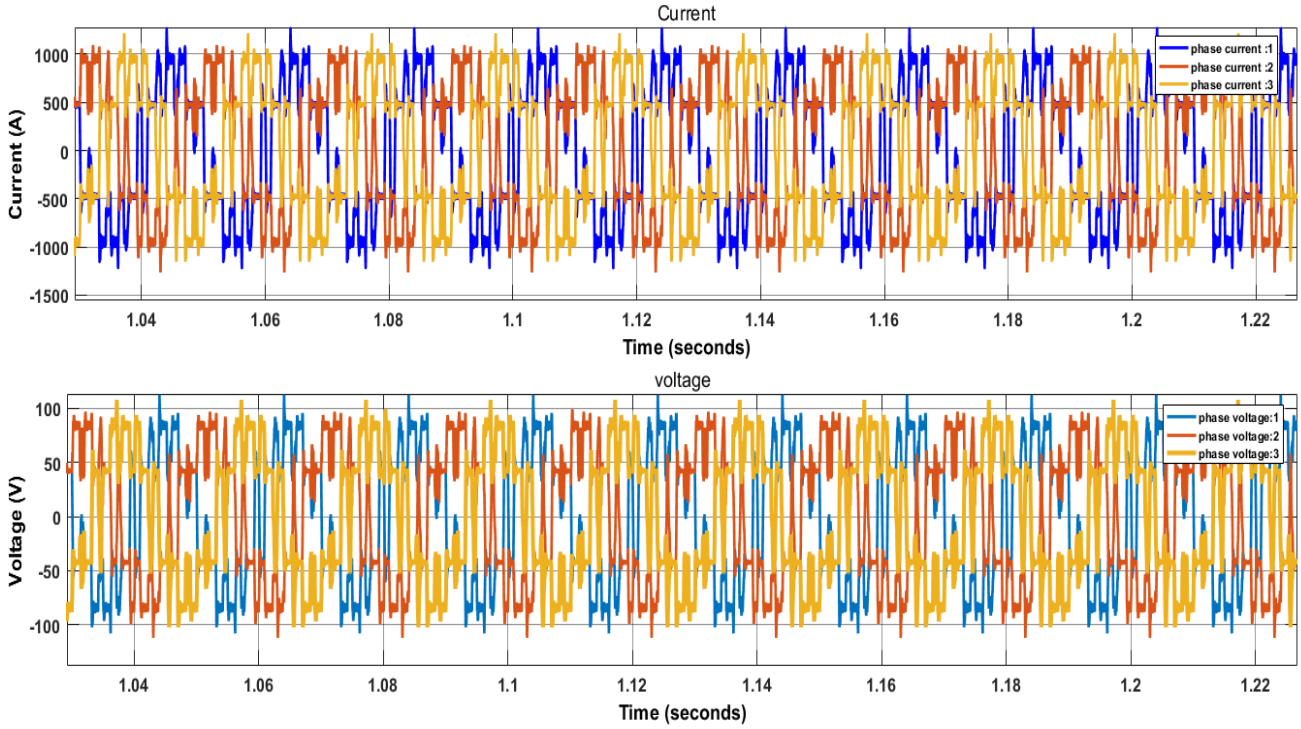

Fig. 4.31 Three phase current and voltage output when cell no 250

The above Fig. 4.31 represents the three-phase voltage and current after DC to AC conversion for 250 cell number. For phase current 1 and phase voltage 1 we have the following Table 4.19-

Table 4.19: Output results of three phase current and voltage output when cell no 250

Contents	**Phase current I_A**	**Phase voltage V_A**
Maximum peak value	1266A	112.5V
Maximum peak value Time	1.684 second.	1.784 second.
Minimum phase value	-1216 A	-108.1 V
Minimum phase value Time	1.996 second	1.996 second
Peak to peak value	2482A	220.6V
Rams value	661.1A	58.75V
Rise time	122.308us	122.308us
Fall time	125.49 us	125.49 us
Overshoot	18.559%	18.559%

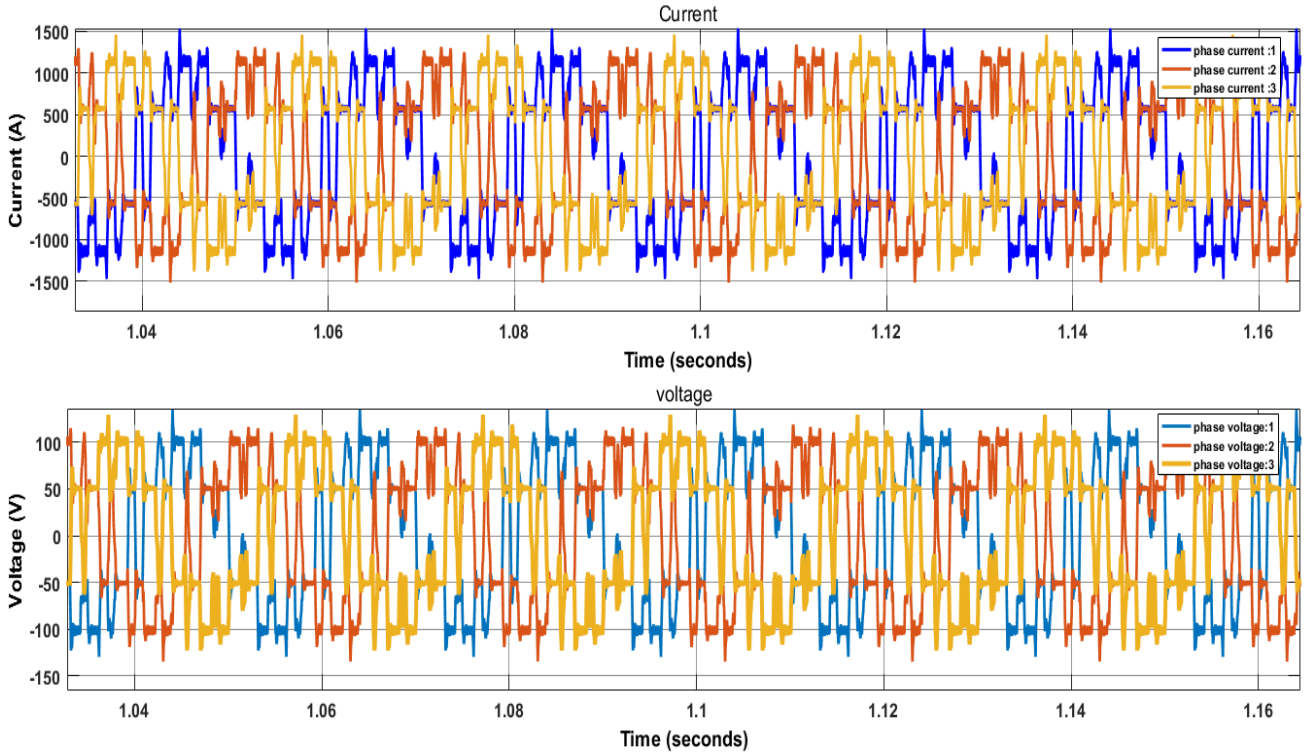

Fig. 4.32 Three phase current and voltage output when cell no 300

The above Fig. 4.32 represents the three-phase voltage and current after DC to AC conversion for 300 cell number. For phase current 1 and phase voltage 1 we have the following Table 4.20-

Table 4.20: Output results of three phase current and voltage output when cell no 300

Contents	**Phase current I_A**	**Phase voltage V_A**
Maximum peak value	1519 A	135V
Maximum peak value Time	1.684 second.	1.784 second.
Minimum phase value	-1460 A	-129.7V
Minimum phase value Time	1.996 second	1.996 second
Peak to peak value	2979A	264.7V
Rams value	793.4A	70.5V
Rise time	122.308us	122.308us
Fall time	125.49 us	125.49 us
Overshoot	18.559%	18.559%

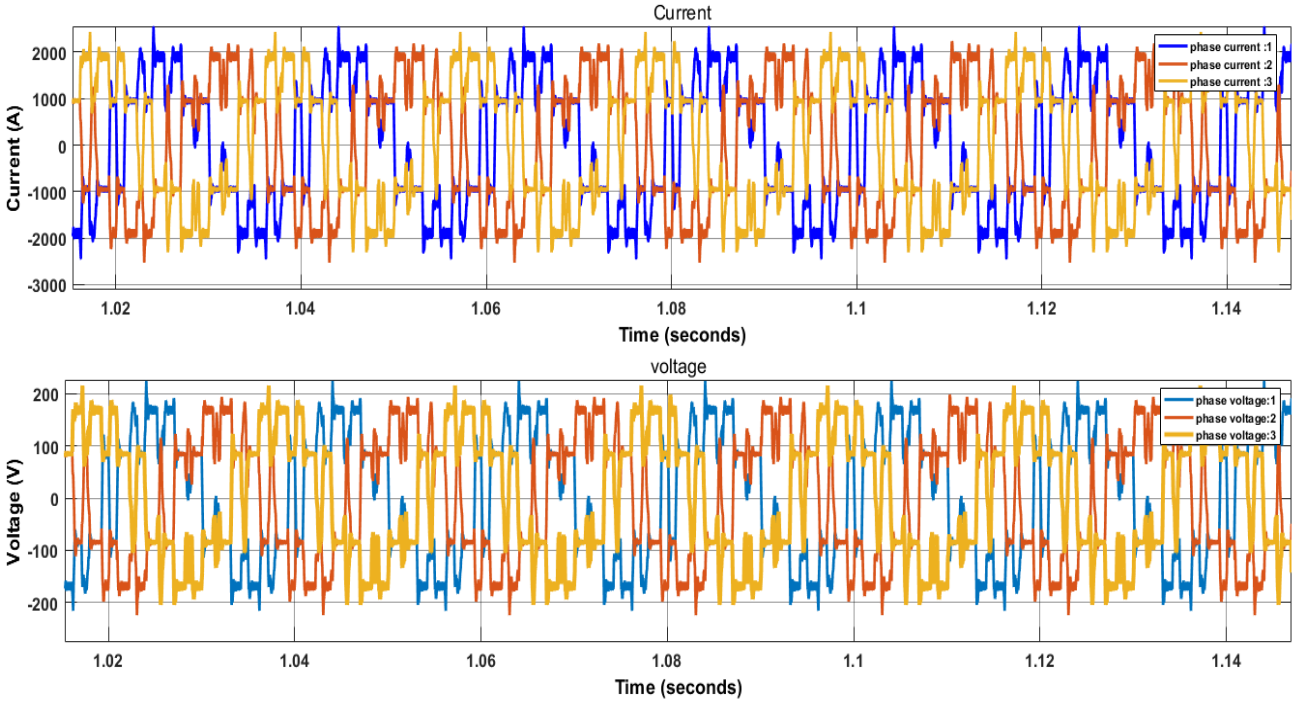

Fig. 4.33 Three phase current and voltage output when cell no 500

The above Fig. 4.33 represents the three-phase voltage and current after DC to AC conversion for 500 cell number. For phase current 1 and phase voltage 1 we have the following Table 4.21-

Table 4.21: Output results of three phase current and voltage output when cell no 500

Contents	**Phase current I_A**	**Phase voltage V_A**
Maximum peak value	2531A	224.9V
Maximum peak value Time	1.684 second.	1.784 second.
Minimum phase value	-2433A	-216.2 V
Minimum phase value Time	1.996 second	1.996 second
Peak to peak value	4964A	441.1 V
Rams value	1322A	117.5V
Rise time	122.308us	122.308us
Fall time	125.49 us	125.49 us
Overshoot	18.559%	18.559%

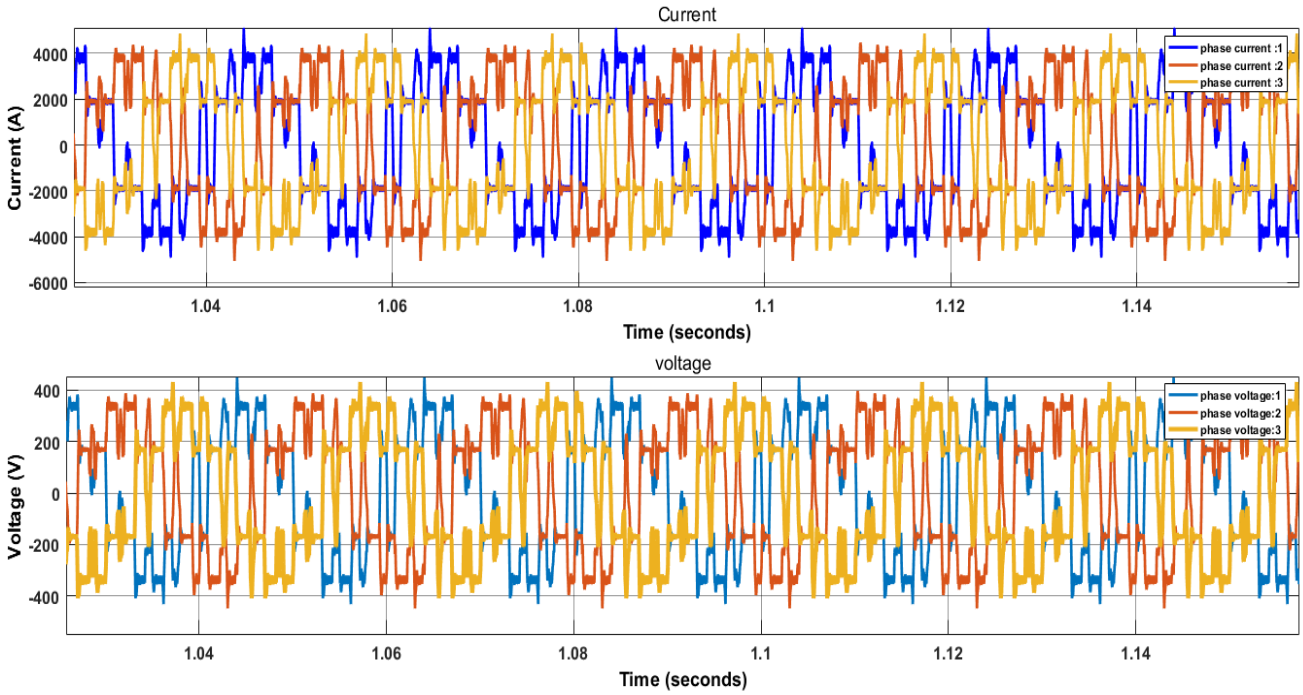

Fig. 4.34 Three phase current and voltage output when cell no 1000

The above Fig. 4.34 represents the three-phase voltage and current after DC to AC conversion for 1000 cell number. For phase current 1 and phase voltage 1 we have the following Table 4.22-

Table 4.22: Output results of three phase current and voltage output when cell no 1000

Contents	**Phase current I_A**	**Phase voltage V_A**
Maximum peak value	5063A	449.9V
Maximum peak value Time	1.684 second.	1.784 second.
Minimum phase value	-4866 A	-432.4V
Minimum phase value Time	1.996 second	1.996 second
Peak to peak value	9929A	882.3V
Rams value	2645A	235V
Rise time	122.308us	122.308us
Fall time	125.49 us	125.49 us
Overshoot	18.559%	18.559%

4.5 Output of inverter section for continuous time analysis:

The output results of inverter section for continuous time analysis has shown below in Table 4.23

Table 4.23: Output results of inverter section for continuous time analysis

SL	Cell no	Power P_{ac}	P_{dc}	I_{rms} (A)	V_{rms} (V)	Efficiency %
01	65	6.37KW	13.15KW	154.6	13.74	48.44
02	75	8.48KW	17.51KW	178.3	15.85	48.43
03	85	10.89KW	22.49KW	202.1	17.96	48.42
04	100	15.08KW	31.12KW	237.8	21.13	48.46
05	150	33.92Kw	70.02KW	356.7	31.7	48.44
06	200	60.31KW	124.49KW	475.7	42.27	48.45
07	250	94.24KW	194.51KW	594.6	52.83	48.45
08	300	135.7KW	280.1KW	713.4	63.4	48.45
09	500	376.9KW	0.778MW	1189	105.7	48.44
10	1000	1.51MW	3.11MW	2378	211.3	48.55

From the continuous time analysis table 4.23 it can be seen that by varying the number of cell, output result also increases. The current and voltage seems shows a linear characteristic while power shows an exponential characteristic. For a cell number of 1000 it can be seen that DC output power is 3.11 MW while in the inverter section this value is reduced to 1.51 MW due to loss in inversion process. As for voltage and current for a 1000 number cell, they show 211.3 V and 2378 A respectively. While the overall efficiency stays around 48%.

4.5.1 Variation of V_{rms} with varying cell number of MCFC stack:

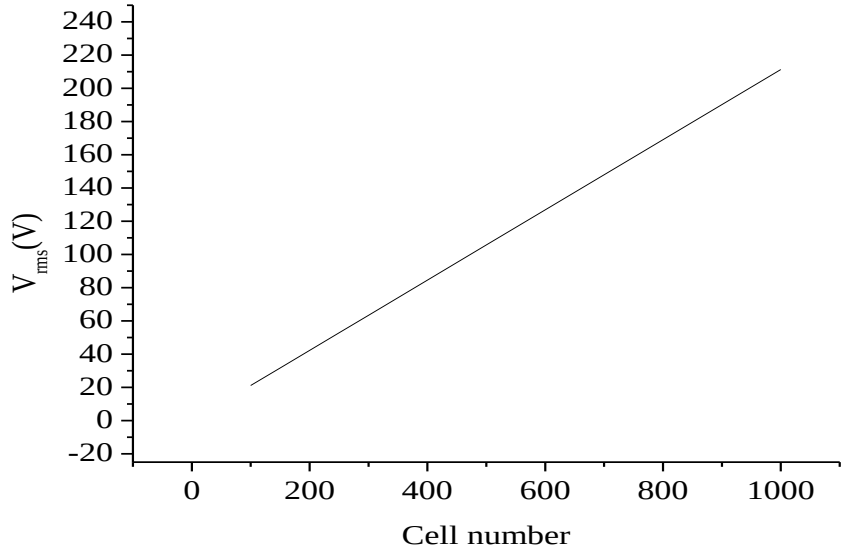

Fig. 4.35 Cell number Vs V_{rms} for continuous time inverter operation.

From the above Fig. 4.35 it is clear that, V_{rms} shows a liner relationship with the varying cell number. Whereas the cell number increases V_{rms} also increases. We have the minimum V_{rms} =13.74V at cell number 65 and maximum V_{rms} =211.3 V value at cell number 1000.

4.5.2 Variation of I_{rms} with varying cell number of MCFC stack:

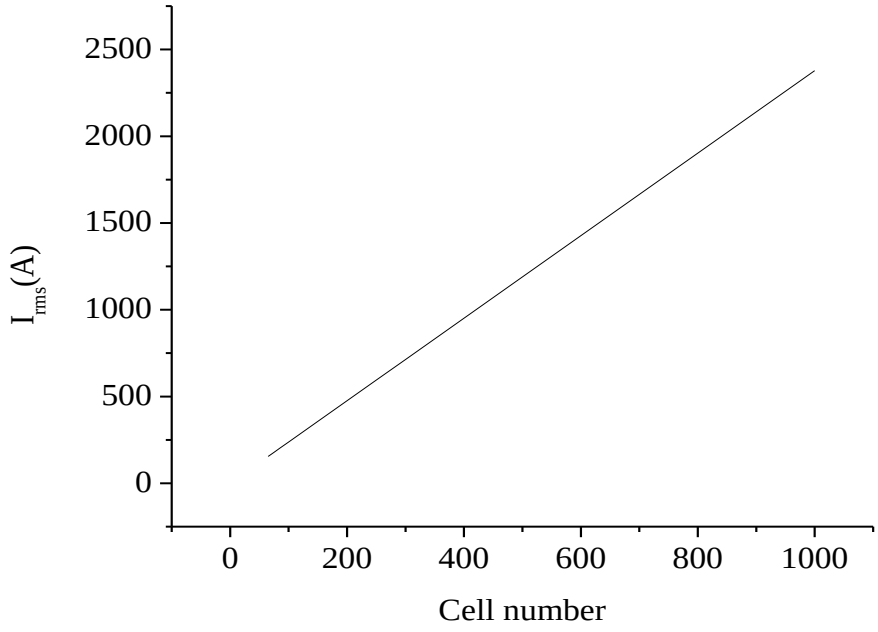

Fig. 4.36 Cell number Vs I_{rms} for continuous time inverter operation

From the above Fig. 4.36 it is clear that, I_{rms} shows a liner relationship with the varying cell number. Whereas the cell number increases I_{rms} also increases. We have the

minimum I_{rms} =154.6A at cell number 65 and maximum I_{rms} =2378 A value at cell number 1000.

4.5.3 Variation of P_{ac} with varying cell number of MCFC stack:

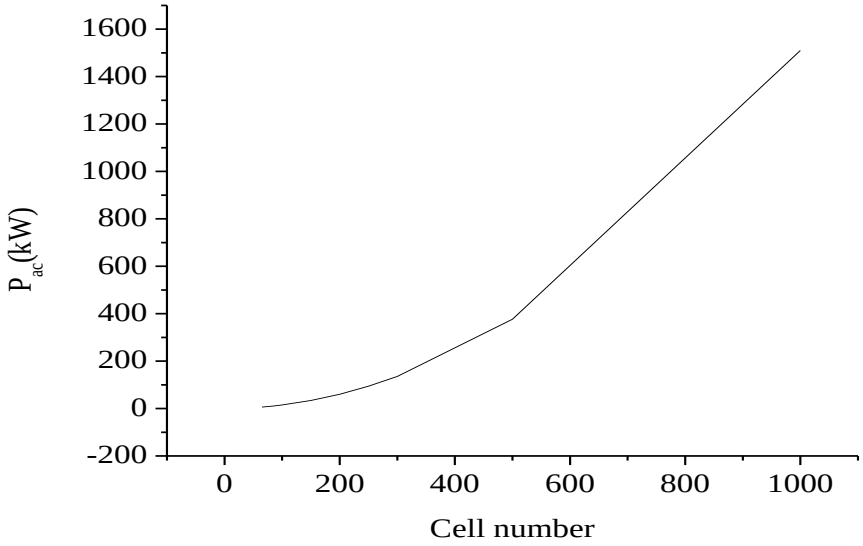

Fig. 4.37 Cell number Vs P_{ac} for continuous time inverter operation

From the above Fig. 4.37 it is clear that, P_{ac} shows an exponential relationship with the varying cell number. As the cell number increases P_{ac} also increases. Here, we minimum P_{ac}=6.37KW at cell number 65. Again, we have maximum P_{ac}=1.51MW.

4.5.4 Variation of efficiency of inverter with varying cell number of MCFC stack:

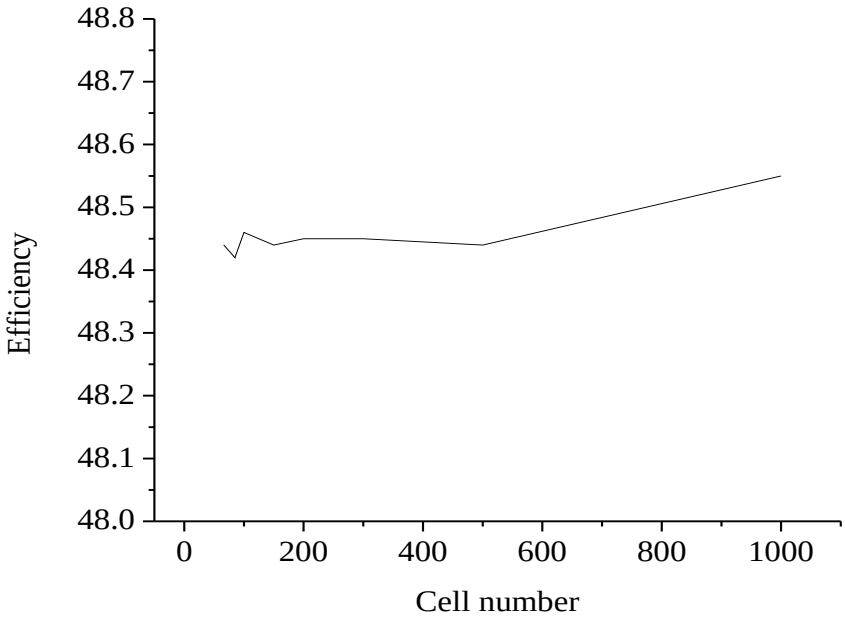

Fig. 4.38 Cell Vs inverter efficiency for continuous time operation

From the above Fig. 4.38 it is clear that, we have maximum efficiency 48.55% at cell number 1000. Minimum efficiency 48.42% at the cell number 85.

4.5.5 Output characteristics of single phase current and voltage:

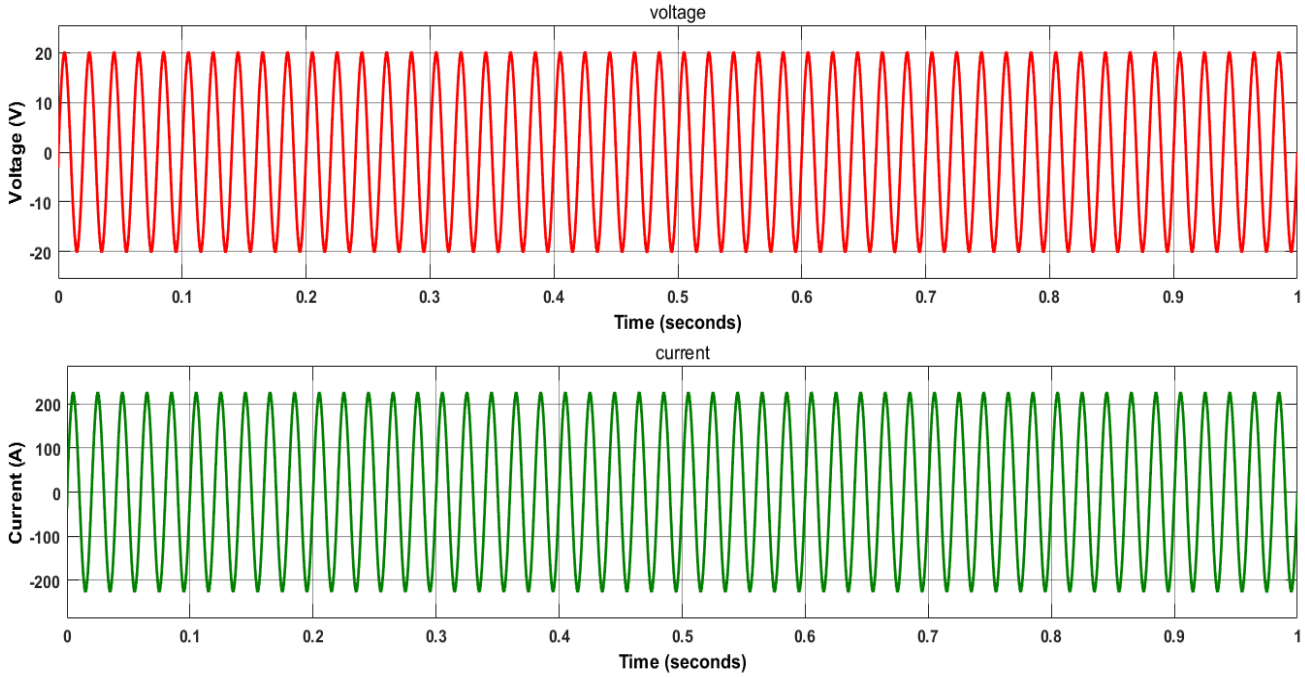

Fig. 4.39 Single phase current and voltage output when cell no 65

The above Fig. 4.39 represents the single-phase voltage and current after DC to AC conversion for 65 cell number. For phase current 1 and phase voltage 1 we have the following Table 4.24-

Table 4.24: Output results of single phase current and voltage output when cell no 65

Contents	**Phase current I_A**	**Phase voltage V_A**
Maximum peak value	227.5 A	20.22 V
Maximum peak value Time	0.825 second.	0.825 second.
Minimum phase value	-227.5A	-20.22 V
Minimum phase value Time	1.175second	0.175 second
Peak to peak value	455A	40.44V
Rams value	156.6 A	13.87 V
Rise time	5.656 ms	5.656 ms
Fall time	5.718 ms	5.719 ms
Overshoot	2.620%	2.620%

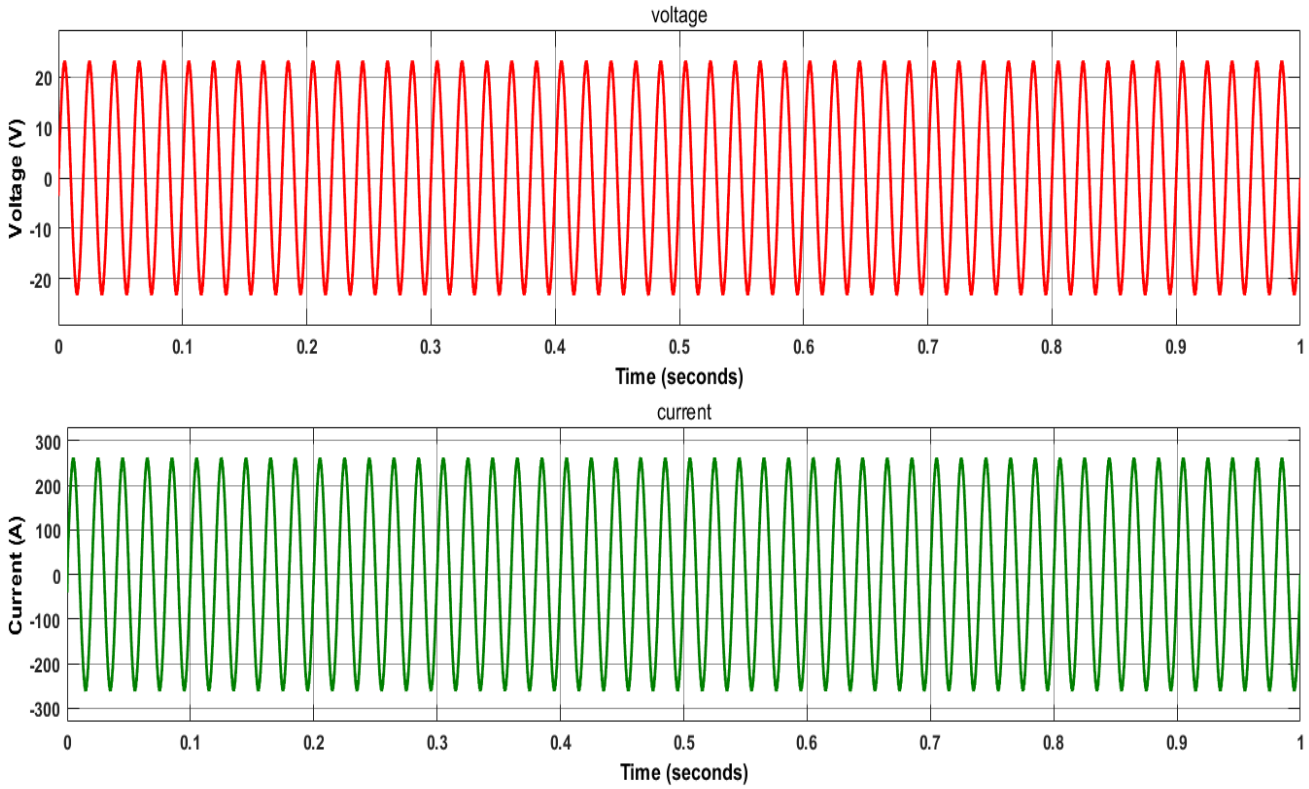

Fig. 4.40 Single phase current and voltage output when cell no 75

The above Fig. 4.40 represents the single-phase voltage and current after DC to AC conversion for 65 cell number. For phase current 1 and phase voltage 1 we have the following Table 4.25-

Table 4.25: Output results of single phase current and voltage output when cell no 75

Contents	**Phase current I_A**	**Phase voltage V_A**
Maximum peak value	262.5 A	23.33 V
Maximum peak value Time	0.805 second.	0.805 second.
Minimum phase value	-262.5 A	-23.33 V
Minimum phase value Time	0.855 second	0.855 second
Peak to peak value	525A	46.65V
Rams value	181.2 A	16.1 V
Rise time	5.656 ms	5.656 ms
Fall time	5.718 ms	5.718 ms
Overshoot	2.628%	2.620%

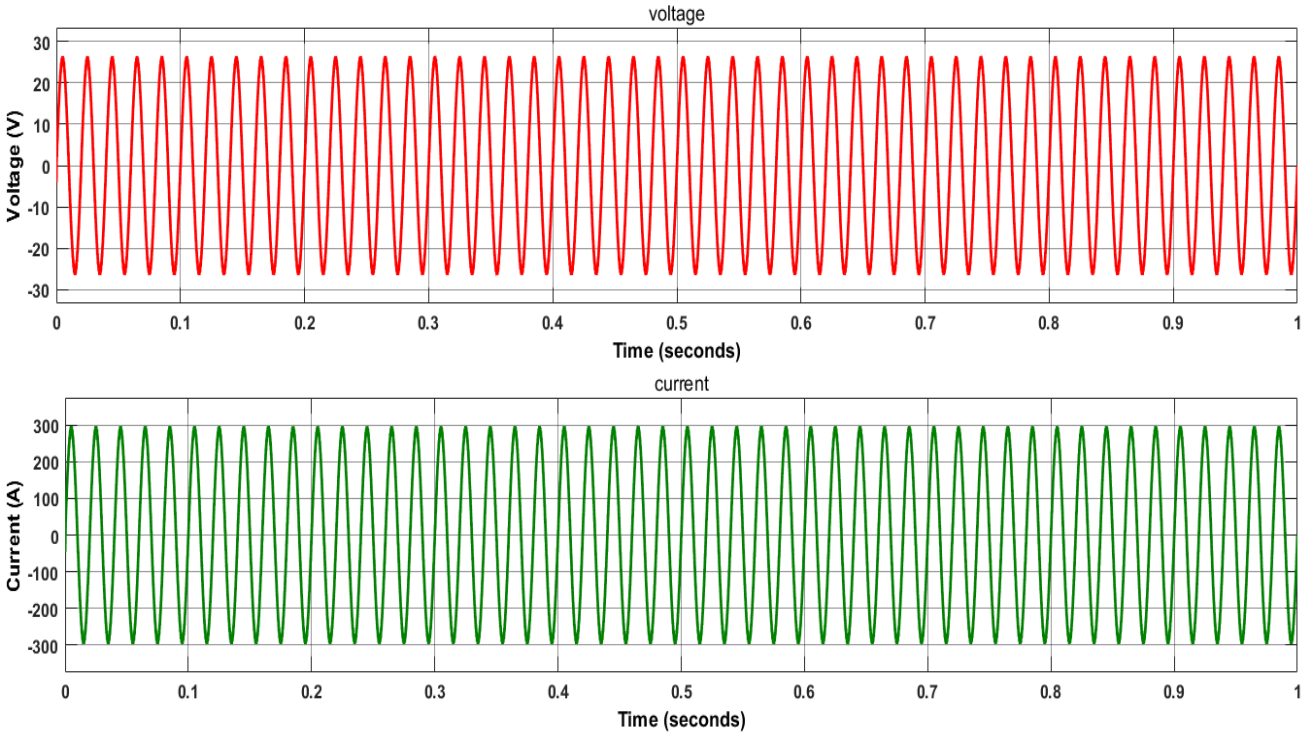

Fig. 4.41 Single phase current and voltage output when cell no 85

The above Fig. 4.41 represents the Single-phase voltage and current after DC to AC conversion for 85 cell number. For phase current 1 and phase voltage 1 we have the following Table 4.26-

Table 4.26: Output results of single phase current and voltage output when cell no 85

Contents	**Phase current I_A**	**Phase voltage V_A**
Maximum peak value	297.5 A	26.44 V
Maximum peak value Time	0.785 second.	0.785 second.
Minimum phase value	-297.5A	-26.44 V
Minimum phase value Time	0.855 second	0.855 second
Peak to peak value	595A	52.87 V
Rams value	204 A	18.13 V
Rise time	5.656 ms	5.656 ms
Fall time	5.718 ms	5.718 ms
Overshoot	2.619%	2.619%

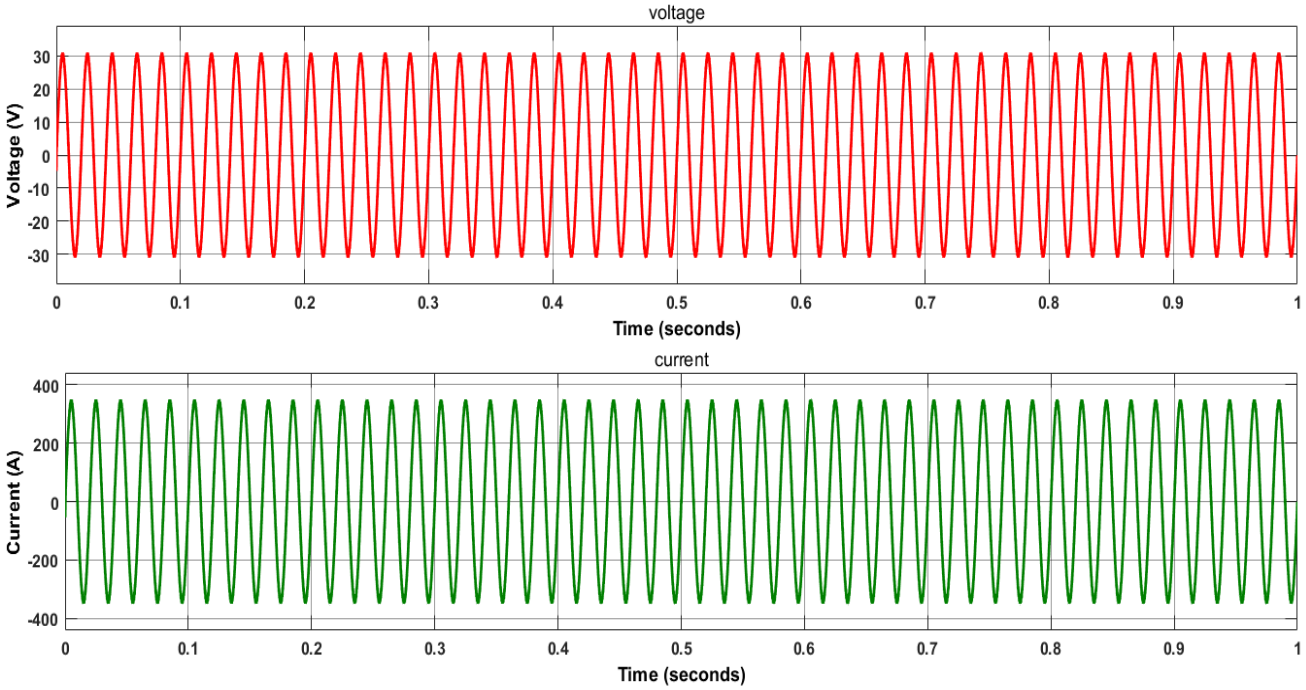

Fig. 4.42 Single phase current and voltage output when cell no 100

The above Fig. 4.42 represents the Single-phase voltage and current after DC to AC conversion for 100 cell number. For phase current 1 and phase voltage 1 we have the following Table 4.27-

Table 4.27: Output results of single phase current and voltage output when cell no 100

Contents	**Phase current I_A**	**Phase voltage V_A**
Maximum peak value	350 A	31.11 V
Maximum peak value Time	0.745 second.	0.745 second.
Minimum phase value	-350 A	-31.11 V
Minimum phase value Time	0.175second	0.175 second
Peak to peak value	700A	62.22 V
Rams value	239.4 A	21.27 V
Rise time	5.656 ms	5.656 ms
Fall time	5.718 ms	5.718 ms
Overshoot	2.623%	2.623%

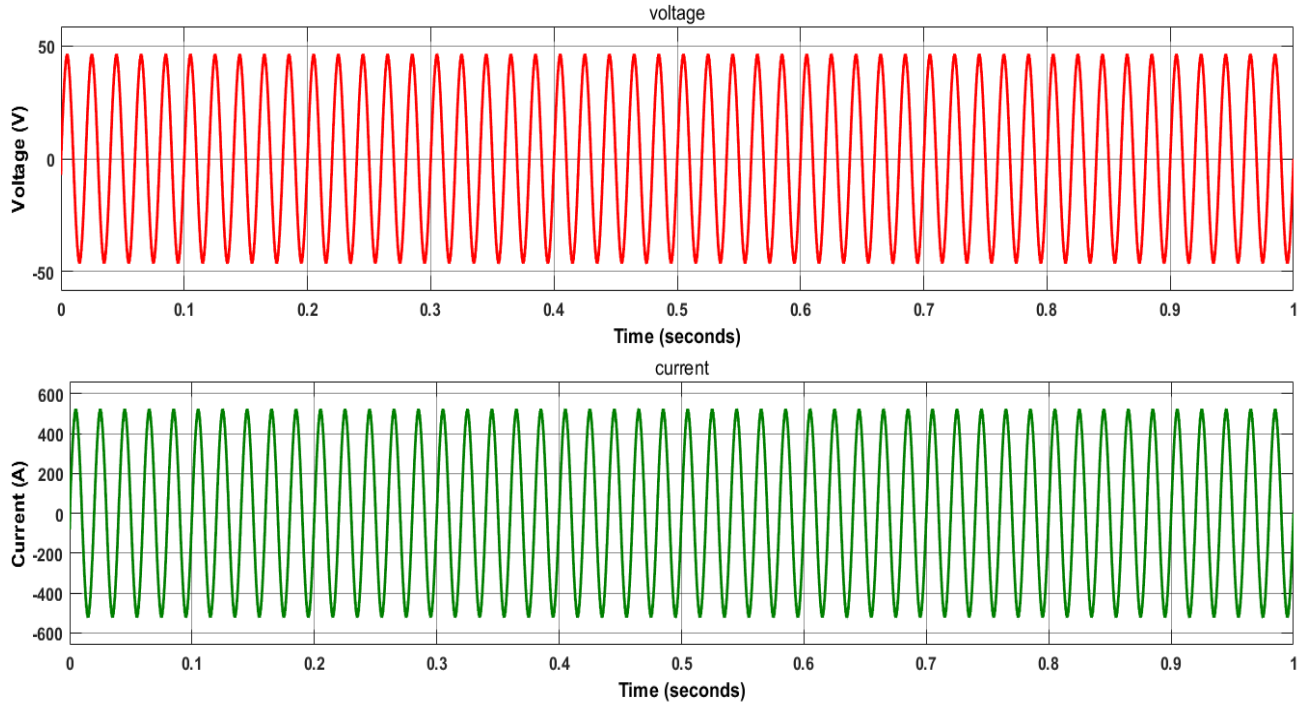

Fig. 4.43 Single phase current and voltage output when cell no 150

The above Fig. 4.43 represents the single-phase voltage and current after DC to AC conversion for 150 cell number. For phase current 1 and phase voltage 1 we have the following Table 4.28-

Table 4.28: Output results of single phase current and voltage output when cell no 150

Contents	**Phase current I_A**	**Phase voltage V_A**
Maximum peak value	525.1 A	46.66 V
Maximum peak value Time	0.805second.	0.805 second.
Minimum phase value	-525.1 A	-46.66V
Minimum phase value Time	0.175 second	0.175 second
Peak to peak value	1050.2A	93.32 V
Rams value	358.2 A	31.89 V
Rise time	5.656 ms	5.656 ms
Fall time	5.719 ms	5.719 ms
Overshoot	2.621%	2.621%

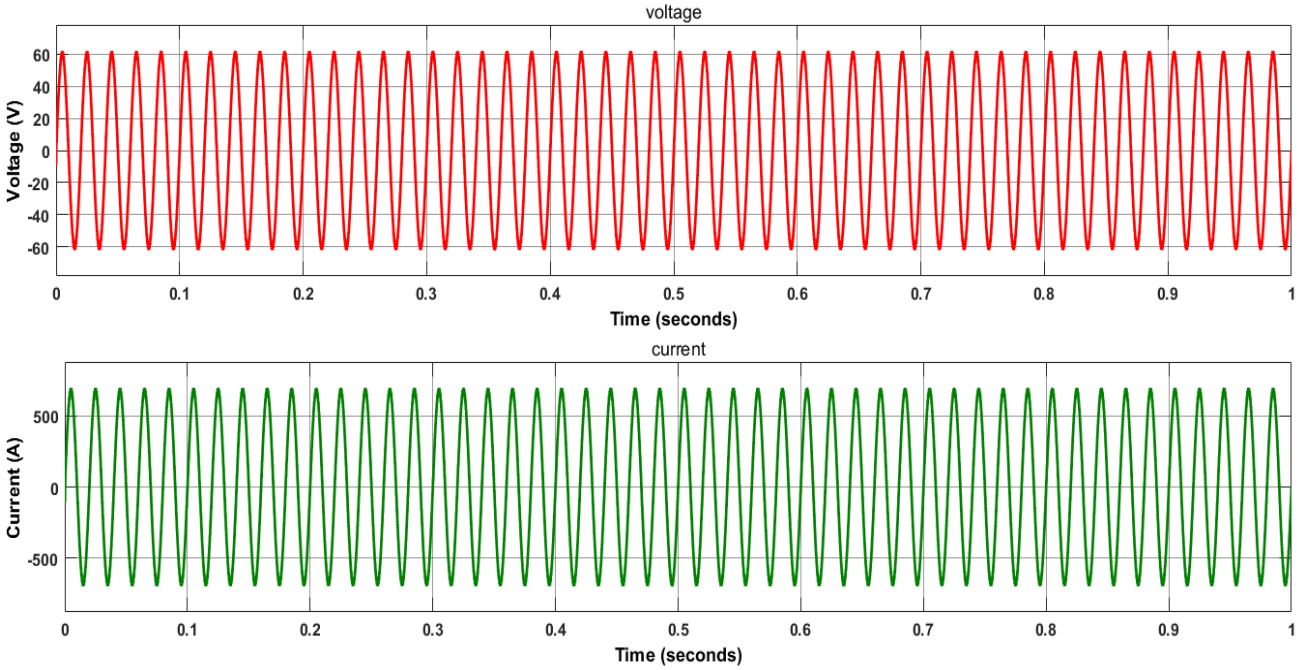

Fig. 4.44 Single phase current and voltage output when cell no 200

The above Fig. 4.44 represents the single-phase voltage and current after DC to AC conversion for 200 cell number. For phase current 1 and phase voltage 1 we have the following Table 4.29-

Table 4.29: Output results of single phase current and voltage output when cell no 200

Contents	**Phase current I_A**	**Phase voltage V_A**
Maximum peak value	700 A	62.21 V
Maximum peak value Time	0.725 second.	0.725 second.
Minimum phase value	-700A	-62.21V
Minimum phase value Time	0.815 second	0.815 second
Peak to peak value	1400 A	124.42 V
Rams value	478.4 A	42.41V
Rise time	5.656 ms	5.656 ms
Fall time	5.718 ms	5.718 ms
Overshoot	2.626%	2.626%

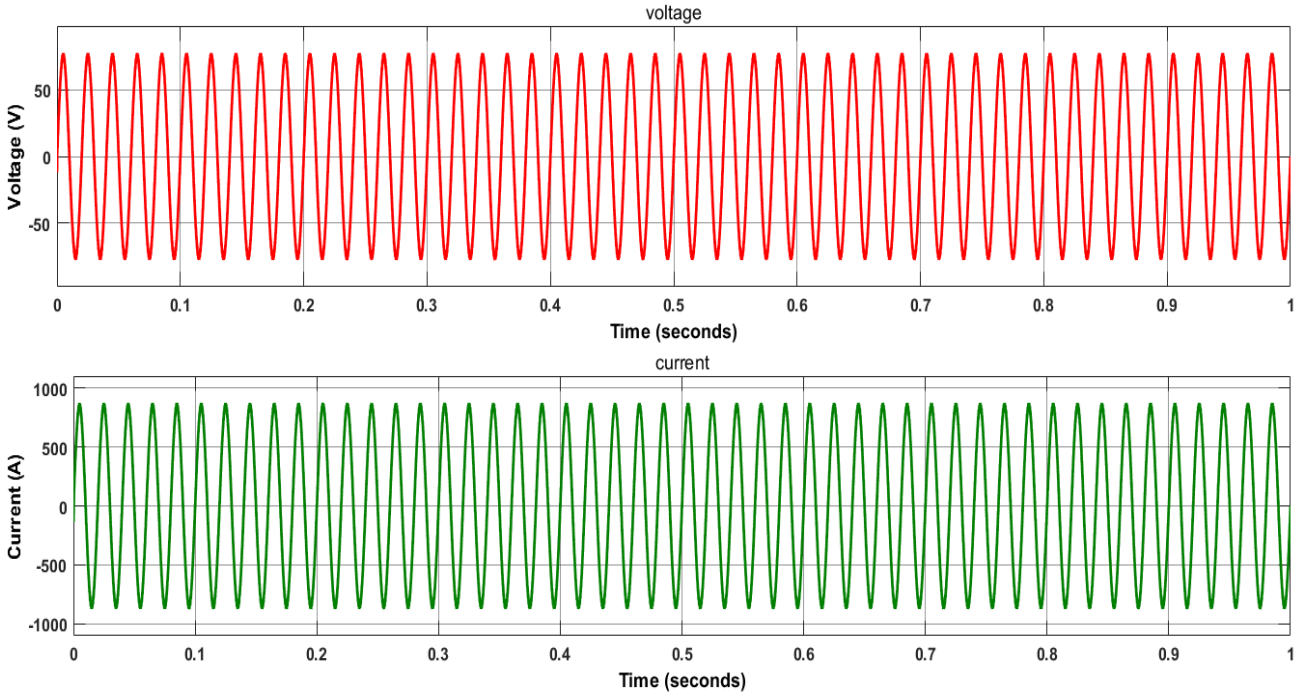

Fig. 4.45 Single phase current and voltage output when cell no 250

The above Fig. 4.45 represents the Single-phase voltage and current after DC to AC conversion for 250 cell number. For phase current 1 and phase voltage 1 we have the following Table 4.30-

Table 4.30: Output results of single phase current and voltage output when cell no 250

Contents	**Phase current I_A**	**Phase voltage V_A**
Maximum peak value	875 A	77.76 V
Maximum peak value Time	0.725second.	0.725 second.
Minimum phase value	-875.1A	-77.76V
Minimum phase value Time	0.175 second	0.175 second
Peak to peak value	1750.1 A	155.5 V
Rams value	602 A	53.50 V
Rise time	5.656 ms	5.656 ms
Fall time	5.718 ms	5.718 ms
Overshoot	2.627%	2.627%

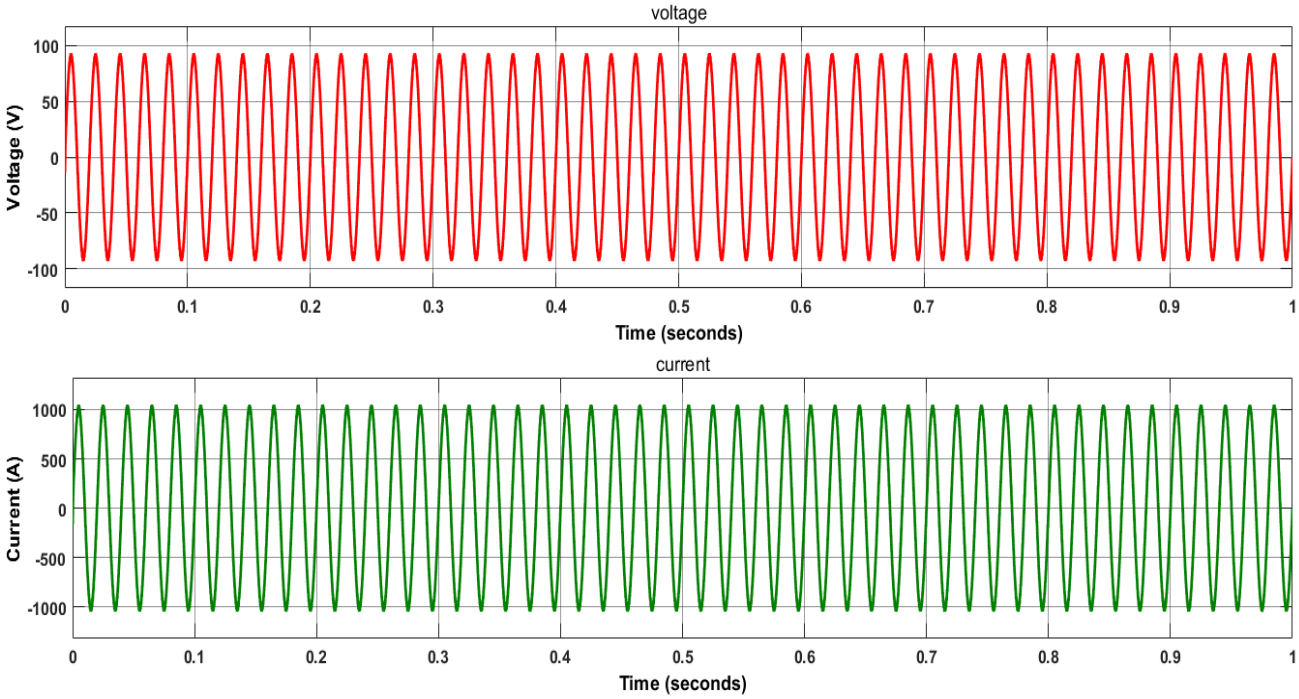

Fig. 4.46 Single phase current and voltage output when cell no 300

The above Fig. 4.46 represents the single-phase voltage and current after DC to AC conversion for 300 cell number. For phase current 1 and phase voltage 1 we have the following Table 4.31-

Table 4.31: Output results of single phase current and voltage output when cell no 300

Contents	**Phase current I_A**	**Phase voltage V_A**
Maximum peak value	1050 A	93.31 V
Maximum peak value Time	0.825 second.	0.825 second.
Minimum phase value	-1050A	-93.31 V
Minimum phase value Time	0.175 second	0.175 second
Peak to peak value	2100 A	186.6 V
Rams value	721.2 A	64.09 V
Rise time	5.656 ms	5.656 ms
Fall time	5.718 ms	5.718 ms
Overshoot	2.627%	2.627%

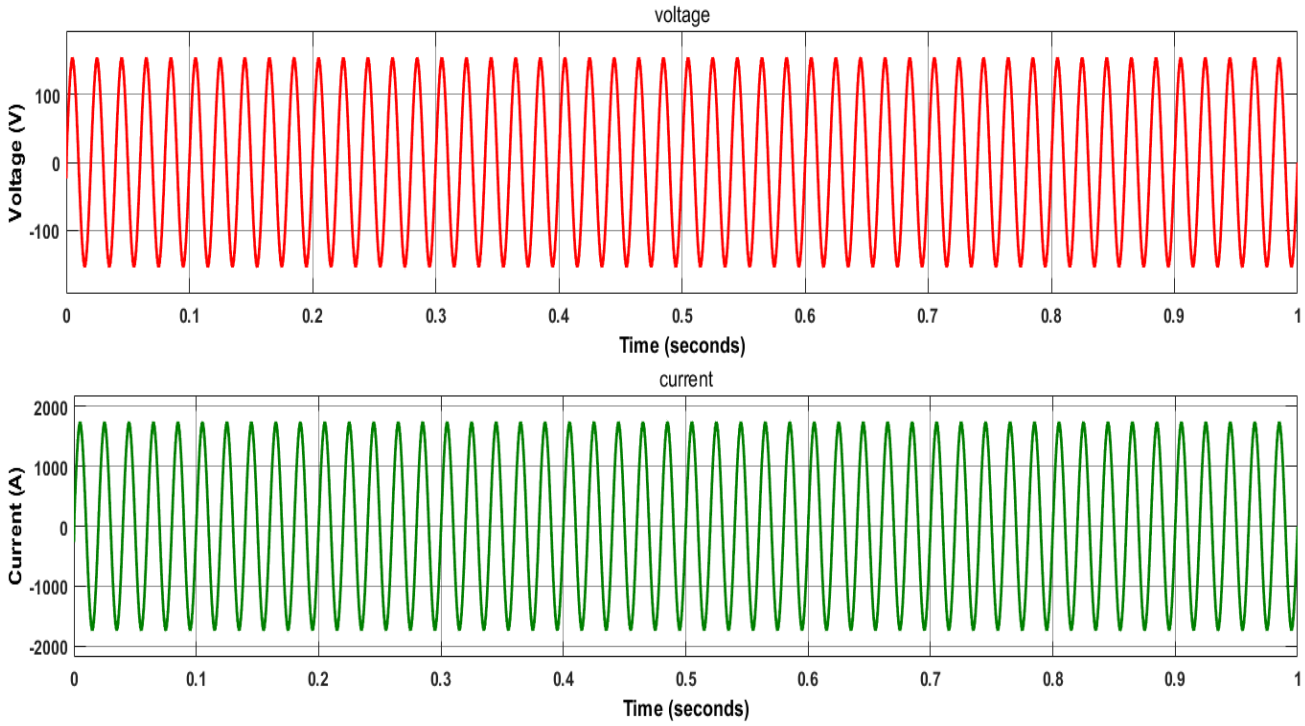

Fig. 4.46 Single phase current and voltage output when cell no 500

The above Fig. 4.46 represents the single-phase voltage and current after DC to AC conversion for 500 cell number. For phase current 1 and phase voltage 1 we have the following Table 4.32-

Table 4.32: Output results of single phase current and voltage output when cell no 500

Contents	**Phase current I_A**	**Phase voltage V_A**
Maximum peak value	1750 A	155.5 V
Maximum peak value Time	0.805 second.	0.805 second.
Minimum phase value	-1750A	-155.5V
Minimum phase value Time	0.175 second	0.175 second
Peak to peak value	3500 A	310.1 V
Rams value	1195 A	106.2 V
Rise time	5.656 ms	5.656 ms
Fall time	5.718 ms	5.718 ms
Overshoot	2.628%	2.628%

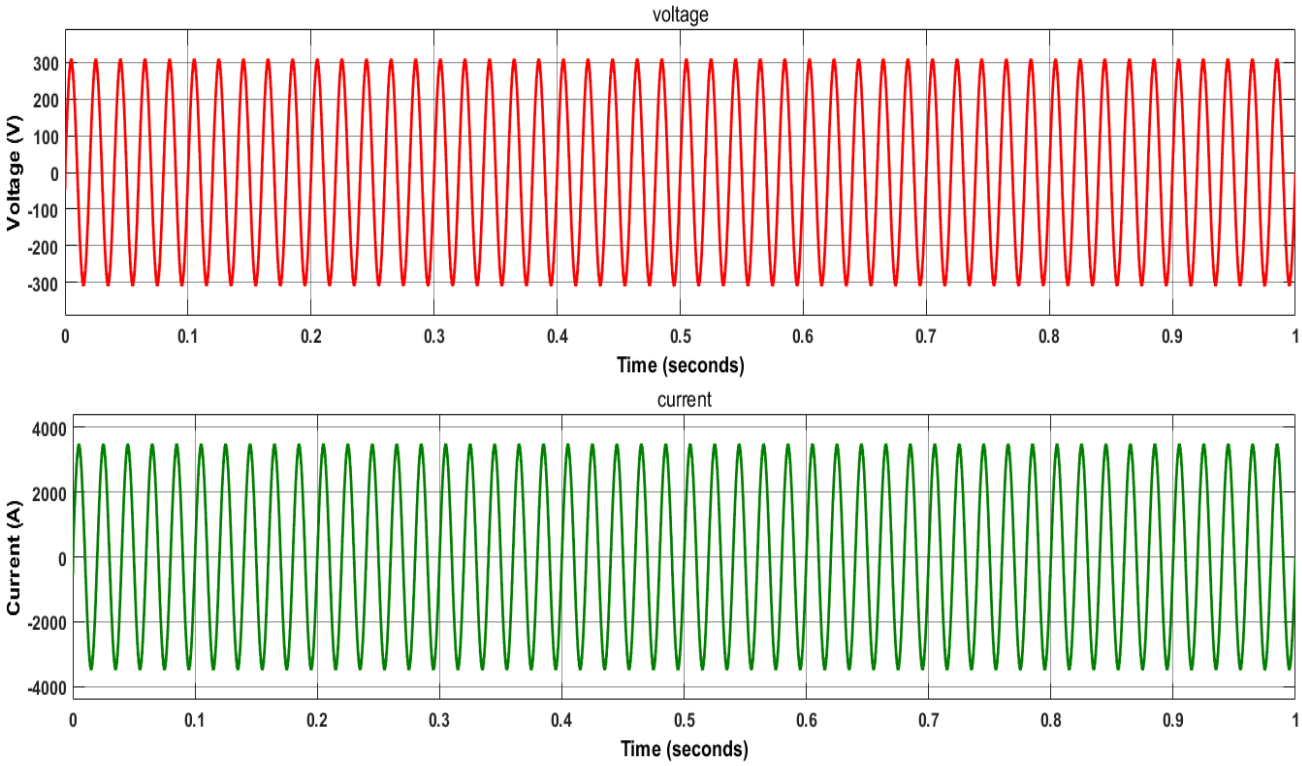

Fig. 4.47 Single phase current and voltage output when cell no 1000

The above Fig. 4.47 represents the single-phase voltage and current after DC to AC conversion for 1000 cell number. For phase current 1 and phase voltage 1 we have the following Table 4.33-

Table 4.33: Output results of single phase current and voltage output when cell no 1000

Contents	**Phase current I_A**	**Phase voltage V_A**
Maximum peak value	3500 A	310 V
Maximum peak value Time	0.725 second.	0.725 second.
Minimum phase value	-3500 A	-311.1 V
Minimum phase value Time	-0.175 second	0.175 second
Peak to peak value	7000 A	621.1 V
Rams value	2412 A	214.3 V
Rise time	5.656 ms	5.656 ms
Fall time	5.718 ms	5.718 ms
Overshoot	2.630%	2.630%

4.5.2 Output characteristics of three phase current and voltage:

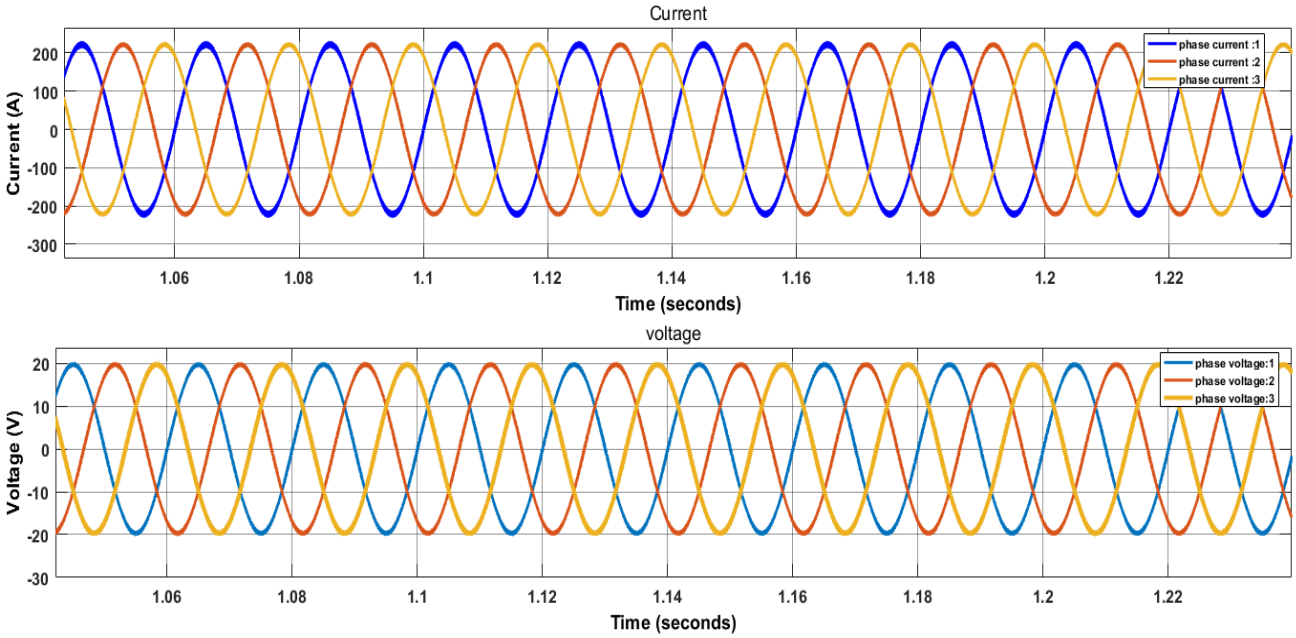

Fig. 4.48 Three phase current and voltage output when cell no 65

The above Fig. 4.48 represents the three-phase voltage and current after DC to AC conversion for 65 cell number. For phase current 1 and phase voltage 1 we have the following Table 4.34-

Table 4.34: Output results of three phase current and voltage output when cell no 65

Contents	**Phase current I_A**	**Phase voltage V_A**
Maximum peak value	227.5 A	19.21 V
Maximum peak value Time	1.105 second.	1.825 second.
Minimum phase value	-227.5 A	-19.21 V
Minimum phase value Time	1.175second	1.175 second
Peak to peak value	455A	40.44V
Rams value	156.6 A	13.87 V
Rise time	5.656 ms	5.656 ms
Fall time	5.718 ms	5.719 ms
Overshoot	2.628%	2.620%

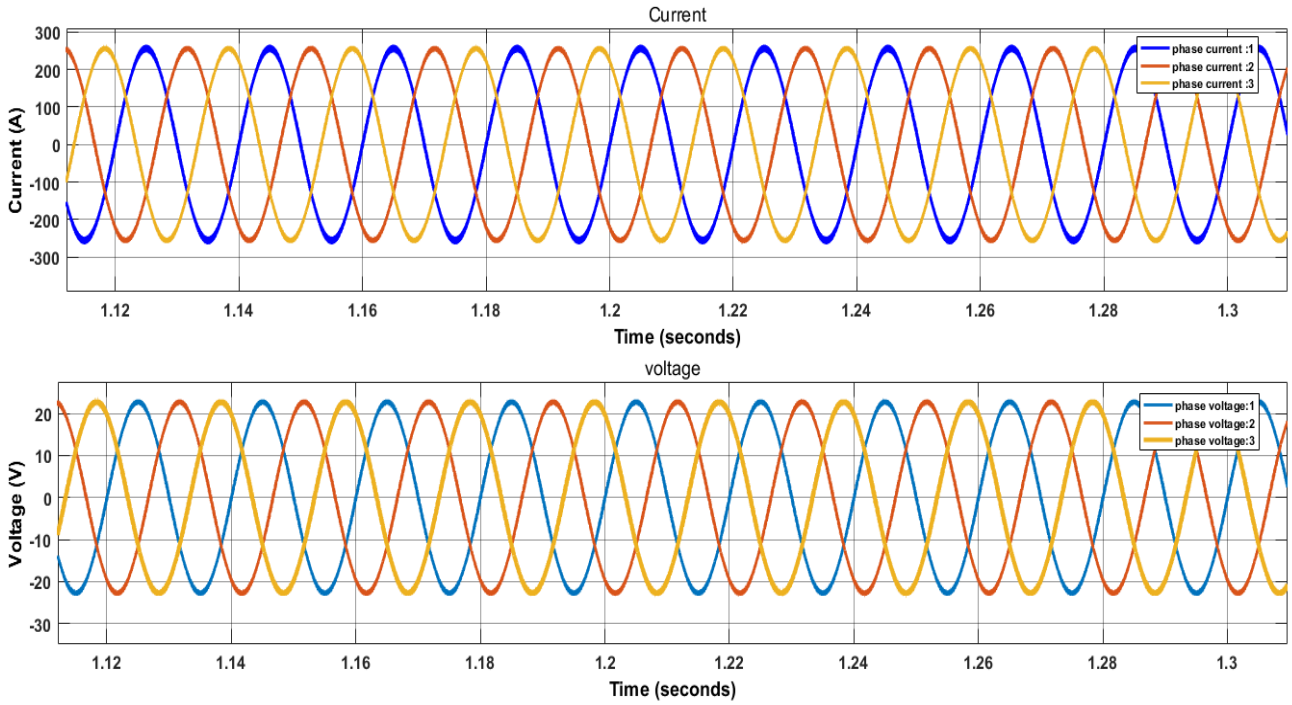

Fig. 4.48 Three phase current and voltage output when cell no 75

The above Fig. 4.48 represents the three-phase voltage and current after DC to AC conversion for 65 cell number. For phase current 1 and phase voltage 1 we have the following Table 4.35-

Table 4.35: Output results of three phase current and voltage output when cell no 75

Contents	**Phase current I_A**	**Phase voltage V_A**
Maximum peak value	262.5 A	23.33 V
Maximum peak value Time	1.245 second.	1.245 second.
Minimum phase value	-262.5 A	-23.33 V
Minimum phase value Time	1.175second	1.175 second
Peak to peak value	525A	46.65V
Rams value	181.2 A	16.1 V
Rise time	5.656 ms	5.656 ms
Fall time	5.718 ms	5.718 ms
Overshoot	2.628%	2.620%

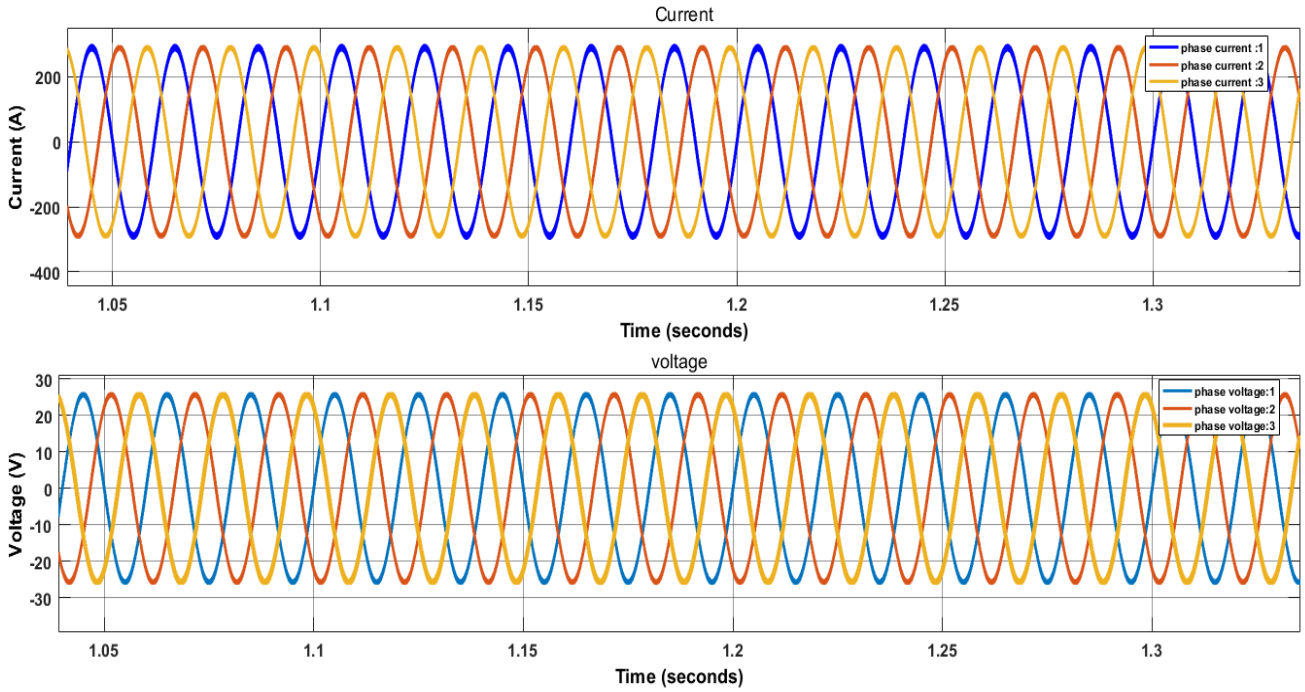

Fig. 4.49 Three phase current and voltage output when cell no 85

The above Fig. 4.49 represents the three-phase voltage and current after DC to AC conversion for 85 cell number. For phase current 1 and phase voltage 1 we have the following Table 4.36-

Table 4.36: Output results of three phase current and voltage output when cell no 85

Contents	**Phase current I_A**	**Phase voltage V_A**
Maximum peak value	297.5 A	26.44 V
Maximum peak value Time	1.225 second.	1.225 second.
Minimum phase value	-297.5A	-26.44 V
Minimum phase value Time	1.175second	1.175 second
Peak to peak value	595A	52.87 V
Rams value	204 A	18.13 V
Rise time	5.656 ms	5.656 ms
Fall time	5.718 ms	5.718 ms
Overshoot	2.629%	2.629%

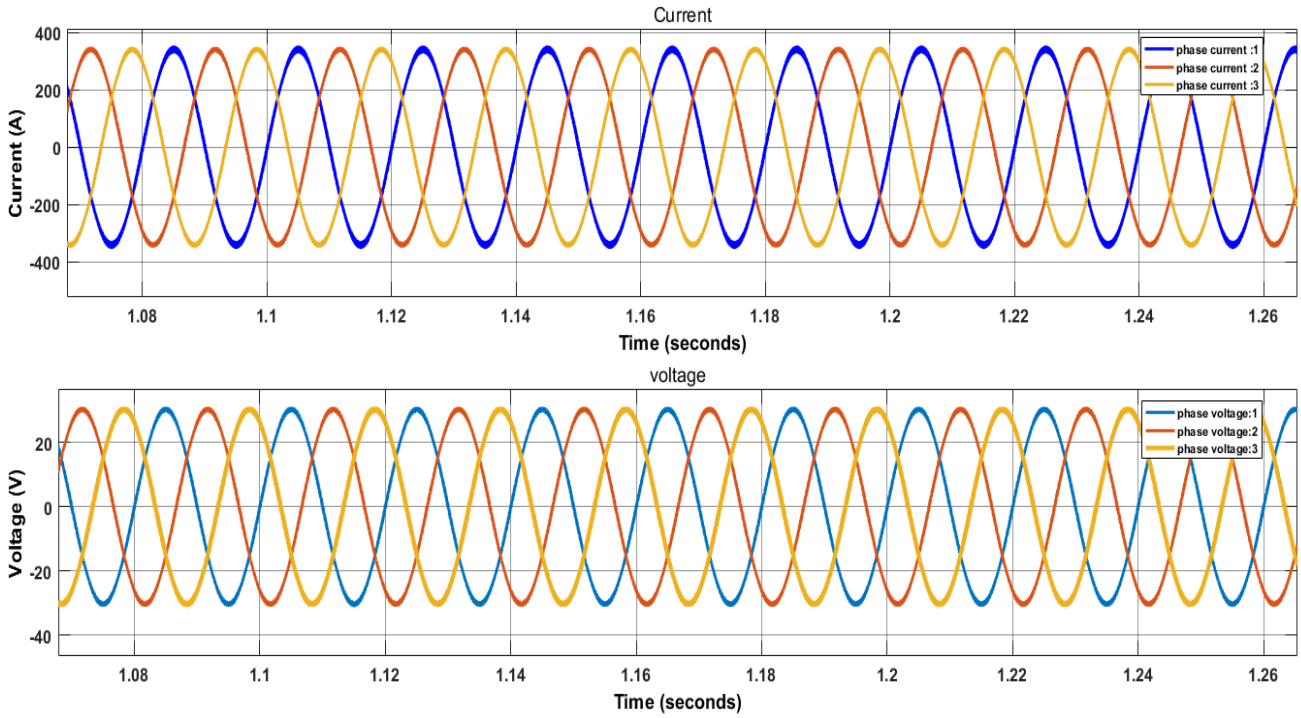

Fig. 4.50 Three phase current and voltage output when cell no 100

The above Fig. 4.50 represents the three-phase voltage and current after DC to AC conversion for 100 cell number. For phase current 1 and phase voltage 1 we have the following Table 4.37-

Table 4.37: Output results of three phase current and voltage output when cell no 100

Contents	**Phase current I_A**	**Phase voltage V_A**
Maximum peak value	350 A	31.11 V
Maximum peak value Time	1.105 second.	1.105 second.
Minimum phase value	-350 A	-31.11 V
Minimum phase value Time	1.175second	1.175 second
Peak to peak value	700A	62.22 V
Rams value	239.4 A	21.27 V
Rise time	5.656 ms	5.656 ms
Fall time	5.718 ms	5.718 ms
Overshoot	2.623%	2.623%

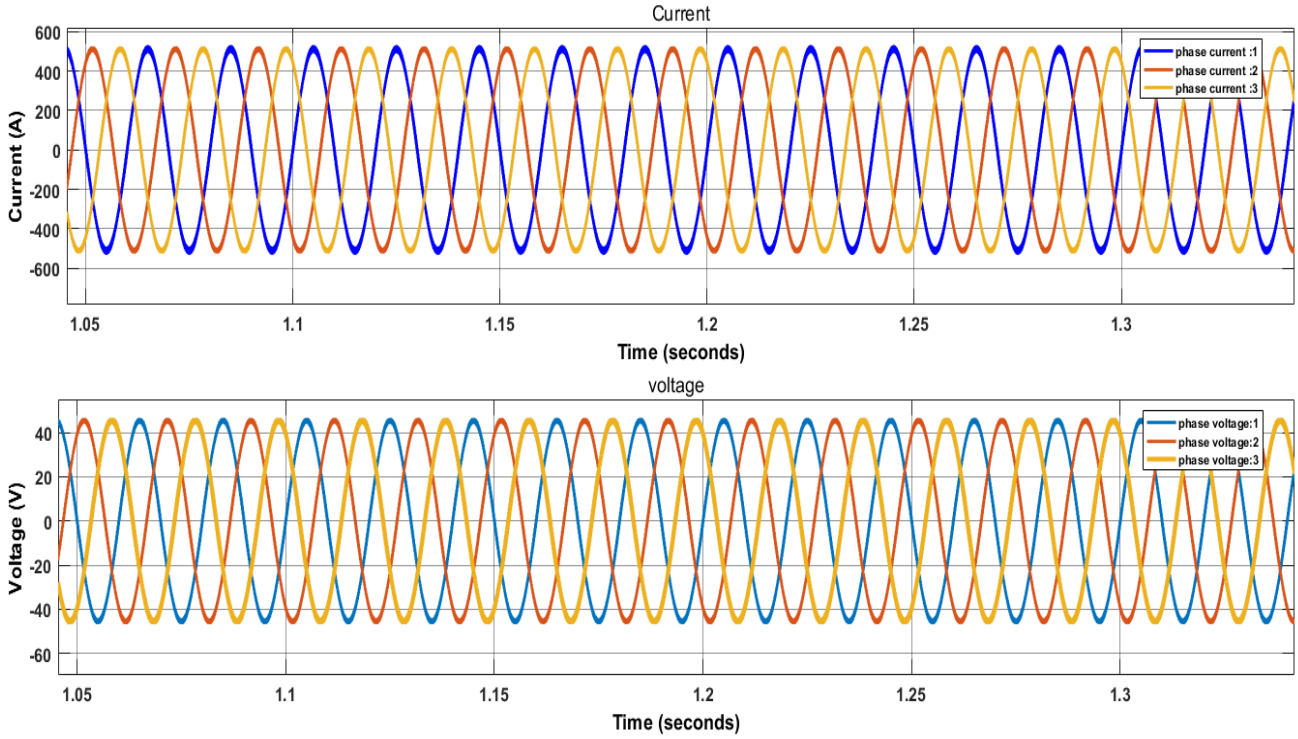

Fig. 4.51 Three phase current and voltage output when cell no 150

The above Fig. 4.51 represents the three-phase voltage and current after DC to AC conversion for 150 cell number. For phase current 1 and phase voltage 1 we have the following Table 4.38-

Table 4.38: Output results of three phase current and voltage output when cell no 150

Contents	**Phase current I_A**	**Phase voltage V_A**
Maximum peak value	525.1 A	46.66 V
Maximum peak value Time	1.105 second.	1.105 second.
Minimum phase value	-525.1 A	-46.66V
Minimum phase value Time	1.175second	1.175 second
Peak to peak value	1050.2A	93.32 V
Rams value	358.2 A	31.89 V
Rise time	5.656 ms	5.656 ms
Fall time	5.719 ms	5.719 ms
Overshoot	2.621%	2.621%

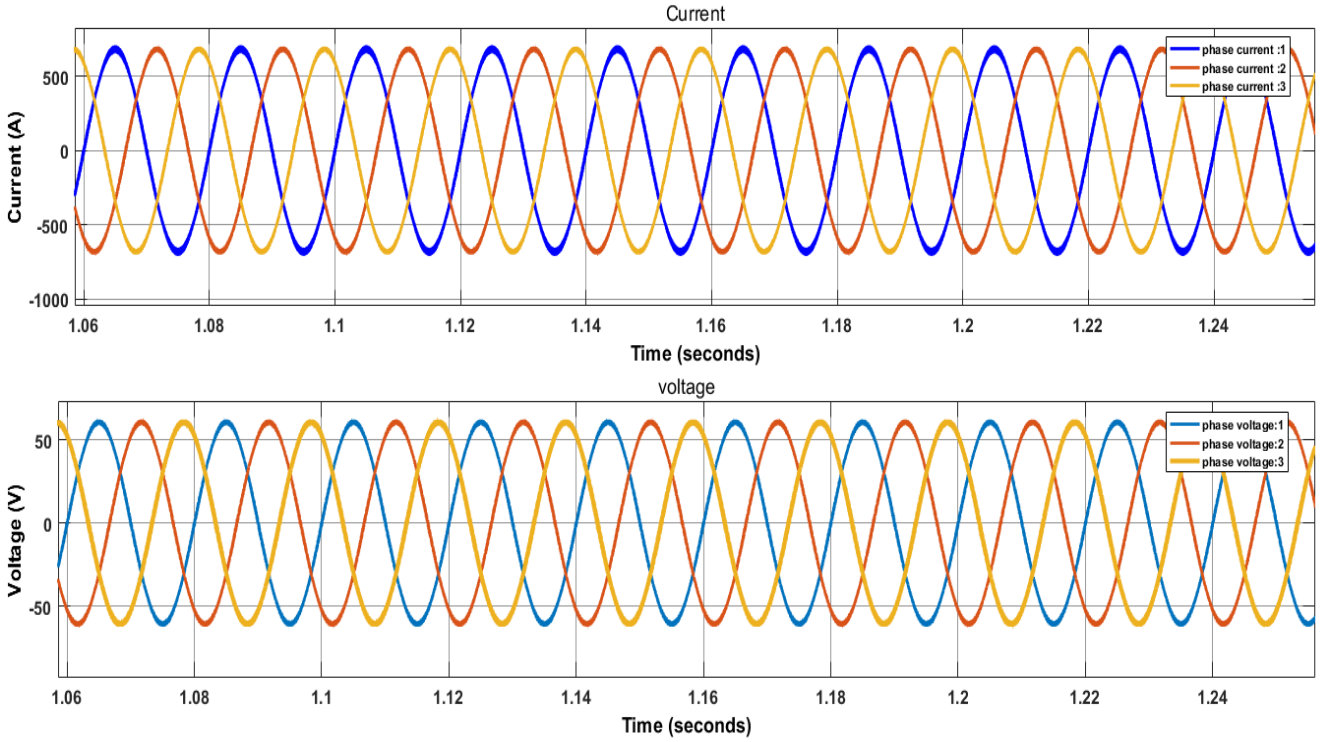

Fig. 4.52 Three phase current and voltage output when cell no 200

The above Fig. 4.52 represents the three-phase voltage and current after DC to AC conversion for 200 cell number. For phase current 1 and phase voltage 1 we have the following Table 4.39-

Table 4.39: Output results of three phase current and voltage output when cell no 200

Contents	**Phase current I_A**	**Phase voltage V_A**
Maximum peak value	700 A	62.21 V
Maximum peak value Time	1.105 second.	1.105 second.
Minimum phase value	-700A	-62.21V
Minimum phase value Time	1.175second	1.175 second
Peak to peak value	1400 A	124.42 V
Rams value	478.4 A	42.41V
Rise time	5.656 ms	5.656 ms
Fall time	5.718 ms	5.718 ms
Overshoot	2.626%	2.626%

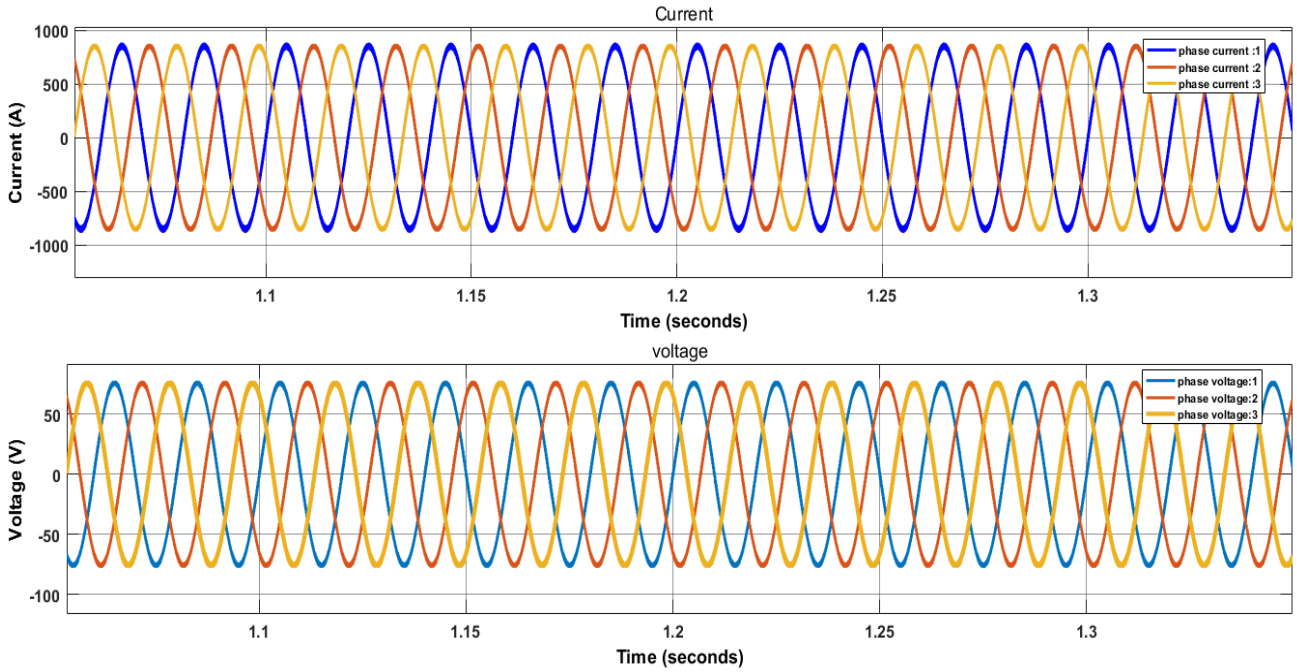

Fig. 4.53 Three phase current and voltage output when cell no 250

The above Fig. 4.53 represents the three-phase voltage and current after DC to AC conversion for 250 cell number. For phase current 1 and phase voltage 1 we have the following Table 4.40-

Table 4.40: Output results of three phase current and voltage output when cell no 250

Contents	**Phase current I_A**	**Phase voltage V_A**
Maximum peak value	875 A	77.76 V
Maximum peak value Time	1.105 second.	1.105 second.
Minimum phase value	-875.1A	-77.76V
Minimum phase value Time	1.175second	1.175 second
Peak to peak value	1750.1 A	155.5 V
Rams value	602 A	53.50 V
Rise time	5.656 ms	5.656 ms
Fall time	5.718 ms	5.718 ms
Overshoot	2.627%	2.627%

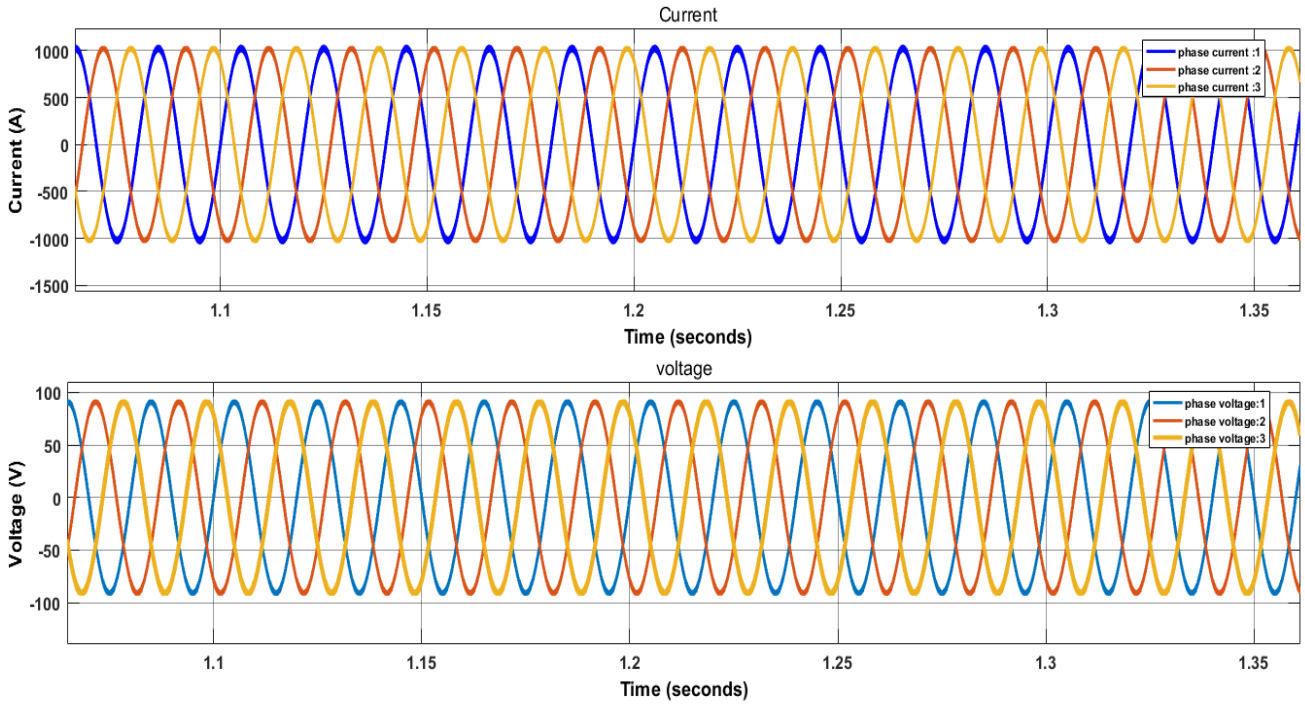

Fig. 4.54 Three phase current and voltage output when cell no 300

The above Fig. 4.54 represents the three-phase voltage and current after DC to AC conversion for 300 cell number. For phase current 1 and phase voltage 1 we have the following Table 4.41-

Table 4.41: Output results of three phase current and voltage output when cell no 300

Contents	**Phase current I_A**	**Phase voltage V_A**
Maximum peak value	1050 A	93.31 V
Maximum peak value Time	1.105 second.	1.105 second.
Minimum phase value	-1050A	-93.31 V
Minimum phase value Time	1.175second	1.175 second
Peak to peak value	2100 A	186.6 V
Rams value	721.2 A	64.09 V
Rise time	5.656 ms	5.656 ms
Fall time	5.718 ms	5.718 ms
Overshoot	2.627%	2.627%

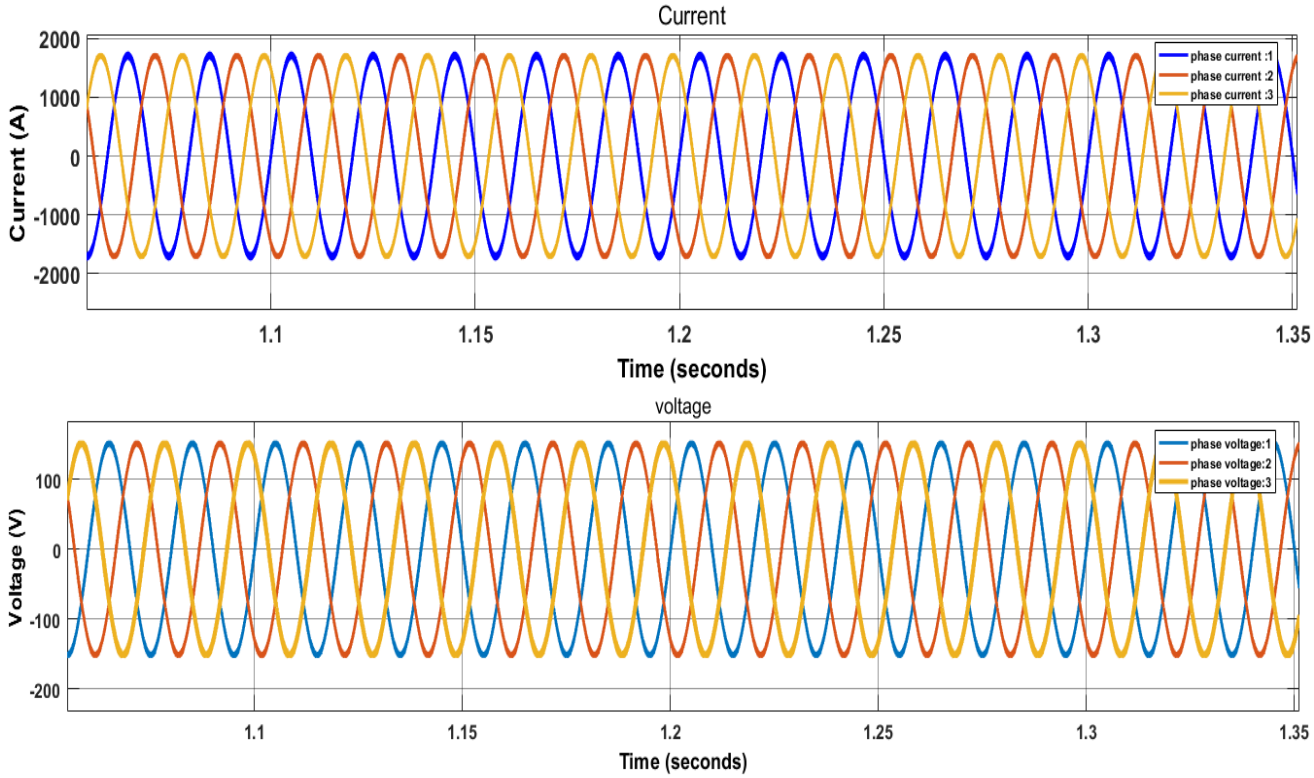

Fig. 4.55 Three phase current and voltage output when cell no 500

The above Fig. 4.55 represents the three-phase voltage and current after DC to AC conversion for 500 cell number. For phase current 1 and phase voltage 1 we have the following Table 4.42-

Table 4.42: Output results of three phase current and voltage output when cell no 500

Contents	**Phase current I_A**	**Phase voltage V_A**
Maximum peak value	1750 A	155.5 V
Maximum peak value Time	1.125 second.	1.105 second.
Minimum phase value	-1750A	-155.5V
Minimum phase value Time	1.175second	1.175 second
Peak to peak value	3500 A	310.1 V
Rams value	1195 A	106.2 V
Rise time	5.656 ms	5.656 ms
Fall time	5.718 ms	5.718 ms
Overshoot	2.628%	2.628%

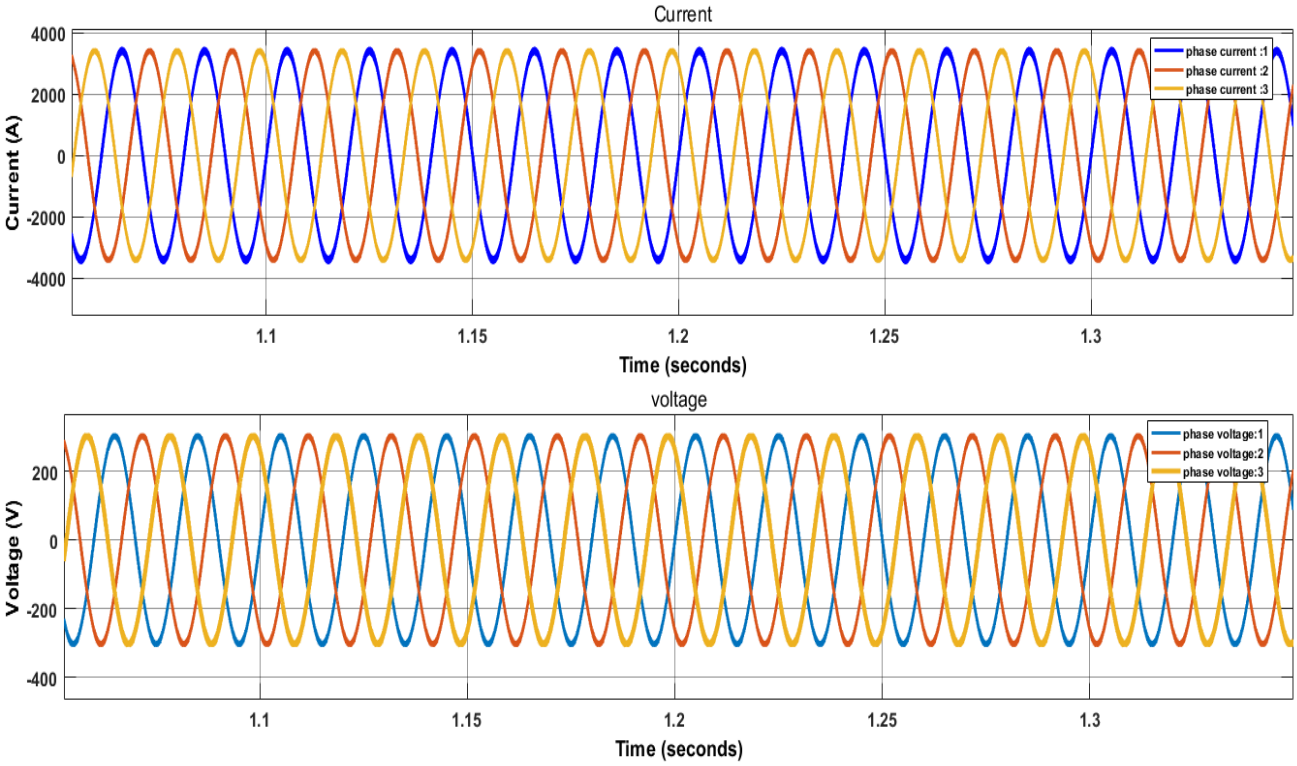

Fig. 4.56 Three phase current and voltage output when cell no 1000

The above Fig. 4.56 represents the three-phase voltage and current after DC to AC conversion for 1000 cell number. For phase current 1 and phase voltage 1 we have the following Table 4.43-

Table 4.43: Output results of three phase current and voltage output when cell no 1000

Contents	**Phase current I_A**	**Phase voltage V_A**
Maximum peak value	3500 A	310 V
Maximum peak value Time	1.065 second.	1.065 second.
Minimum phase value	-3500 A	-311.1 V
Minimum phase value Time	1.175second	1.175 second
Peak to peak value	7000 A	621.1 V
Rams value	2412 A	214.3 V
Rise time	5.656 ms	5.656 ms
Fall time	5.718 ms	5.718 ms
Overshoot	2.630%	2.630%

4.6 Economical Aspects:

4.6.1 Condition of carbon reduction after implementation of MCFC:

Fig. 4.57 below has been made from Table 1.1 where top ten emitters of CO_2 were shown. Basically, the graph below shows what would be the condition of CO_2 emission before and after implementation of MCFC. Where, the CO_2 reduction capability of MCFC was considered to be 70%.

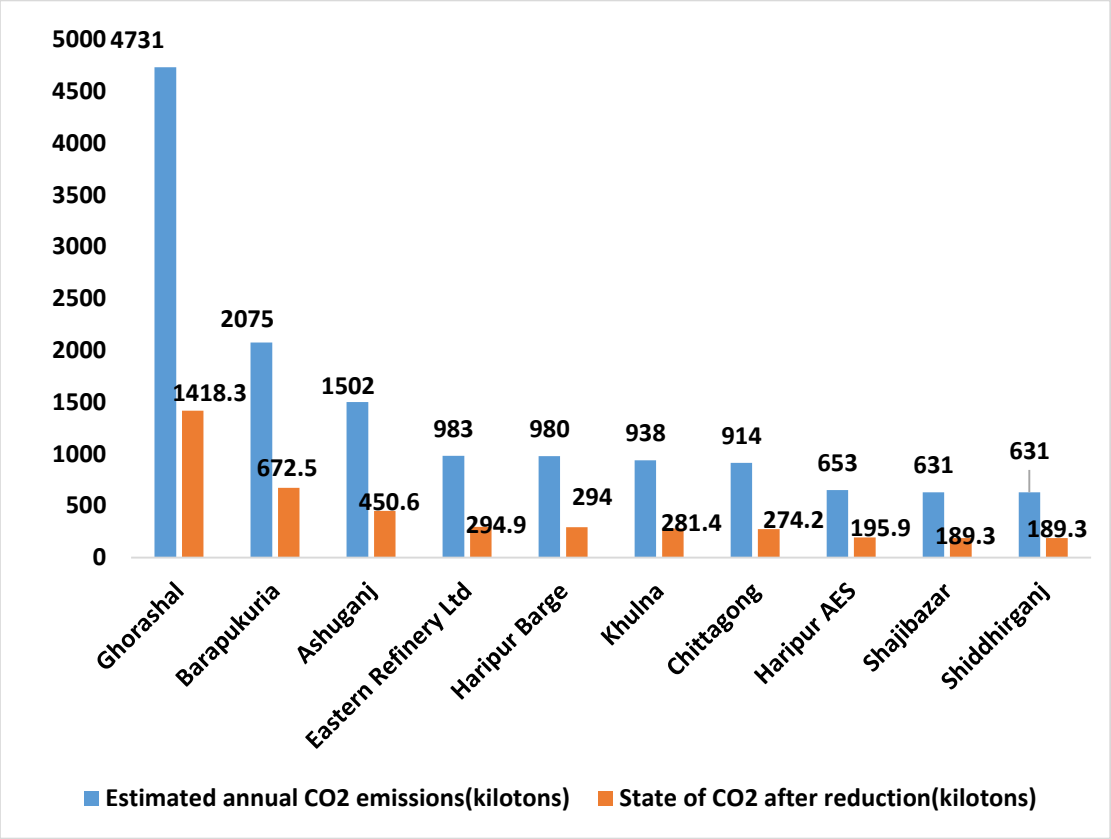

Fig. 4.57 Condition of carbon emission after Implementation of MCFC

4.6.2 If MCFC is implemented in Ghorashal power plant:

This power plant emits 4,731 kiloton CO_2 in per year. In one hour, it emits

$$=4{,}731/(365\times24) \text{ kilotons}$$

$$=0.54 \text{ kilotons(approx.)}.$$

Here, 40% of 0.54 kilotons mean that 0.216 kilotons can be converted into fuel.

From 0.216 kilotons, we can produce =(247,500×0.216)KWh

=53,460 KWh

=53.46 MWh .

Total cost per year = (53460×24×30×12×20.28)

=9,367,218,432 BDT.

As the value of money changes over time it is assumed that the interest rate after a year is 6 percent.

So, the total cost value of money per year must be

= (total cost per year + interest rate of total cost per year

=(9,367,218,432+6% of 9,367,218,432)

=9,929,251,537.92 BDT.

Income:

While considering 1KWh=8 BDT

Total income per year= (53,460×24×30×12×8)

= 3,695,155,200 BDT

Payback:

So, Payback period=(Total system cost)/(Total annual income)

=(9,929,251,537/36,951,555,200)

=2.68 year.

By using values from TABLE 1 and using the mathematical procedure as shown above the following Table 4.44 was created in order to show just how much electrical energy can be produced from the following power plants and refineries while at the same time

how CO_2 can be reduced. Here the amount of CO_2 reduction capability of MCFC has been considered to be 70%.

Table 4.44: Power generation and CO_2 reduction for different power sectors using MCFC

Name of sector	**Installation name**	**Generated electrical energy**	**Reduced CO_2 (kilotons)**
Power	Ghorashal	53.46 MWh	3311.7
Power	Barapukuria	23.45 MWh	1452.5
Power	Ashuganj	16.97 MWh	1052.4
Refinery	Eastern Refinery Ltd	11.11 MWh	688.1
Power	Haripur Barge	11.10 MWh	686

Now let's take a look at how much additional land would be required and how many houses could be powered from the given amount of power along with the cost incorporated with it. For this, two power plants namely Ghorashal and Ashuganj have been used and the average daily consumption per household has been considered to be 1kwh in the following Table 4.45. These two sites were selected for this observation because MCFC units require a considerable amount of land and it came into our attention that these two power plants had adequate space in their vicinity for further expansions.

Table 4.45: Economical perspectives and power generation capability of MCFC in combination with Ghorashal and Ashuganj:

Power plant	**Area required**	**Power production per hour from MCFC**	**System cost per year (BDT)**	**Power providing capability to household**
Ghorashal	2.54 Acre	53.46 MW	950 crores	53000 houses
Ashuganj	0.804 Acre	16.97 MW	412 crores	16000 houses

4.7 Summary:

In this section the results and discussion of both MATLAB Simulink and Comsol has been discussed. The economical prospective of MCFC has also been shown here. From this section it can also be summed up that for the cell number of 1000 in a stack we can get maximum efficiency. At 1000 cell numbers, the MCFC stack can extract 41.19% efficiency. To make sure of the efficient implementation of MCFC stack with the existing natural and coal based power plant (installed capacity above 400 MVA), we need to use cell number of 1000 or above. To connect the output of the MCFC stack with the grid an inverter has been designed in Simulink. In this inverter section we observed two operations, one in discrete time and the other in continuous time. For 1000 cell numbers in the discrete time operation we got maximum efficiency of 59.8% and in continuous time we got 48.6%. But in discrete time, overshoot level is 16.36% higher than the continuous operation. In perspective of efficiency level, discrete time is preferable.

CHAPTER 5

CONCULSIONS AND FUTURE WORK

5.1 Conclusions:

Over the last few decades' earth is experiencing an alarming rise of CO_2 in its atmosphere. So, to overcome this obstacle many industries, factories or power manufacturers are looking for a way to reduce the CO_2 produced by them. In the past, many would suggest to hide the CO_2 underground using the carbon capture storage method. While the process does help in reducing the CO_2 but this expensive process does not give any economic benefit. But with the help of MCFC technology we can not only reduce CO_2 but can also be a sustainable source of power development. Bangladesh could also try to implement MCFC in their power plants as it would not only help produce much needed power for the country, it will also help increase the GDP growth rate of the country as many economical proposals were turned down due to shortage of power. So, an example was shown by implementing MCFC at Ghorashal, Barapukuria, Ashuganj, Eastern Refinery Ltd and Haripur Barge power plant to show a scenario as to what can be expected from MCFC. We have also shown many output results in Comsol and MATLAB. In MATLAB we tried simulate how much power we can get by varying the cell numbers both in continuous and discrete time. The grid connection with output results with inverters has also been showed here. In the Comsol section we have shown various outputs regarding gas diffusion layer of a MCFC. While the process of MCFC is fairly expensive at present time it will surely fall with further advancement in this technology. Also taking into consideration that the world is facing great threat of global warming expense of MCFC is surely a small price to pay for the future of our environment.

5.2 Future suggestions:

- Incorporating with different power generation companies to share our findings
- To be able to test out our theatrical assumption in real world scenario.
- To tryout replacing different materials in Comsol to see if there are any efficiency boost to the system.
- And lastly to be able to contribute to the country.

REFERENCES

[1] "Bangladesh Power Development Board (BPDB)." [Online]. Available: http://www.bpdb.gov.bd/bpdb/. [Accessed: 07-Oct-2017].

[2] "Power Generation Units (Fuel Type Wise)." [Online]. Available: http://www.bpdb.gov.bd/bpdb/index.php?option=com_content&view=article&id=150&Itemid=16 . [Accessed: 08-Aug-2017].

[3] "CO2 sources in Bangladesh | Global CCS Institute." [Online]. Available: https://hub.globalccsinstitute.com/publications/regional-assessment-potential-co2-storage-indian-subcontinent/41-co2-sources-bangladesh. [Accessed: 08-Aug-2017].

[4] "Bangladesh CO2 Emissions from Fossil-fuel CO2 emissions from fossil-fuels." [Online]. Available: https://knoema.com/atlas/Bangladesh/topics/Environment/CO2-Emissions-from-Fossil-fuel/CO2-emissions-from-fossil-fuels. [Accessed: 11-Aug-2017].

[5] O. R. N. L. Environmental Sciences Division, "United States of America Fossil-Fuel CO2 Emissions," 01-Jan-2011. [Online]. Available: http://cdiac.ornl.gov/ftp/trends/co2_emis/ban.dat. [Accessed: 08-Aug-2017].

[6] "Rampal power station." [Online]. Available: https://www.sourcewatch.org/index.php/Rampal_power_station. [Accessed: 27-Oct-2017].

[7] "Chittagong power station (S Alam)." [Online]. Available: https://www.sourcewatch.org/index.php/Chittagong_power_station_(S_Alam). [Accessed: 27-Oct-2017].

[8] F. Elahi and N. I. Khan, "A Study on the Effects of Global Warming in Bangladesh," *Int. J. Environ. Monit. Anal.*, vol. 3, no. 3, p. 118, 2015.

[9] P. Gour and R. Nikose, "Application of fuel cell in power plant to reduce the carbon-dioxide emission," *Int. J. Core Eng. Manag.*, vol. 1, no. 5, pp. 76–82, 2014.

[10] M. L. Perry and T. F. Fuller, "An ECS Centennial Series Article A Historical Perspective of Fuel Cell Technology in the 20th Century," pp. 59–67, 2002.

[11] A. L. Dicks, "FUEL CELLS – MOLTEN CARBONATE FUEL CELLS | Overview A2 - Garche, Jürgen BT - Encyclopedia of Electrochemical Power Sources," Amsterdam: Elsevier, 2009, pp. 446–453.

[12] S. J. Mcphail, P. Hsieh, and J. R. Selman, *Molten Carbonate Fuel Cells*, vol. 4. Elsevier Ltd., 2012.

[13] Z. Ma, R. Venkataraman, M. Farooque, and F. Energy, "Cell and Stack Modeling Approach and Methodology," *Encycl. Electrochem. Power Sources*, 2009.

[14] S. J. Mcphail, L. Leto, M. Della Pietra, V. Cigolotti, and A. Moreno, "International Status of Molten Carbonate Fuel Cells 2015," *Enea*, 2015.

[15] H. Kim, J. Ho, K. Soon, S. Yook, and W. Jung, "Modeling and Control System Design of an MCFC System," pp. 84–89, 2011.

[16] P. Chiesa, S. Campanari, and G. Manzolini, "CO2 cryogenic separation from combined cycles integrated with molten carbonate fuel cells," *Int. J. Hydrogen Energy*, vol. 36, no. 16, pp. 10355–10365, 2011.

[17] B. Kim, D. H. Kim, J. Lee, S. W. Kang, and H. C. Lim, “The operation results of a 125kW molten carbonate fuel cell system,” *Renew. Energy*, vol. 42, pp. 145–151, 2012.

[18] J. Milewski and J. Lewandowski, “Separating CO2 from Flue Gases Using a Molten Carbonate Fuel Cell,” *IERI Procedia*, vol. 1, no. 48, pp. 232–237, 2012.

[19] D. Sánchez, S. Ubertini, J. M. Muñoz De Escalona, and R. Chacartegui, “Potential of molten carbonate fuel cells to reduce the carbon footprint of large reciprocating engines,” *Int. J. Hydrogen Energy*, vol. 39, no. 8, pp. 4081–4088, 2014.

[20] A. Haghighat Mamaghani, B. Najafi, A. Shirazi, and F. Rinaldi, “4E analysis and multi-objective optimization of an integrated MCFC (molten carbonate fuel cell) and ORC (organic Rankine cycle) system,” *Energy*, vol. 82, pp. 650–663, 2015.

[21] A. H. Mamaghani, B. Najafi, A. Shirazi, and F. Rinaldi, “Exergetic, economic, and environmental evaluations and multi-objective optimization of a combined molten carbonate fuel cell-gas turbine system,” *Appl. Therm. Eng.*, vol. 77, pp. 1–11, 2015.

[22] L. Duan, K. Xia, T. Feng, S. Jia, and J. Bian, “Study on coal-fired power plant with CO2 capture by integrating molten carbonate fuel cell system,” *Energy*, vol. 117, pp. 578–589, 2016.

[23] “Aspen Plus.” [Online]. Available: http://home.aspentech.com/products/engineering/aspen-plus. [Accessed: 07-Oct-2017].

[24] S. Samanta and S. Ghosh, “A thermo-economic analysis of repowering of a 250 MW coal fired power plant through integration of Molten Carbonate Fuel Cell with carbon capture,” *Int. J. Greenh. Gas Control*, vol. 51, pp. 48–55, 2016.

[25] R. Taylor and R. Krishna, *Multicomponent Mass Transfer*. JOHN WILEY & SONS, INC., 1993.

[26] M. Brenna, F. Foiadelli, and G. Manzolini, “Grid connection of MCFC applied to power plant with CO2 capture,” *Int. J. Electr. Power Energy Syst.*, vol. 53, pp. 980–986, 2013.

APPENDIX

Parameters used Comsol

Name	Expression	Value	Description
kappa_s	1000[S/m]	1000[S/m]	Conductivity, solid phase
kappa_m	9[S/m]	9[S/m]	Conductivity,membrane
V_cell	0.7[V]	0.7 V	Cell voltage
T	923.15[K]	923.15 K	Temperature
kappa_p	1e-13[m^2]	1.0000E-13 m²	GDL permeability
eta	2.1e-5[Pa*s]	2.1000E-5 Pa·s	Fluid viscosity
p_ref	1[atm]	1.0133E5 Pa	Reference pressure
p_a_in	1.1*p_ref	1.1146E5 Pa	Anode inlet pressure
p_c_in	1.1*p_ref	1.1146E5 Pa	Cathode inlet pressure
drag	3	3	Proton-Water drag coefficient through membrane
E_eq_a	0 V	0 V	Equilibrium potential, anode
E_eq_c	1[V]	1 V	Equilibrium potential, cathode
i0_a	1e5[A/m^2]	1.0000E5 A/m²	Exchange current density, anode
i0_c	1[A/m^2]	1 A/m²	Exchange current density, cathode
S	1e7[m^2/m^3]	1.0000E7 1/m	Specific surface area
R_agg	0.1[um]	1.0000E-7 m	Aggregate radius
eps_mic	0.2	0.2	Microscopic porosity inside agglomerates
eps_mac	0.4	0.4	Macroscopic porosity between agglomerates
D_agg	1.2e-10[m^2/s]* ((1-eps_mac)*eps_mic)^1.5	4.9883E-12 m²/s	Effective diffusion coefficient inside agglomerates

D_effH2_H2O	0.915e-4[m^2/s]* (T/307.1[K])^1.5*(eps_mac)^1.5	1.2064E-4 m²/s	Effective binary diffusivity, H2_H20
D_effO2_CO2	0.22e-4[m^2/s]* (T/293.2[K])^1.5*(eps_mac)^1.5	3.1094E-5 m²/s	Effective binary diffusivity, O2_CO2
D_effH2O_CO2	0.256e-4[m^2/s]* (T/307.5[K])^1.5*(eps_mac)^1.5	3.3688E-5 m²/s	Effective binary diffusivity, H2O_CO2
D_effO2_H2O	0.282e-4[m^2/s]* (T/308.1[K])^1.5*(eps_mac)^1.5	3.7001E-5 m²/s	Effective binary diffusivity, O2_H2O
wH2_in	0.1	0.1	Inlet weight fraction H2
wO2_in	0.21*0.8	0.168	Inlet weight fraction O2
wH2Oc_in	0.2	0.2	Cathode inlet weight fraction, H2O
MH2	2[g/mol]	0.002 kg/mol	Molar mass, H2
MO2	32[g/mol]	0.032 kg/mol	Molar mass, O2
MH2O	18[g/mol]	0.018 kg/mol	Molar mass, H2O
MCO2	44[g/mol]	0.044 kg/mol	Molar mass, CO2
xH2_in	(wH2_in/MH2)/(wH2_in/MH2+ (1-wH2_in)/MH2O)	0.5	Inlet molar fraction, H2
KH2	3.9e4[Pa*m^3/mol]	39000 Pa·m³/mol	Henry's law constant, H2 in agglomerate
KO2	3.2e4[Pa*m^3/mol]	32000 Pa·m³/mol	Henry's law constant, O2 in agglomerate
cH2_ref	xH2_in*p_ref/KH2	1.299 mol/m³	Reference concentration, H2
cO2_ref	xO2_in*p_ref/KO2	0.54105 mol/m³	Reference concentration, O2
l_act	10[um]	1.0000E-5 m	Active layer thickness
xO2_in	(wO2_in/MO2)/ (wO2_in/MO2+wH2Oc_in/MH2O+ (1-wO2_in-wH2Oc_in)/MCO2)	0.17087	Inlet molar fraction, O2
K	-6*l_act*(1- eps_mac)*F_const*D_agg/R_agg^2	-1732.7 m·A/mol	Agglomerate current density subexpression

Darcy's Law: Darcy's law for porous media states that the gradient of pressure, the viscosity of the fluid, and the structure of the porous media determine the velocity:

$$u = \frac{k_p}{\eta} \nabla p$$

Parameters used in Cost calculation

*To produce 1khw by natural gas fired power plant required 2-3tk

*To produce 1khw by coal fired power plant required 5tk
*1Mcf=10Ccf
*1ccf=0.004tons
Or,10*1ccf=0.04tons
Or,1Mcf=0.04tons
*1kiloton=907.1874metricton
Or,1metricton=0.001kiloton
*Again 1-ton coal can produce 1,927kwh
Or,1kiloton coal produce 1,927,000kwh
*1ton natural gas can produce 247.5kwh
Or,1kilo ton gas can produce 247,500 kwh

MCFC initial cost(BDT)	**Maintenance cost(BDT)**	**Equipment and construction (1st year)**	**Equipment and construction (2nd year)**	**Generation cost(kwh)**
60,800,000	30,400,000/40,000 hour	60,800,000(BDT)	30,400,000(BDT)	20.28(BDT)